# Proteomic and metabolomic signature of Dravet Syndrome: analysis in a genetic *Scn1a*-A1783V mouse model

**Nina Miljanović**

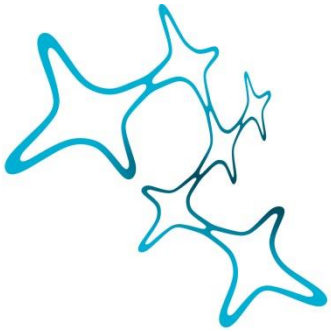

Graduate School of
Systemic Neurosciences
LMU Munich


Dissertation der
Graduate School of Systemic Neurosciences der
Ludwig-Maximilians-Universität München

March 12, 2021

Supervisor
Prof. Dr. med. vet. Heidrun Potschka
Institute of Pharmacology, Toxicology and Pharmacy
Ludwig-Maximilians-Universität München

First Reviewer: Prof. Dr. med. vet. Heidrun Potschka
Second Reviewer: Prof. Dr. med. Soheyl Noachtar
External Reviewer: Prof. Dr. med. Yvonne Weber

Date of Submission: 12.03.2021
Date of Defense: 14.06.2021

Correction to the article by Miljanovic et al. (2021)

This erratum is to correct errors in the article "Metabolomic signature of the Dravet syndrome: A genetic mouse model study" published in Epilepsia on July 5th, 2021.

In Results section 3.1 on page 2003, the second sentence should read: “Genotype differences between Dravet and WT mice were identified for 68 metabolites in the hippocampus…” instead of “…for 72 metabolites…”.
The plasma data for corticosterone, allocholic acid, cholic acid, and malic acid were presented without FDR correction. Therefore, in Results section 3.2 on page 2004, paragraph 3, it should read as follows: “Analysis of the plasma metabolome in CD-fed mice, pointed toward a downregulation of corticosterone, allocholic, and cholic bile acid and an upregulation of malic acid in Dravet mice (Figure 3A-C; unpaired t test).” The last sentence in the legend for figure 3A-C should read as follows: “Data shown are from 20 WT mice (10 CD, 10 KD) and 21 Dravet mice (10 CD, 11 KD) (A-C, unpaired t-test, * = $p < .05$, mean ± SEM; D-F, Two-way ANOVA, FDR correction, Bonferroni post hoc test, * = $p < .05$, mean ± SEM; differences illustrated for the following comparisons: groups with the same genotype KD vs. CD and groups with the same diet Dra vs. WT).”

*“Do not go where the path may lead, go instead where there is no path and leave a trail.”*

Ralph Waldo Emerson

# Table of content

Table of content

# ABSTRACT

Dravet syndrome is a rare, severe form of pediatric epilepsy, accompanied by cognitive, behavioral and motor disturbances. Haploinsufficiency of the *Scn1a* gene, encoding the function of sodium channels on GABAergic neurons, has been detected in over 80 % of patients. Thus, it is considered the main cause of hyperexcitability. Albeit few drugs have received orphan drug status over the past years, pharmacoresistance remains the biggest challenge in the treatment of Dravet syndrome. Therefore, novel therapeutic strategies are urgently needed.

Characterization of a novel, conditional, *Scn1a*-A1783V knock-in mouse model confirmed an increased seizure susceptibility, behavioral and motor alterations and thus demonstrated excellent face validity for the further investigation of Dravet syndrome.

The untargeted proteomic screening displayed more pronounced changes following the onset of spontaneous seizures, dominated by the down-regulation of proteins involved in synaptic and glutamatergic signaling in the hippocampus of Dravet mice. The proteomic data was complemented by metabolome data that detected lower levels of glutamate and GABA in the hippocampus, suggesting a disturbed glutamate/GABA-glutamine cycle and an increased GABA:glutamate ratio. This can later be supported by GABAergic drugs.

A comparison of proteomic data to published data from animal models of acquired epilepsies revealed common molecular alterations between genetic and acquired epilepsies comprising proteins linked with synaptic plasticity, astrogliosis and angiogenesis.

Metabolomic screening of hippocampal tissue in Dravet mice showed pronounced alterations in energy metabolism and an impact of Dravet genotype on concentrations of several glycolysis and tricarboxylic acid (TCA) cycle intermediates. These changes in energy metabolism may contribute to seizure susceptibility and ictogenesis. Furthermore, they could explain the

therapeutic potential of a ketogenic diet, which aims to shift energy metabolism towards a more fat-based energy supply. This diet improved the motor deficits observed in Dravet mice.

Overall, the proteome and metabolome analysis in a mouse model of Dravet syndrome demonstrated complex molecular alterations in the hippocampus. Whether these alterations may contribute to hyperexcitability or, instead, represent a compensatory mechanism, will have to be confirmed by further investigations. The proteomic data indicated more complex pathophysiological mechanisms during the course of the disease, which should be considered in the management of Dravet syndrome. However, future studies investigating the functional relevance of the aforementioned molecular changes may confirm our data and provide valuable guidance on the development of novel therapeutic options.

# INTRODUCTION

## *1. Epilepsy: history and definition*

The mention of epilepsy and epileptic seizures dates back to the year 2000 B.C. and the Assyrian empire, where epilepsy and seizures were believed to be a manifestation of evil spirits. Over the centuries, these beliefs remained through other civilizations up until the ancient Greeks who called it a sacred disease. Hippocrates was the first to describe it as the medical condition known today, believing its cause originates in the brain. He named it the great disease, which would later become the globally accepted term for generalized seizures (*grand-mal*) (Magiorkinis et al., 2010).

According to The International League Against Epilepsy (ILAE), an epileptic seizure is defined as "a transient occurrence of signs and/or symptoms due to abnormal excessive or synchronous neuronal activity in the brain." (Fisher et al., 2005). Over the years, the exact definition of epilepsy has changed. Today, ILAE's practical clinical definition describes epilepsy as a brain disease including one of three conditions: (1) at least two unprovoked seizures occurring within a 24-hour interval; (2) one unprovoked seizure and high risk for recurrent seizures occurring within the next 10 years or (3) an epilepsy syndrome diagnosis (Fisher et al., 2014).

# *2. Dravet Syndrome*

## *2.1. Epidemiology*

Dravet syndrome is a rare, severe, lifelong form of epileptic encephalopathy that begins within the first year of life (Dravet, 2011). It is defined as a syndrome, due to its specific clinical picture and accompanying electroencephalogram (EEG) abnormalities (Scheffer et al., 2016). Previously known as Severe Myoclonic Epilepsy of Infancy (SMEI), Dravet syndrome was first described by doctor Charlotte Dravet in 1978 (Dravet, 2011), after whom it was later named. Besides frequent and/or prolonged seizures, the syndrome comprises of intellectual and motor disabilities, behavioral and developmental delays, poor immune responses etc. The worldwide Dravet syndrome prevalence is one in 40,000 individuals. Thus, the syndrome is listed as a rare disease (https://www.orpha.net/consor/cgi-bin/OC_Exp.php?Expert=33069&lng=EN, ORPHA: 33069).

## *2.2. Scn1a mutation*

Until 2001, it was not known that Dravet syndrome is caused by a genetic deficiency of the *Scn1a* gene in the majority of patients. The *Scn1a* gene encodes the $Na_V1.1$ sodium channel α subunit (Claes et al., 2001) that is widely expressed throughout the brain. It is localized to the cell body, dendrites and the initial axonal segments of fast-spiking parvalbumin-positive neurons (Ogiwara et al., 2007) and somatostatin-positive neurons (Tai et al., 2014). The channel is comprised of four homologous domains (I–IV), each consisting of six transmembrane segments (S1–S6) (Escayg and Goldin, 2010). Although numerous mutations in the *Scn1a* gene have been identified, most causing Dravet syndrome were found in the transmembrane region (Lossin, 2009). The current state of knowledge is that the mutation causes deficits in action potential firing of GABA inhibitory interneurons thus leading to abnormal excitability and encephalopathy (Catterall, 2018). Therefore, Dravet syndrome is also considered a channelopathy.

Over the years, increasing proportions of patients with Dravet syndrome tested positive for the *SCN1A* mutation, reaching a prevalence of over 80% (Rosander and Hallbook, 2015). Interestingly, mutations in the same gene can also provoke Generalized Epilepsy with Febrile Seizures Plus (GEFS+), usually linked to a missense *SCN1A* mutation and a milder clinical picture (Catterall et al., 2010; Meisler and Kearney, 2005). Furthermore, mutations causing the abnormal ion selectivity (segments S5, S6 and S5-S6 linker of $Na_V1.1$ channel) are more frequent in Dravet syndrome (Kanai et al., 2004). In Dravet patients, mutations in *SCN1A* mostly result in loss of function (Escayg and Goldin, 2010). While all *SCN1A* mutations are dominantly inherited (Escayg and Goldin, 2010), the majority of mutations in Dravet patients occur *de novo* (Poryo et al., 2017), frequently originating from the paternal chromosomes (Heron et al., 2010; Sun et al., 2010). Nonetheless, a large proportion of patients have a family history of epilepsy or febrile seizures, with or without *SCN1A* mutations (Dravet, 2011). Interestingly, truncating mutations found in 40-50 % of patients are associated with earlier seizure onset and a more severe phenotype (Zuberi et al., 2011). Slightly less abundant were missense (40%) and splice site mutations (0-10%). Interestingly, all inherited *SCN1A* mutations were missense (Connolly, 2016).

## *2.3. Disease phases*

The first disease phase is known as the “febrile stage” (Dravet, 2011). The initial seizure in Dravet patients occurs within the first year of life, mostly between 5 and 8 months of age. The seizures, most commonly thermally provoked by a hot bath, fever or vaccination, are clonic, unilateral or generalized and frequently prolonged (Dravet, 2011). Vaccination is reported as the trigger for the first seizure in more than 50 % of children (Tro-Baumann et al., 2011; von Spiczak et al., 2011). Although this link was thought to be due to a provoked fever, a shift towards a pro-inflammatory profile in Dravet patients has been demonstrated *in vitro* (Auvin et al., 2018). Nonetheless, disease progression is reported to be the same in patients whose first

seizure is not associated with vaccination (McIntosh et al., 2010). Prior to the first convulsive seizure, focal myoclonic jerking has been reported in some patients (Dravet, 2011).

Following the first seizure, repeated febrile or afebrile seizures usually occur once per month up until the end of the first year and frequently do not respond well to benzodiazepines (Gataullina and Dulac, 2017). Whilst diagnosis may point towards febrile seizures, the temperature of Dravet patients is not sufficiently high and seizures are clonic, unilateral, more frequent, prolonged and start at an earlier age (Dravet, 2011). The EEG remains normal for several years with prominent theta activity starting from the second year of life (Bureau and Dalla Bernardina, 2011).

Following the first year of life until the age of ten, the "worsening" or "catastrophic stage" takes place (Dravet, 2011). This phase is characterized by the onset of different types of seizures that are the hallmark of Dravet syndrome. Patients start experiencing myoclonic, atypical absence seizures, with or without loss of consciousness, and focal seizures sometimes with secondary generalization. Convulsions are still present and can progress into status epilepticus (SE). Tonic seizures are rarely present (Dravet, 2011; Gataullina and Dulac, 2017). During this stage, EEG abnormalities can be detected that can help diagnosis (Dravet, 2011). Hyperthermia remains a seizure trigger but other common epilepsy triggers also appear such as photosensitivity, noise, altered emotions etc (Dravet, 2011; Gataullina and Dulac, 2017).

After the sixth year of life, the "stabilization stage" begins characterized by reduced seizure frequency and duration (Dravet, 2011). Convulsive seizures frequently occur during sleep, absence and myoclonic seizures may disappear and focal seizures occur with a reduced density. Nevertheless, in several cases epileptic phenotype worsens even after the age of five (Dravet, 2011). Magnetic resonance imaging (MRI) during the stabilization stage does not show

structural abnormalities. However, within the second decade a global volume reduction of white and gray matter has been detected in several brain structures (Gataullina and Dulac, 2017).

## *2.4. Dravet syndrome phenotype*

In Dravet syndrome, it is thought that seizures themselves contribute to brain impairment and the development of cognitive, motor and behavioral alterations (Berg, 2011). Accordingly, cognitive and behavioral impairments are associated with seizure frequency (Brunklaus and Zuberi, 2014). However, nowadays this claim is rather challenged in epileptic encephalopathies where both seizure frequency and phenotype disturbances can be triggered by a particularly aggressive epileptogenic process (Avanzini et al., 2013). Preclinical studies have also pointed towards $Na_V1.1$ dysfunction in different brain regions affecting the complete phenotype in Dravet syndrome (Brunklaus and Zuberi, 2014). For instance, defects in the action potential firing of cerebellar GABAergic Purkinje cells are known to cause ataxia (Kalume et al., 2007).

In patients older than 5 years, whereafter seizures generally decline (Dravet, 2011), at least one bad phenotype outcome has been reported, with learning deficits being the most common, then speech and motor impairments, autism, attention deficit hyperactivity syndrome and other behavioral difficulties (Lagae et al., 2018).

### *2.4.1. Intellectual disability*

Cognitive deterioration is a hallmark of Dravet syndrome. Children develop normally in the first few months of life, showing the first deficits in the second or third year (Cassé-Perrot et al., 2001). However, pre-cognitive abilities such as vision, are affected even before the first seizure (Chieffo et al., 2011). Children show slower language development, with a stronger effect on speech production than on comprehension (Acha et al., 2015; Chieffo et al., 2016). Between 2 and 6 years of age, children develop dysarthria and poor articulation (Chieffo et al., 2016). Intellectual disability varies from mild to severe mental retardation accompanied by

different clinical symptoms. Teenagers with Dravet syndrome and milder retardation mostly show visuo-motor disabilities with preserved verbal skills, while moderately and severely retarded patients show pronounced cognitive decline (Olivieri et al., 2016). Some patients experience attention deficit hyperactivity disorder with hyperkinesia to the detriment of their learning abilities. Additionally, over 30 % of patients with Dravet syndrome exhibit autistic behaviors, with a higher prevalence of social reserve observed in male patients (Gataullina and Dulac, 2017; Villas et al., 2017).

Children who experience the early appearance of myoclonus, absence seizures and worse seizure control, show a poorer cognitive profile (Catarino et al., 2011; Ragona et al., 2011). As a consequence of the total seizure accumulation and poor pharmacoresponse, cognitive decline increases with age (Acha et al., 2015; Catarino et al., 2011). In line with this, speech alterations positively correlate with higher seizure frequency (Lagae et al., 2018).

### *2.4.2. Motor dysfunction*

Motor disabilities are frequently observed in Dravet patients. The symptoms seem to deteriorate with age. The first clinical sign of motor disabilities is the delayed onset of independent sitting and walking by 3 and 8 months on average, respectively (Gitiaux et al., 2016; Verheyen et al., 2019). Up to the age of six, gait is frequently described as normal or with possible hypermobility and ataxia (Gitiaux et al., 2016; Rodda et al., 2012). Most patients develop a crouched gait following 6 years of age which worsens during adolescence (Gitiaux et al., 2016; Rilstone et al., 2012; Rodda et al., 2012; Wyers et al., 2019). This is characterized by hip and passive knee flexion extension, lateral tibial torsion and feet planoabductovalgus (Gitiaux et al., 2016). Additionally, ataxia and spasticity progress with age (Gataullina and Dulac, 2017; Rodda et al., 2012) while parkinsonian gait, antecollis and extrapyramidal signs are frequently observed in adults (Aljaafari et al., 2017; Fasano et al., 2014). Overall, motor disabilities in Dravet patients

vary, ranging from mild motor impairments to immobility and the need for a wheelchair (Rodda et al., 2012).

Though frequent seizures can worsen gait and ataxia, there is a strong connection between gait disturbances and *SCN1A* mutations in patients with Dravet syndrome. Namely, $Na_V1.1$ channels located on nodes of Ranvier and the initial axonal segment are crucial for the electrical outputs of neurons. Their dysfunction could explain motor deficits, gait disturbance and crouching in Dravet syndrome (Duflocq et al., 2008). Additionally, the impact of these channels' dysfunction on the basal ganglia is linked to parkinsonian features. Severe *SCN1A* deficiency is linked to an earlier onset of symptoms in children (Aljaafari et al., 2017). Importantly, these patients showed a good response to levodopa treatment (Fasano et al., 2014). Lastly, data from animal models imply the role of impaired GABAergic firing of Purkinje cells as a mechanism of ataxia (Kalume et al., 2007; Ogiwara et al., 2007; Yu et al., 2006).

### *2.4.3. Sleep disturbances*

Sleep disturbances are frequently reported by caregivers of patients with Dravet syndrome (Gataullina and Dulac, 2017; Villas et al., 2017). They are considered a risk factor for nocturnal seizures, which occur more frequently after the age of 10 (Dravet and Oguni, 2013). Patients usually experience difficulties with initiating and maintaining sleep, sleep-wake transitions and sleep breathing (Licheni et al., 2018; Schoonjans et al., 2019). Excessive somnolence and daytime sleepiness are consequences of these disturbances. Melatonin has shown some beneficial effect on sleep initiation and maintenance, contributing to a better quality of life (Myers et al., 2018).

While data from humans do not provide information about circadian rhythm, preclinical models indicate that it may be impaired in Dravet syndrome. Patients show a fragmented rhythm of non-rapid eye movement (NREM) sleep and a prolonged circadian period (Sanchez et al.,

2019). Interestingly, $Na_V1.1$ channels are located in the suprachiasmatic nucleus, whose dysfunction could explain the slow EEG background rhythm and sleep impairments starting from the second year of life (Gataullina and Dulac, 2017). Moreover, in a mouse model of Dravet syndrome, an imbalance between excitatory and inhibitory neurons in the thalamic ventrobasal and reticular nucleus could further delay the onset and maintenance of sleep (Kalume et al., 2015b).

#### *2.4.4. Other symptoms of Dravet syndrome*

Caregivers frequently report problems with thermoregulation, overheating and insufficient sweating in patients with Dravet syndrome, altogether increasing the risk of thermally provoked seizures. Furthermore, Dravet patients frequently suffer from slowed growth, digestion issues and constipation (Skluzacek et al., 2011). Osteopenia and increased fracture risk are mentioned as major concerns in drug-resistant epilepsy (Connolly, 2016). Additionally, a poor immune response with frequent respiratory and urinary tract infections is another concern in Dravet patients (Skluzacek et al., 2011). Cardiovascular irregularities are also observed in some patients (Skluzacek et al., 2011).

## *2.5. Sudden unexpected death in epilepsy*

Dravet syndrome has a high rate of premature death ranging from 3.1 to 20.8 % (Connolly, 2016). Children from 3 to 7 years of age seem to have the highest death incidence (Sakauchi et al., 2011). Sudden unexpected death in epilepsy (SUDEP) is known as the leading cause of death, explaining over 50 % of mortalities in patients with Dravet syndrome (Sakauchi et al., 2011; Skluzacek et al., 2011). SUDEP is defined as sudden, unexpected death in patients suffering from epilepsy when no other disease, drowning or injury can be considered causative. It may occur with or without confirmed seizures, but status epilepticus (SE) does not precede the death (Nashef et al., 2012). In Dravet syndrome, the risk of SUDEP is roughly 15 times higher than in other childhood epilepsies (Skluzacek et al., 2011). Besides SUDEP, SE and

accidents with drowning are the next leading causes of death (Connolly, 2016; Sakauchi et al., 2011). The exact mechanism of SUDEP is not yet fully understood but current data from patients imply a role of peri-ictal respiratory dysfunction leading to central apnea, bradycardia and heart arrest (Kim, 2017). Heart rate variability has also been shown to be a biomarker of SUDEP in some patients (Myers et al., 2018). Further research in Dravet patients is still necessary to establish the exact mechanisms behind SUDEP and validate the findings from animal models.

## *2.6. Diagnosis*

Today, according to the 2017 consensus of North American neurologists with expertise in Dravet syndrome (Wirrell et al., 2017), the diagnosis of the syndrome is purely clinical using the following criteria:

- typical disease onset within the first year of life, on average 5.2 months (Cetica et al., 2017; Wirrell et al., 2017)
- children experience recurrent convulsive or hemiconvulsive seizures, which are frequently prolonged
- myoclonic seizures appear by the age of two, followed by obtundation status, focal seizures with loss of consciousness and atypical absence seizures
- patients are susceptible to thermally provoked seizures with fever, vaccination and warm baths as the most frequent triggers
- photosensitivity, eating, and bowel movements are observed as potential seizure triggers
- children develop normally until disease onset
- sodium channel agents are contraindicated and may exacerbate seizures

In older children and adults the clinical picture consists of:

- persistent seizures with less frequent and obvious SE over time
- decreased sensitivity to hyperthermia over time

- intellectual disability presenting between 18 and 60 months
- motor impairment: crouch gait, lack of coordination and muscle tonus, impaired physical dexterity
- normal MRI with mild generalized atrophy and/or hippocampal sclerosis
- EEG potentially showing diffuse background slowing with multifocal and/or generalized interictal discharges

## *3. Animal models*

A major step in filling the gaps in knowledge about Dravet syndrome was the development of an animal model back in 2006 (Yu et al., 2006). Today, there are several other models accessible to a broad scientific community that have improved our understanding of the pathophysiological mechanisms underlying the disease, providing a solid foundation for the development of novel treatment candidates in Dravet syndrome.

Following the discovery of *SCN1A* deficiency in Dravet children, the exact mechanism of epileptogenesis was explained using an *Scn1a* knock-out mouse model (Ogiwara et al., 2007; Yu et al., 2006). These studies elucidated why a loss of function mutation in sodium channels leads to seizures by showing that the mutation reduces sodium currents and neuronal firing of GABAergic hippocampal interneurons, leading to general hyperexcitability and a lower seizure threshold (Ogiwara et al., 2007; Yu et al., 2006).

Whilst Dravet mutations are present from birth, both mice and humans only experience the first seizure later in life. The reason behind this phenomenon was clarified in an animal model of Dravet syndrome (Cheah et al., 2012). Namely, the expression of $Na_V1.1$ channels is low at birth and increases with age. On the contrary, the expression of $Na_V1.3$ sodium channels declines with age in mice, reaching the lowest expression levels around 3 weeks of age, corresponding to weaning age. Over these 3 weeks, $Na_V1.1$ deficits in Dravet mice are rescued by an up-regulation of $Na_V1.3$ channels in hippocampal interneurons. Thus, the natural decrease in $Na_V1.3$ expression along with the failure of $Na_V1.1$ channels to replace their function defines the starting point for developing Dravet syndrome, characterized by the disinhibition of neuronal circuits, seizures, and other comorbidities (Cheah et al., 2013). Importantly, the same pattern was noted in humans, showing that the decline of $Na_V1.3$ and the increase of $Na_V1.1$ expression at the age of 5-6 months corresponds to the approximate age of seizure onset in Dravet patients (Cheah et al., 2013).

In addition to neuronal hyperexcitation, the $Na_V1.1$ channelopathy was linked to motor deficits including ataxia. Experimental proof came from homozygous *Scn1a*$^{-/-}$ mice, which related to the lack of $Na_V1.1$-positive cerebellar Purkinje cells, exhibit impaired firing of Purkinje cells and severe ataxia (Ogiwara et al., 2007; Yu et al., 2006).

Similarly, a selective $Na_V1.1$ deletion and impaired GABAegic neurotransmission in the prefrontal cortex was linked to autistic-like behavior and spatial learning and memory deficits in Dravet mice. Low-dose clonazepam fully rescued these social and cognitive deficits in Dravet mice, thus demonstrating impaired GABAergic neurotransmission as a cause of *Scn1a* haploinsuficiency (Han et al., 2012). Furthermore, another study has shown that the selective blockade of $Na_V1.1$ channels in the basal forebrain region leads to learning and memory impairment but no spontaneous seizures (Bender et al., 2013). These findings suggest that impaired GABAergic neurotransmission may not only lead to seizure protection but also to improved behavioral and motor phenotypes in patients.

Great progress has been made in understanding the mechanism of SUDEP using animal models of Dravet syndrome. Video monitoring of *Scn1a* heterozygous knock-out mice observed SUDEP shortly after generalized tonic-clonic seizures (Kalume, 2013). Moreover, the study showed that SUDEP is triggered by increased parasympathetic activity following tonic-clonic seizures, resulting in ventricle electrical dysfunction and lethal bradycardia (Kalume, 2013).

On the other hand, a high rate of seizure-related respiratory difficulties including hypoventilation and apnea have been reported in most witnessed SUDEP cases, listing it as a possible cause of SUDEP. Additionally, patients who suffered from SUDEP reported impaired respiratory function throughout earlier seizures (Kalume, 2013; Langan, 2000). A recent study in Dravet mice expressing an *Scn1a* mutation demonstrated disordered breathing comprised of hypoventilation, apnea and diminished $CO_2$ ventilatory response. Hypoexcitability of inhibitory

brainstem neurons and hyperexcitability of glutamatergic chemosensitive neurons, responsible for the $CO_2/H^+$ ventilatory response, were observed in the retrotrapezoid nucleus of Dravet mice. This has therefore been proposed as a possible underlying mechanism in SUDEP (Kuo et al., 2019).

Lastly, animal models of Dravet syndrome used in preclinical drug discovery and development studies have been instrumental in the licensing of new therapeutics for Dravet syndrome. For instance, some preclinical studies in Dravet animal models provided critical evidence for the efficacy and tolerability of cannabidiol, stiripentol and fenfluramine (Cao et al., 2012; Kaplan et al., 2017; Zhang et al., 2015) facilitating their approval for the treatment of Dravet syndrome in subsequent years. Similarly, the efficacy of a ketogenic diet in seizure protection and reducing susceptibility to SUDEP was confirmed in mouse models of Dravet syndrome (Dutton et al., 2011; Teran et al., 2019). More details are provided in the following section.

## *4. Current therapeutic options in the treatment of Dravet syndrome*

Currently, the treatment of Dravet syndrome remains very challenging. Medication has to be tailored to the types of seizures which demonstrate great interpatient variability. During the "febrile" stage, the aim of therapy is to prevent prolonged seizures including SE, which frequently require medical intervention (Knupp and Wirrell, 2018). During the "worsening" phase, patients require better control of nonconvulsive seizures, which can further contribute towards cognitive decline (Ragona, 2011; Ragona et al., 2011). During the "stabilization" phase, the focus of therapy is to reduce convulsive nocturnal seizures which are a great risk factor for SUDEP (Genton et al., 2011; Knupp and Wirrell, 2018).

Most patients with Dravet syndrome have an *SCN1A* sodium channel mutation. The use of sodium channels agents is therefore strongly contraindicated as they may exacerbate seizures. Moreover, truncating mutations in *SCN1A* gene can serve as biomarkers predicting a bad prognosis to sodium channel blockers (Weber et al., 2014). Thus, carbamazepine, oxcarbazepine, phenytoin, lamotrigine and rufinamide should be avoided in the treatment of Dravet syndrome. Additionally, an irreversible inhibitor of GABA aminotransferase (vigabatrin) should be avoided due to its proconvulsant effect in Dravet patients (Knupp and Wirrell, 2018).

### *4.1. Stiripentol*

In 2007, Stiripentol (Diacomit) was the first drug approved for the treatment of Dravet patients (older than 2 years) in the European Union (EU). Approved as an add-on medication in combination with clobazam or valproate, stiripentol is indicated for the treatment of generalized tonic-clonic seizures (EU/3/01/071). Recently, the Food and Drug Administration (FDA) also approved its use in the United States if combined with clobazam (reference ID: 4309499).

Stiripentol is a novel drug that is structurally different from other antiepileptic drugs. There are several proposed mechanisms of action. Stiripentol enhances GABAergic neurotransmission by increasing $GABA_A$ receptor activity (Fisher, 2011). Due to its effect on α4- and δ-containing $GABA_A$ receptors, it does not lose efficacy during prolonged SE as a consequence of receptor internalization (Grosenbaugh and Mott, 2013). Additionally, stiripentol inhibits lactate dehydrogenase leading to neuronal hyperpolarization (Sada et al., 2015) and blocks calcium- and sodium-channel mediated neurotoxicity (Verleye et al., 2016). It must be considered that stiripentol interacts with CYP2C19 and CYP3A4, thus affecting the pharmacokinetics of other drugs such as clobazam and valproate (Chiron, 2005; Jogamoto et al., 2017). Therefore, it is necessary to adjust its dose when used in combination with other antiseizure drugs.

The first randomized placebo-controlled clinical studies demonstrated stiripentol's efficacy in the treatment of Dravet syndrome, with 67 and 71 % of patients exhibiting a reduction in the frequency of convulsive seizures by more than 50 %, compared to 9 and 5 % observed in the placebo groups (Chiron, 2007; Chiron et al., 2000). Further studies confirmed its efficacy for generalized tonic-clonic and focal seizures (Myers et al., 2018) as well as for the prevention of SE (Buck and Goodkin, 2019). It is considered a safe therapeutic, with anorexia and somnolence as the most common adverse events (Buck and Goodkin, 2019).

## *4.2. Cannabidiol*

Cannabinoids or derivatives of *Cannabis sativa* have been used for centuries in herbal medicine to treat epilepsy. The story of Charlotte Figi, a girl with Dravet syndrome, whose seizures almost completely disappeared with cannabidiol-enriched extract attracted a lot of media attention (Maa and Figi, 2014). As one of the dominant non-psychoactive components in cannabis, cannabidiol has been widely used in children with Dravet syndrome and reported as very promising by their parents (Porter and Jacobson, 2013). Preclinical studies confirmed its efficacy in both seizure management and improving social deficits (Kaplan et al., 2017). A

double-blind, placebo-controlled clinical study showed that cannabidiol reduces seizures by ≥ 50 % in 43 % of Dravet patients, as compared to 27 % observed in the placebo group (Devinsky et al., 2018b). Furthermore, seizure frequencies of all but non-convulsive seizures were reduced and the treatment was well tolerated. Diarrhea, fatigue, somnolence, decreased appetite and elevated liver transaminases were the most common adverse events (Devinsky et al., 2018b).

The proposed mechanism of action is the modulation of intracellular calcium and adenosine uptake by antagonizing GPR55-mediated increased excitotoxicity, desensitizing TRPV1 channels and inhibiting nucleoside transporters (ENT1) (Nichol et al., 2019). Cannabidiol can strongly increase the concentration of clobazam and its active metabolite when applied together (Geffrey et al., 2015). Thus, dose optimization should be kept in mind.

In 2019, cannabidiol (Epidiolex) was the first drug approved by the FDA as a single-use therapy for Dravet patients older than 2 years, thus receiving orphan drug designation (https://www.centerwatch.com/directories/1067-fda-approved-drugs/listing/3466-epidiolex-cannabidiol; ID: 4282447). A year later, cannabidiol was also approved by the EU as an add-on therapy (EU/3/14/1339).

## *4.3. Fenfluramine*

The most recent drug to receive orphan drug designation for the treatment of Dravet syndrome is fenfluramine. The drug was approved for the treatment of patients over 2 years of age by the FDA (reference ID: 4631810) and as an add-on therapy by the European Medicines Agency (EMA) (EU/3/14/1219).

Fenfluramine is an amphetamine derivate, previously registered as an appetite suppressor in the treatment of obesity. Its frequent combination with the monoamine oxidase inhibitor phentermine, raised pulmonary hypertension (Douglas et al., 1981). Later on, severe cardiovascular adverse events were observed, leading to its withdrawal from the market

(Connolly et al., 1997; Gardin et al., 2000). Nevertheless, a great improvement was observed in seizure control in patients with self-induced epilepsy, among which were patients with Dravet syndrome. The drug was further examined in lower doses (Schoonjans et al., 2015). In comparison to up to 120 mg/day used for appetite suppression, fenfluramine was tested in doses under 1 mg/kg/day, thus minimizing risk for cardiac side effects (Knupp and Wirrell, 2018). Additionally, Belgian Dravet patients were continuously treated with fenfluramine (10-20 mg/day) over 28 years with no signs of cardiac valve disease or pulmonary hypertension, thus providing the first valid safety data in Dravet patients (Schoonjans et al., 2017). A recent long-term open-label study further confirmed this finding (Lai et al., 2020).

Whilst the exact mechanism of action is still unclear, it is know that fenfluramine hydrochloride is a serotonin 5HT-2 receptor agonist that inhibits serotonin transporters thereby increasing extracellular serotonin availability (Knupp and Wirrell, 2018). Recent findings demonstrated that fenfluramine also acts as a positive allosteric modulator of sigma-1 receptors (Martin et al., 2020).

Two double-blind placebo-controlled randomized clinical trials provided crucial data for fenfluramine's approval. The first study showed a clinically relevant seizure frequency reduction (≥ 50 %) in 74.9 % of patients treated with fenfluramine hydrochloride as compared to 19.2 % observed in the placebo group (Lagae et al., 2019). Additionally, compared to placebo, the monthly convulsive seizure frequency was reduced by 62.3 % and 32.4 % with 0.7 and 0.2 mg/kg/day fenfluramine hydrochloride, respectively (Lagae et al., 2019). The other study confirmed its clinical efficacy by reducing monthly convulsive seizure frequency (≥ 50 %) in 54 % of patients as compared to 5 % in the placebo group (Nabbout et al., 2020). The main adverse effects were decreased appetite and body weight, diarrhea, fatigue, pyrexia, lethargy and somnolence (Lagae et al., 2019; Nabbout et al., 2020).

## *4.4. Other antiseizure drugs*

While medicating Dravet patients remains very individualized, several standard antiepileptic drugs have shown promising effects. As first-line therapeutics, valproic acid and clobazam are commonly used (Wirrell et al., 2017). The efficacy of these drugs individually has not shown promising results and so they are frequently combined with second-line therapeutics such as stiripentol and topiramate. Bromides, zonisamide, levetiracetam, phenobarbital or clonazepam serve as third-line therapeutics (Knupp and Wirrell, 2018; Wirrell et al., 2017). In addition, ethosuximid can be used for the treatment of absence seizures (Wirrell et al., 2017).

Buccal or rectal benzodiazepines are indicated in persistent seizures lasting more than 5 minutes, while intravenous benzodiazepines are indicated in the case of SE (Gataullina and Dulac, 2017). According to ILAE, "Tonic-clonic SE is a condition resulting either from the failure of the mechanisms responsible for seizure termination or from the initiation of mechanisms which lead to abnormally prolonged seizures (> 5 minutes). It is a condition that can have long-term consequences if lasting over 30 minutes." Importantly, after frequent usage tolerance to benzodiazepines can develop due to $GABA_A$ receptor internalization (Hu and Ticku, 1994).

## *4.5. Adjunctive therapy*

Although a variety of drugs are available for Dravet patients, the results of individual drug trials are often disappointing. Thus, doctors frequently prescribe adjunctive therapies, among which a ketogenic diet is commonly used. Both the traditional and modified ketogenic diets are commonly prescribed as second-line treatments (Wirrell et al., 2017). The diet consists of a high fat to carbohydrate and fat to protein ratio (3:1 to 4:1 respectively), thereby replacing glucose with ketone bodies as the main fuel in the central nervous system (Knupp and Wirrell, 2018).

Vagal nerve stimulation is another treatment option. The left cervical vagus nerve is stimulated with electrical impulses through a stimulator device consisting of a helical electrode connected to a pulse generator. The device emits electrical signals to the brainstem, which further sends signals to certain areas in the brain. The treatment has shown encouraging results, reducing seizures by more than 50 % in 52.9 % of Dravet patients (Dibué-Adjei et al., 2017). Currently, it is considered as a third-line treatment in Dravet patients (Wirrell et al., 2017). The right vagal nerve should be avoided except in specific circumstances since its innervation of the sinoatrial node could provoke bradycardia, asystole and further cardiac side effects (Giordano et al., 2017).

Corpus callosotomy and temporal lobectomy (in cases of temporal sclerosis) have been tested in a small number of Dravet patients. However, the success of these procedures was rather limited with more than 50 % seizure reduction achieved only in single patients (Dlouhy et al., 2016; Wirrell et al., 2017).

### *4.6. Polytherapy*

Although there are several therapeutic options available, polytherapy seems to be predominantly prescribed in Dravet patients of which 40 % use three and 25 % use four different antiepileptic drugs (Aras et al., 2015). In Europe, the most frequently prescribed antiseizure drugs are valproate, clobazam, topiramate, and stiripentol, used by 86, 55, 44, and 42 % of patients with Dravet syndrome, respectively (Brigo et al., 2018). Moreover, a combination of stiripentol, clobazam and valproate was the most commonly used combination, prescribed in 29 % of patients (Brigo et al., 2018).

The main challenge in Dravet syndrome is the achievement of seizure-freedom. Over time, certain algorithms for its treatment have been developed, such as the current one proposed by the North American Consensus Panel shown in Figure 1 (Wirrell et al., 2017).

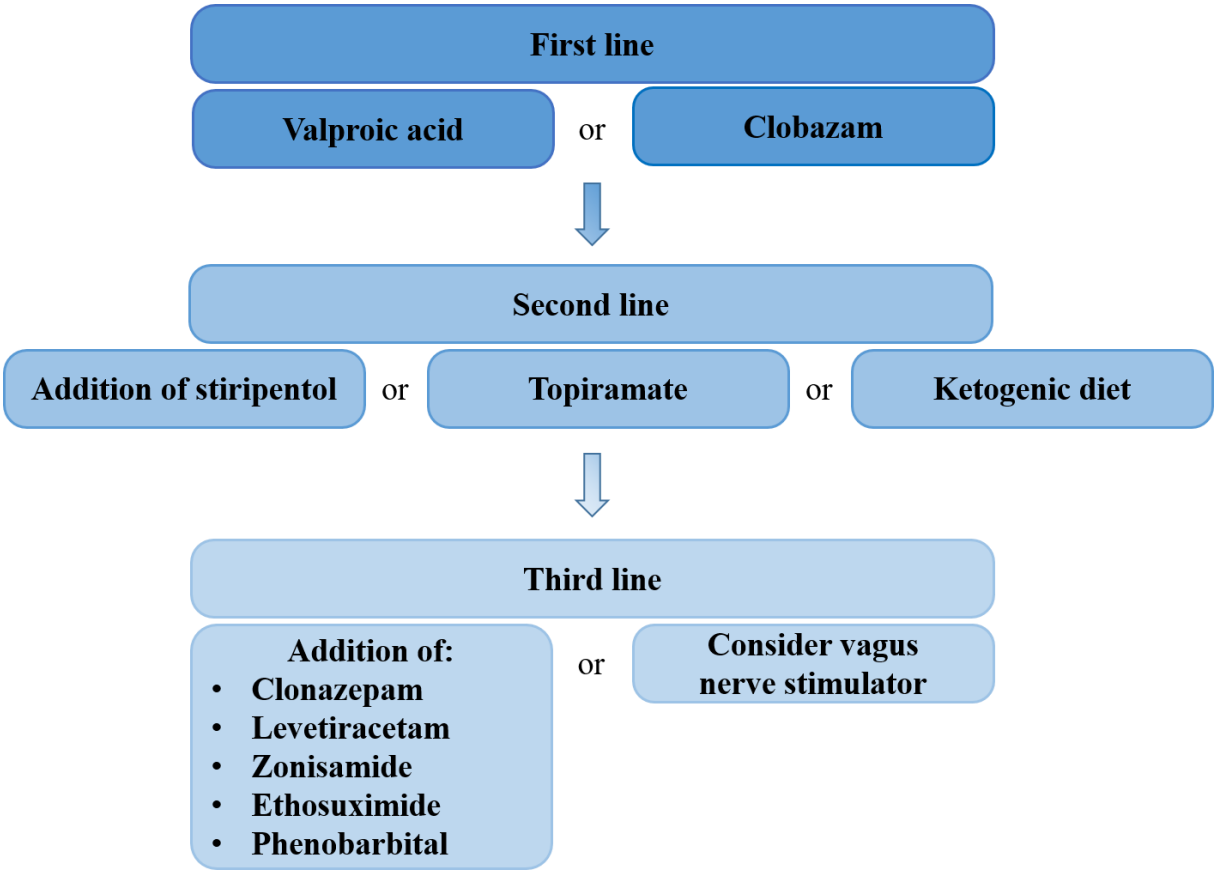


**Figure 1.** Algorithm for the treatment of Dravet syndrome proposed by the North American Consensus Panel. Adapted from Wirrel et al., 2017.

# *5. Ketogenic diet*

## *5.1 Origin and subtypes*

Fasting has been implemented in human medicine to treat epilepsy since at least 500 BC. It was also the only therapeutic measure mentioned in the Hippocratic collection (Wheless, 2008). Several centuries later, fasting appeared in the bible as a therapy for seizures, believed to be a demonic possession. The bible states that Jesus recommended fasting along with praying for curing convulsing demon possession (Wheless, 2008).

In 1921, an important observation was made. Specifically, both starvation and a diet with high-fat and low-carbohydrate content resulted in increased β-hydroxybutyrate and acetone production, today recognized as ketone bodies along with acetoacetate (Peterman, 1924; Woodyatt, 1921). In the same year, the ketogenic diet was offered to epileptic patients as a substitution for fasting (WILDER, 1921). Even though the diet showed promising effects with improvements in both seizure and behavioral outcomes, it was placed aside for decades due to the discovery of antiseizure drugs in the late 1930s (Wheless, 2008). In 1997, a captive television drama about a two-year-old boy, Charlie, suffering from intractable generalized seizures who became seizure-free following the introduction of a ketogenic diet over the next 5 years, placed the scientific focus back on the ketogenic diet (Wheless, 2008). Numerous studies have been executed, leading to the discovery of the emerging role of the diet, not only in epilepsy, but also in other diseases (Freeman et al., 2007). Today, a ketogenic diet is the first choice in the treatment of glucose transporter deficiency syndrome (Glut1DS) and pyruvate dehydrogenase deficiency (PDHD) and second choice in the treatment of Dravet syndrome. In addition, it may be one of the early choices in the treatment for epilepsy with myoclonic-atonic seizures, febrile infection-related epilepsy syndrome (FIRES), Angelman syndrome, infantile spasms, and tuberous sclerosis complex (Kossoff et al., 2018).

Currently, there are four different types of ketogenic diet. The classical, traditional diet is defined by a 3:1 to 4:1 mass ratio of fats to combined carbohydrates and proteins. On average, about 90 % of calories are ingested from fats. The medium chain triglyceride diet is based on the consumption of more ketogenic oil, which due to its shorter chains of fatty acids allows more carbohydrates in the diet. The low glycemic index diet allows an increased intake of low glycemic index carbohydrates, leading to a lower calorie intake from fats (around 60 %). Finally, the modified Atkins diet is based on greater food variety, yet carbohydrates are limited to only 10-20 g per day (Knupp and Wirrell, 2018).

Overall, the ketogenic diet is generally well tolerated in patients. Hypoglycemia, hyperlipidemia, acidosis, dehydration, lethargy, gastrointestinal symptoms, weight loss and kidney stones are the main side effects (Tian et al., 2019).

## *5.2. Mechanism of action in epilepsy management*

The exact mechanism underlying the anticonvulsive effects of the ketogenic diet remains a mystery. Although several hypotheses have been proposed, it seems like the ketogenic diet targets multiple pathophysiological mechanisms that can contribute to neuronal hyperexcitability (Rho, 2017).

For instance, ketone bodies demonstrated a direct anti-seizure effect in several animal models (Likhodii et al., 2003; Rho et al., 2002). In addition, ketone bodies can indirectly affect neurotransmission by increasing GABA and adenosine levels (Masino et al., 2012; Yudkoff et al., 2005), activating ATP-sensitive potassium channels (Rho, 2017), enhancing mitochondrial biogenesis and reducing oxidative stress (Bough et al., 2006; Rowley and Patel, 2013).

Furthermore, the ketogenic diet reduces glycolysis by switching the cell's metabolism to a more fat-based energy supply including fatty acids and ketone bodies (Masino and Rho, 2012). Additionally, it increases the level of neuroprotective polyunsaturated fatty acids (Michael-

Titus and Priestley, 2014). Modulation of the tricarboxylic cycle by refilling its intermediates with acetyl-CoA produced from the oxidation of ketone bodies or fatty acids and increasing ATP production, represents another possible anti-seizure mechanism of the ketogenic diet (Rho, 2017). The diet is indicated in patients with pyruvate dehydrogenase deficiency, the enzyme that converts pyruvate to acetyl-CoA. This deficiency limits cell bioenergetics, which can be compensated for by using ketone bodies for the direct synthesis of acetyl-CoA and enhancement of the TCA cycle (Wexler et al., 1997).

As previously mentioned, the ketogenic diet is also indicated in patients with Glut1 deficiency. GLUT-1 transports glucose across the blood-brain barrier and its deficiency causes brain hypoglycemia that is associated with infantile seizures, acquired microcephaly, ataxia and spasticity. The ketogenic diet provides ketone bodies as an alternative brain fuel. They have the ability to enter the brain via the monocarboxylic acid transporter (Koch and Weber, 2019).

### *5.3. Ketogenic diet for the treatment of Dravet syndrome*

Evidence for the efficacy of the ketogenic diet in the treatment of Dravet syndrome is constantly emerging. Several studies presented promising results by showing a diet response rate with ≥ 50 % in seizure reduction in 52-77 % of patients. The outcome largely depended on the length of treatment. The effect was observed for all seizure types including generalized convulsions, hemiconvulsions, myoclonic seizures, atypical absence seizures, and status epilepticus (Caraballo, 2011; Dressler et al., 2015; Laux and Blackford, 2013; Nabbout et al., 2011; Tian et al., 2019; Yan et al., 2018). In addition, EEG abnormalities showed an improvement, especially in patients with better seizure protection (Caraballo, 2011). Furthermore, a significant improvement in cognition, language production, hyperactivity, attention and motor function was observed (Laux and Blackford, 2013; Nabbout et al., 2011; Tian et al., 2019; Yan et al., 2018) altogether implying that a ketogenic diet can greatly improve the quality of life in Dravet patients. In line with this finding, some patients with no relevant impact on seizures

continued the diet because of its positive behavioral and cognitive effects (Nabbout et al., 2011). Aditionally, fewer antiseizure drugs were prescribed with the application of the diet (Caraballo, 2011; Yan et al., 2018). Overall, the diet was well tolerated among patients and the main reason for termination was lack of efficacy.

Adverse events arising during the first 2 weeks of the diet application are usually transient. They include hypoglycemia, ketosis, irritability, lethargy, lack of appetite and gastrointestinal symptoms (Yan et al., 2018). During diet maintenance, the main side effects comprise gastrointestinal symptoms (severe vomiting, constipation and diarrhea) and metabolic disorders (transitory anorexia, hyperlipidemia, acidosis) (Caraballo, 2011; Nabbout et al., 2011; Tian et al., 2019; Yan et al., 2018). With adjustments of the diet, some of the side effects like kidney stones, liver dysfunction and gastrointestinal symptoms were reduced to a tolerable level (Tian et al., 2019). The diet also showed advantages over pharmacological treatments including fewer neurotoxic adverse events such as lethargy, behavioral and cognitive symptoms (Laux and Blackford, 2013).

Lastly, the ketogenic diet has been compared to other antiseizure drugs in Dravet syndrome. Surprisingly, it proved to be equally or more efficacious in seizure reduction than antiseizure drugs, including the gold standard combination of clobazam, stiripentol and valproate (Dressler et al., 2015).

As a result, the ketogenic diet is proposed as an alternative treatment strategy in Dravet patients who did not reach sufficient improvement in seizures profile with three to four different antiseizure drugs (Cross et al., 2019; Wirrell et al., 2017). The traditional ketogenic diet is indicated for children under 2 years of age, the traditional or modified Atkins diet for children between 2 and 12 years, and a modified Atkins diet for children over 12 years of age (Wirrell et al., 2017).

## *5.4. Ketogenic diet for other indications*

Over the last 20 years, the potential of the ketogenic diet in the treatment of other disorders has been established. The diet seems to be protective in many neurodegenerative disorders due to the improvement of mitochondrial function. For instance, impaired activity of mitochondrial complex I in Parkinson's disease is assumed to be associated with the death of substantia nigra dopaminergic neurons and the development of motor symptoms. Ketone bodies are hypothesized to replace glucose as an energy source and therefore bypass the dysfunctional mitochondrial complex I (Barañano and Hartman, 2008). In Alzheimer's disease, ketone bodies are postulated to overcome amyloid-induced pyruvate dehydrogenase and GLUT deficiency, mitochondrial dysfunction, and possibly protect against extracellular amyloid-β deposition (Barañano and Hartman, 2008; Paoli et al., 2014). Moreover, the ketogenic diet has been linked to the preservation of motor function in amyotrophic lateral sclerosis, possibly by increasing mitochondrial ATP production or reducing cell oxidative stress (Barañano and Hartman, 2008). Lastly, it has demonstrated protective effects in brain trauma and ischemia, possibly because ketones are the preferred energy source in an injured brain (Prins, 2008).

The ketogenic diet also caused a marked improvement in the treatment of autism-spectrum disorders, depression, migraine and narcolepsy. However, the disease-modifying mechanisms remain unknown (Barañano and Hartman, 2008).

The diet has also proved efficacious in the management of some metabolic diseases including phosphofructokinase deficiency and McArdle disease, with a specific glycogen phosphorylase deficiency, by improving energy deficits and switching to an alternative energy source (ketone bodies). In addition, the diet has been successful in the treatment of diabetes mellitus type 2, obesity and metabolic syndrome. By restricting carbohydrate ingestion, glycemic control is increased therefore reducing variations in insulin concentration and increasing fats beneficial for reducing a risk of cardiovascular diseases (Accurso et al., 2008).

Interestingly, the ketogenic diet may also play a role in the treatment of cancer. The underlying mechanism may comprise a lower metabolic flexibility of malignant cells, which cannot equally adjust to ketones as a novel energy substrate in comparison to normal cells (Seyfried and Mukherjee, 2005). In contrast to glucose, ketone bodies cannot produce essential products for the growth of proliferative cells, thus resulting in restricted tumor growth (Deberardinis et al., 2008).

# *6. Omics techniques*

## *6.1. Definition, application, benefits and limitations*

Over the past decades, the investigation of cellular and subcellular processes in different pathologies has become available using a range of new techniques, including "Omics" techniques. The beginning of the "Omics" era tracks back to 2003, when the entire human genome was sequenced as part of the human genome project (HGP). "Omics" comprises branches of science based on novel technologies for high-throughput biomolecular analysis, which enables simultaneous quantification of up to thousands of molecules at different cellular function levels (Vasilopoulou et al., 2016). The main aim of "Omics" is to fully characterize and quantify pools of biological molecules, thus gathering knowledge about the complete network of genes and gene products in a biological system (Vidal et al., 2011). Therefore, instead of regular hypothesis-driven studies, these studies are exploratory and knowledge-based systemic investigations. All "Omics" techniques share a name ending with the same suffix -omics, such as proteomics, genomics, metabolomics etc.

The central nervous system represents one of the most complex networks in the human body, due to various synergistic and complementary interactions between different brain regions. In order to fully understand its architecture and function, a systemic investigation with comprehensive brain function mapping combined with should be used and the high-throughput quantitative approaches of "Omics" studies could provide a valuable contribution (Vasilopoulou et al., 2016). Among these, connectomics are already widely used for mapping neuronal connections (Lichtman et al., 2014) whilst proteomics, transcriptomics and metabolomics are used for molecular fingerprinting showing proteins, genes and metabolites profiles, respectively (Geschwind and Konopka, 2009). Altogether, these data could advance our current state of knowledge and identify novel disease biomarkers and diagnostic tools as well as lead to the discovery of personalized medicine approaches (Vasilopoulou et al., 2016).

Proteomic profiling is comprised of complete proteome characterization looking at protein structure, function, expression, interaction and any kind of modifications (Domon and Aebersold, 2006). It provides comprehensive information about gene function and is considered the most valuable dataset for biological system characterization. In contrast to transcriptomics, which relies on mRNA expression, proteomic profiling measures proteins that are biological function effectors, thus capturing not only their expression, but also any proteome modifications due to the cellular response to any perturbation at the protein activation level and downstream consequences of gene expression regulation (Cox and Mann, 2007).

Metabolomics is the newest "Omics" discipline. It detects and quantifies free metabolites with a low molecular weight. As the metabolite concentration depends on metabolic reactions, the profiling provides a metabolic physiology fingerprint and information about *in vivo* enzymatic activity and regulation. In contrast, other screening techniques like transcriptomics or proteomics, only capture current gene or protein expression without quantification of the ongoing biochemical processes leading to those changes (Hollywood et al., 2006; Kanani et al., 2008; Patti et al., 2012). Metabolomic screening is particularly relevant for brain research, where it combines molecular biology and neurophysiology, thus giving a completely new insight into systems biology (Vasilopoulou et al., 2016).

While this area of research can provide extensive information about early disease diagnosis and monitoring, detection of disease biomarkers and novel drug target molecules, the main limitations of these technique remain to be the reproducibility and higher costs (Vasilopoulou et al., 2016). Therefore, hypothesis-driven techniques are still necessary for confirmatory research.

Another limitation in human "Omics" studies is the difficulty in obtaining biopsies. Only bodily fluids such as blood, plasma, serum or cerebrospinal fluid and post-mortem tissue can be used.

Animal models therefore play a crucial role in collecting valuable information about neurological diseases. They can be used for the comprehensive screening of brain tissue (Chen et al., 2015b; Constantinou et al., 2011; Davidovic et al., 2011; González-Domínguez et al., 2015; Salek et al., 2010), thus avoiding concerns regarding post-mortem tissue (different causes of death, processing and sampling time etc). However, interspecies differences need be considered.

In addition, metabolome, proteome or genome changes may vary depending on how well the model recapitulates disease pathology (McGonigle and Ruggeri, 2014; Suvorov and Takser, 2008). Moreover, depending on the pathology in the model, one or more brain regions of interest should be carefully chosen for investigation (Ivanisevic et al., 2014; Salek et al., 2010). For accuracy, a critical amount of tissue is required, which is hard to obtain in rodents due to their small brain size. Therefore, samples are frequently pooled (Vasilopoulou et al., 2016). The examination of brain metabolomics in animal models can lead to the discovery of metabolic alterations contributing to brain dysfunction. Therefore, metabolomic data can help to understand the molecular basis of various neurological and psychiatric diseases (Vasilopoulou et al., 2016).

“Omics” studies are very practical for broad data screening; however, their main limitation is the lack of precision. For instance, while proteomics studies can quantify the abundance of a certain protein in a specific brain region, they provide no data on protein distribution either within the cell layers or in individual cells and elucidate nothing about protein function. Therefore, these studies frequently serve as a research starting point to generate hypotheses.

Lastly, metabolomics experiments should be thoroughly designed in advance in order to ensure that research aims can be accomplished. For example, tissue selection and preparation should be in line with project objectives, sample size should be calculated with possible sex, age and

genetic differences taken into account, and sampling times as well as the necessity for fasting should be determined. All aforementioned factors can significantly impact metabolome results and lead to unreliable data.

## *6.2. "Omics" studies in epilepsy research*

Proteomics data have provided crucial information about physiological and pathophysiological brain function and contributed to the identification of disease-associated processes, pathway modifications and novel drug candidates (Khurana et al., 2020). Similarly, in epilepsy research, the application of molecular techniques could help elucidate molecular alterations underlying epileptogenesis and ictogenesis (Bosque et al., 2019). To date, most data comes from animal models of acquired structural epilepsy, which have provided evidence for molecular alterations associated with neuronal inflammation, synaptic and cellular plasticity, microglial activation, angiogenesis, cell stress, blood-brain barrier perturbation, cytoskeleton modification etc (Bitsika et al., 2016; Keck et al., 2017; Keck et al., 2018; Li et al., 2010; Liu et al., 2008; Walker et al., 2016). Data from the genetic epilepsies have so far been limited to genetic absence epilepsy and fragile X syndrome. These findings pointed towards a change in the regulation of proteins involved in energy generation, synaptic transmission, inflammatory processes, membrane conductance and ribosomal translation (Danış et al., 2011a; Liao et al., 2008b; Xu et al., 2018). A single transcriptomic study in a mouse model of Dravet syndrome showed developmental deficits in neural connectivity (Tsai et al., 2015). As of yet, a broad large-scale proteomic data set from Dravet syndrome has not been acquired.

One of the first metabolomic studies in epileptology demonstrated that glutamate reuptake and glutamate-glutamine cycling are affected in patients with epilepsy leading to the accumulation of extracellular glutamate, cell toxicity and poor glucose and lactate utilization, thus resulting in energetic deficiency (Cavus et al., 2005). Further metabolomic screening of brain tissue from

patients with epilepsy identified numerous biomarkers of disease, pharmacological targets, and evidence of epilepsy (Donatti et al., 2020).

Recently, the term “metabolic epilepsies” has been introduced for all epilepsies with a metabolic etiology (Scheffer et al., 2016). Importantly, most patients with these disorders also possess a genetic defect (Scheffer et al., 2016). Therefore, there is a strong interest in the investigation of genetic epilepsies including Dravet syndrome to determine the associated metabolic changes and assess if their management could improve patients’ responsiveness to antiseizure drugs.

## *7. Future directions in Dravet syndrome treatment – knowledge gap*

The facilitation of orphan drug approval by the Orphan Drug Act in the USA (1983) and in the EU (2000) combined with technology advancement, led to greater higher interest and investment from pharma companies in the development of treatments for rare diseases, including Dravet syndrome (https://pharmaboardroom.com/articles/investments-and-deal-activity-in-orphan-drug-products/). Over the last decade, progress in the treatment of Dravet syndrome has been made, resulting in three drugs gaining approval for its therapeutic management. However, we are still far away from the main goal of the treatment, which is seizure-freedom. While the available drugs do improve seizure control in some patients, most are not seizure-free even with the combination of several antiepileptic drugs. In addition, other disease symptoms progress drastically over time, the treatment of which is poorly managed. Therefore, the aim of Dravet syndrome treatment may be early disease management which should also prove prophylactic for symptoms occurring later in the disease course.

Most findings regarding the pathophysiological mechanisms underlying the disease are derived from animal models of acquired structural epilepsy, while the knowledge about neurobiological changes associated with genetic epilepsies including Dravet syndrome, is still very limited. A better understanding of these mechanisms and their metabolic consequences may facilitate the identification of alternate targets and the development of therapeutic agents tailored to the patient's needs. Therefore, patients could benefit not only from better seizure management, but also from an improvement of cognitive, motor and behavioral symptoms. In addition, the identification of novel biomarkers may facilitate a more rational selection of drugs or dietary approaches.

# AIMS OF THE THESIS

The aims of this thesis comprise:

1. Characterization of a novel mouse model of Dravet syndrome, evaluating its face validity and suitability for future pharmacological and biomedical evaluation.
2. Understanding the molecular and metabolic consequences of *Scn1a* genetic deficiency and the pathophysiological mechanisms developing through the course of the disease.
3. Identification of possible candidates that could be therapeutically targeted in the treatment of Dravet syndrome.
4. Investigating the effect of the ketogenic diet on the metabolome in Dravet mice.

# MANUSCRIPTS

## *1. Manuscript I*

This chapter contains a manuscript submitted to the journal *Neurobiology of Disease* (doi: 10.1016/j.nbd.2021.105423). The manuscript aimed to provide the first phenotype characterization of a mouse model of Dravet syndrome and highlight relevant proteome alterations in the hippocampal brain region before and following epilepsy manifestation.

## Proteomic signature of the Dravet syndrome in the genetic mouse model *Scn1a*-A1783V.

**Miljanovic N., Hauck SM., van Dijk RM., Di Liberto V., Rezaei A., Potschka H.**

The author of the thesis is the first author of this manuscript. **N.M**. designed and performed all in vivo experiments, completed statistical analysis and provided the original manuscript draft. **S.M.H.** performed proteomic screening and provided raw data. **R.M.v.D.** contributed to study design and statistical analysis. **D.L.V.** contributed to establishing experiment methodology and assisted in experiments. **R.A.** performed immunohistochemical staining. **H.P.** provided conception and funding for the study, wrote sections of the manuscript. All authors contributed to manuscript revision, read and agreed on the submitted version.

# Proteomic signature of the Dravet syndrome in the genetic *Scn1a*-A1783V mouse model

Nina Miljanovic[a,b], Stefanie M. Hauck[c], R. Maarten van Dijk[a,e], Valentina Di Liberto[a,d], Ali Rezaei[a,b], Heidrun Potschka[a]

[a]Institute of Pharmacology, Toxicology & Pharmacy, Ludwig-Maximilians-University (LMU), Munich, Germany

[b]Graduate School of Systemic Neurosciences (GSN), Ludwig-Maximilians-University (LMU), Munich, Germany

[c]Research Unit Protein Science, Helmholtz Zentrum München, German Research Center for Environmental Health (GmbH)

[d]present address: Department of Experimental Biomedicine and Clinical Neurosciences, University of Palermo, Palermo, Italy.

[e]present address: Staburo GmbH, München, Germany.

**Correspondence*: Dr. H. Potschka, Institute of Pharmacology, Toxicology, and Pharmacy, Ludwig-Maximilians-University, Koeniginstr. 16, D-80539 Munich, Germany;
Phone: +49-89-21802662; Fax: +49-89-218016556;
e-mail: potschka@pharmtox.vetmed.uni-muenchen.de

Declarations of interest: none

## *Abstract*

**Background**: Dravet syndrome is a rare, severe pediatric epileptic encephalopathy associated with intellectual and motor disabilities. Proteomic profiling in a mouse model of Dravet syndrome can provide information about the molecular consequences of the genetic deficiency and about pathophysiological mechanisms developing during the disease course.

**Methods**: A knock-in mouse model of Dravet syndrome with *Scn1a* haploinsufficiency was used for whole proteome, seizure and behavioral analysis. Hippocampal tissue was dissected from two- (prior to epilepsy manifestation) and four- (following epilepsy manifestation) week-old male mice and analyzed using LC-MS/MS with label-free quantification. Proteomic data sets were subjected to a bioinformatic analysis including pathway enrichment analysis. Differential expression of selected proteins was confirmed by immunohistochemical staining.

**Results**: Analysis of seizure susceptibility and behavioral patterns confirmed an excellent face validity of the novel Dravet mouse model. As expected, proteomic analysis demonstrated more pronounced alterations following epilepsy manifestation. In particular, proteins involved in neurotransmitter dynamics, receptor and ion channel function, synaptic plasticity, astrogliosis, neoangiogenesis, and nitric oxide signaling showed a pronounced regulation in Dravet mice. Pathway enrichment analysis identified several significantly regulated pathways at the later time point, with pathways linked to synaptic transmission and glutamatergic signaling dominating the list. Interestingly, comparison of these data from a genetic epilepsy model to published data from acquired epilepsies suggests commonalities in molecular alterations comprising protein groups linked with GABAergic, glutamatergic, and dopaminergic neurotransmission, voltage-gated ion channels, synaptic plasticity, astrogliosis, angiogenesis, and nitric oxide signaling.

**Conclusion**: In conclusion, the whole proteome analysis in a mouse model of Dravet syndrome demonstrated complex molecular alterations in the hippocampus. Some of these alterations may have an impact on excitability or may serve a compensatory function, which, however, needs to be further confirmed by future investigations. The proteomic data indicate that due to molecular consequences of the genetic deficiency the pathophysiological mechanisms may become more complex during the course of the disease, and that the management of Dravet syndrome may need to consider further molecular and cellular alterations. Along this line, based on functional follow-up studies, the data set may provide valuable guidance for future development of novel therapeutic approaches.

**Key words:** proteome, genetic epilepsy, epileptic encephalopathy, *Scn1a*, mice.

## *Abbreviation list:*

| | |
|---|---|
| MS | Mass spectrometry |
| LC-MS/MS | Liquid chromatography with tandem mass spectrometry |
| Hprt | Hypoxanthine-guanine phosphoribosyltransferase |
| VEGF | Vascular endothelial growth factor |
| JAK-STAT | The Janus kinase/signal transducers and activators of transcription |
| PSD | Postsynaptic density |
| CaMK | Calcium/calmodulin-dependent protein kinases |
| nNOS | Neuronal nitric oxide synthase |
| NO | Nitric oxide |
| SE | Status epilepticus |

## *Introduction*

In the vast majority of patients with Dravet syndrome an *SCN1A* mutation can be identified, which results in functional deficiency of the encoded sodium channel subunit $Na_v1.1$ (Brunklaus and Zuberi, 2014; Dravet and Oguni, 2013). Dravet syndrome is characterized by seizures with a poor pharmacoresponse to available antiepileptic drugs (Wallace et al., 2016). Moreover, there is a high risk of sudden unexpected death in epilepsy (SUDEP) in Dravet patients (Kalume, 2013). Thus, despite the licensing of orphan drugs for Dravet syndrome there is still a particular need for novel therapeutic approaches tailored to the disease. While knowledge about the genetic cause provides a first basis for rational development of precision medicine approaches (Dugger et al., 2018), the elucidation of the molecular consequences of the genetic deficiency can further improve our understanding of the pathophysiological mechanisms and can provide a broader framework for the identification of novel targets and the subsequent development of innovative therapeutic concepts.

Proteomic large-scale profiling constitutes one of the most promising tools providing comprehensive information about epilepsy-associated alterations at a functionally relevant molecular level. During recent years, first studies have been completed that identified proteome alteration in models of acquired epilepsy (Bitsika et al., 2016; Keck et al., 2017; Keck et al., 2018; Li et al., 2010; Liu et al., 2008; Walker et al., 2016). Respective data for genetic epilepsies are rather limited with a focus on models of genetic absence epilepsy and fragile X syndrome (Danış et al., 2011b; Liao et al., 2008a; Xu et al., 2018). To our knowledge, the molecular consequences of *Scn1a* genetic deficiency have so far not been studied by quantitative whole proteome analysis. The characterization of the molecular signature of the Dravet syndrome may provide important clues to understand disease-associated alterations of neuronal homeostasis.

Here, we completed a large-scale proteomic profiling study in a novel conditional mouse line carrying a human Dravet syndrome *SCN1A* mutation (Kuo et al., 2019; Ricobaraza et al., 2019). The analysis focused on two time points, prior and following onset of spontaneous recurrent

seizures in order to obtain information about both, molecular patterns during epileptogenesis and following epilepsy manifestation. The list of differentially expressed proteins was compared with published data sets from models of acquired epilepsy aiming to identify common epileptogenesis- and epilepsy-associated molecular patterns.

Taken together, our findings improve the understanding of the complex molecular consequences of *SCN1A* genetic deficiency and provide a basis for discovery of novel innovative targets for prevention of disease progression and for therapeutic management of Dravet syndrome.

## *Material and methods*

*Genetic mouse model: breeding and genotyping*

Breeding colonies of the parental lines B6(Cg)-*Scn1a*$^{tm1.1Dsf}$/J (#026133(Kuo et al., 2019; Ricobaraza et al., 2019)) and 129S1/Sv-*Hprt*$^{tm1(CAG-cre)Mnn}$/J (#004302(Tang et al., 2002)) were generated based on breeding pairs purchased from the Jackson Laboratory (Bar Harbor, Maine, USA). Conditional knock-in male mice with floxed *Scn1a* (mutation A1783V in exon 26) were crossed with female mice heterozygous for Cre recombinase (X-linked to neuronal promoter *Hprt* gene). The offspring resulted in heterozygous Dravet mice carrying the A1783V mutation (wildtype or heterozygous for Cre recombinase) or wildtype mice without the A1783V mutation (wildtype or heterozygous for Cre recombinase). Since the presence of Cre did not affect the phenotype, animals were divided into a Dravet group and a wildtype control group depending on the presence of the A1783V-*Scn1a* mutation. The mouse line has been chosen for the experiments considering that A1783V represents one of the clinically relevant mutations affecting the domain IV S6 transmembrane region of the alpha subunit of the type I voltage-gated sodium channel in patients with Dravet syndrome (Lossin, 2009).

The genotype of the animals was confirmed by PCR, using 5′-GCAACTCTTCACATGGTACTTTCA-3′, 5’-GCACCTCTCCTCCTTAGAACA-3’ and 5′-GGAGAAACACGAGCAGGAAG-3′ primers: wildtype, 164 bp; heterozygous pre Cre, 164, 198 and 410 bp; and heterozygous post Cre, 164 and 198 bp (Fig. 1A). Presence of Cre recombinase in mice was also confirmed by PCR, using 5′-CTGGTGCTTTACGGTATCGC-3′, 5’-TTCATAGAGACAAGGAATGTGTCC-3’ and 5′-AATCCAGCAGGTCAGCAAAG-3′ primers: WT allele, 217 bp; Cre allele, 450 bp.

Experiments were approved by the responsible government of Upper Bavaria (license number 55.2-1-54-2532-166-2015 and 55.2-1-54-2532-168-2016). All experiments were conducted in accordance with the EU directive 2010/63/EU for animal experiments and the German Animal

Welfare act. All experiments were planned and carried out considering the ARRIVE guidelines and the Basel declaration (http://www.basel.declaration.org) including the 3R concept.

Twenty mice were used for sampling of brain tissue for proteomic analysis with five animals per genotype and time point. Sections from four wildtype and four Dravet mice aged 4 weeks were used for qualitative immunohistochemical analysis of selected proteins.

Another group of animals was used for characterization of the phenotype and face validity of the line. From 38 heterozygous mutant mice, 23 (11 male; 12 female) survived the phase around weaning, which is characterized by a high seizure-associated mortality rate. Data from these animals were compared with those from 21 wildtype littermate controls (11 male; 10 female). One wildtype and one Dravet female mouse from this group were later used for EEG-telemetry recordings.

In addition, baseline data from 22 heterozygous mutant mice were considered for seizure monitoring based on parallel video monitoring and telemetric EEG recordings. These animals were also prepared for ECG recordings and were further used for a separate study assessing effects of ketogenic diet in Dravet mice (manuscript in preparation).

*Housing of animals*

Each litter was housed in individually ventilated cages (Tecniplast, Hohenpeißenberg, Germany) from birth until weaning time (3 weeks). Following this phase, mice were grouped in 3-5 animals per standard Makrolon type III cage (Ehret, Emmendingen, Germany). Animals used for sampling of brain tissue for proteomic analysis were single caged following weaning in type II open cage (Ehret, Emmendingen, Germany) in order to confirm presence of seizures. Animals used for behavioral assessment were single caged 2 weeks prior to behavioral assessment. The order of cages was randomized (randomizer.org).

Each cage was supplied once weekly with fresh sawdust as a bedding material (Lignocel, Rosenberg, Germany), two nestlets (Ancare, Bellmore, New York, USA), and one animal house

(Tecniplast, Hohenpeißenberg, Germany; Zoonlab GmbH**,** Castrop-Rauxel, Germany). Standard conditions in the animal facility were set to: lights on from 6 am to 6 pm, temperature 22 ± 2˚C, and humidity 50 ± 10 %. Animals received food (ssniff® R/M-H, Sniff, Soest, Germany) and water *ad libitum* with Dietgel76A offered as a supplement (Sniff, Soest, Germany) between postnatal days P14 and P26.

*Brain samples for proteomic analysis*

Brain samples were obtained at two different time points from five mice per genotype and time point. Two-week-old mice (early time point, prior to seizure onset) were sacrificed by decapitation, whilst the four-week-old mice (later time point) were sacrificed by cervical dislocation. Hippocampal tissue from the left hemisphere was dissected and fresh frozen in liquid nitrogen (Besamungsstation München-Grub, Poing, Germany) using 1.5 ml Protein LoBind Tubes (Eppendorf, Wesseling-Berzdorf, Germany. The experimenter was blinded to animals' genotype and order of animals for dissection was randomized (randomizer.org). Once the samples were frozen and stored at -80 °C until analysis. The right brain hemisphere was collected and left in 4% PFA solution for 24 hours and then switched to 30 % sucrose solution. The brain was cut into 40 µm thick slices, which were later used for immunohistochemistry.

*Proteome analysis*

Untargeted proteome analysis was carried out by an experimenter not involved in the *in vivo* experiments, to avoid any expectation-triggered bias. Snap frozen hippocampus samples were directly bead milled with a Precellys homogenizer (Peqlab, Lutterworth, U.K.) in extraction buffer (10mM Tris-HCl pH 7.6 with 1 % NP40, 10 mM NaCl and Complete protease inhibitors) as previously described (Molin et al., 2015). The total protein concentration in sample was measured by the Bradford assay. A modified filter-aided sample preparation (FASP) method was used for digestion of 10 µg of total protein per sample as described (Lepper et al., 2018).

A Q Exactive HF mass spectrometer was used for proteomic screening (ThermoFisher Scientific, Dreieich, Germany) with operation in the data independent acquisition (DIA) mode (Lepper et al., 2018). Per sample one injection unit of the HRM Calibration Kit (Biognosys, Schlieren, Switzerland, #Ki-3003) was used for spiking 1 µg of peptides for indexing of retention time. Samples were loaded automatically onto the UPLC system (Ultimate 3000, Dionex, Sunnyvale, CA). The system contained a nano trap column (inner Ø = 300 µm × 5 mm, packed with Acclaim PepMap100 C18, 5 µm, 100 Å; LC Packings, Sunnyvale, CA). Following 5 minutes of elution from the trap column, the peptides were separated by reversed-phase chromatography (Acquity UPLC M-Class HSS T3 Column, 1.8 µm, 75 µm × 250 mm; Waters, Milford, MA) using a 7−27 % gradient of acetonitrile (flow rate of 250 nL/minute, 90 minutes), followed by two short gradients of 27−41 % acetonitrile (15 minutes) and 41−85 % acetonitrile (5 minutes). After 5 minutes at 85 % acetonitrile, the gradient was reduced to 3 % acetonitrile over 2 minutes and then allowed to equilibrate for 8 minutes. All acetonitrile solutions contained 0.1 % formic acid.

The DIA method comprised alternating mass spectrometry (MS) full scans spanning from 300−1650 m/z at 120,000 resolution, followed by 37 DIA window scans at 30,000 resolution for peptide fragmentation with a variable width ranging from 300−1650 m/z. Normalized collision energy was adjusted to 28, with profile type spectra recording.

The DIA liquid chromatography with tandem MS (LC−MS/MS) raw files were converted (HTRMS converter) and analyzed (Spectronaut version 11, Biognosys, Schlieren, Switzerland) as described (Lepper et al., 2018). An automatic calibration mode was chosen with precision indexed retention time (iRT) alignment enabled for the application of the nonlinear iRT calibration strategy. Peptides were identified by comparison with an in-house accumulated spectral library, which has been obtained from mouse brain samples measured on the same MS set-up with a data-dependent acquisition mode. Peptide identification was filtered for a false discovery rate (FDR) of 1 %. Only proteotypic peptides were considered for quantification of

proteins, applying MS2 area based summed precursor quantities. The data filtering function was set to q-value percentile mode applying a 50 % setting, thus enabling a match between runs. This setting allows only peptide precursor signals passing the FDR threshold of 1 % in over 50 % of all samples to be further considered for identification and quantification, thus working towards a reduction of false positive identifications. The sum of abundances of all unique peptides per protein was log2 transformed, and obtained values were compared between groups with unpaired Student's t-test and $p<0.05$ was set as the level of significance.

*Pathway enrichment analysis*

Pathway enrichment analysis was completed using a publicly available pathway tool (Consensus PathDB over-representation tool, (Kamburov et al., 2009)). A background list was used, comprising of all identified proteins. Only pathways with both, a $p<0.01$ and at least two dysregulated proteins, were considered. Only pathways reaching a $q<0.01$ (=p-value corrected for multiple testing using the FDR method) were considered significant and discussed in this study. Protein abundances of all proteins assigned to significantly changed pathways were visualized in a heat map. Individual fold changes for each animal were calculated by dividing their value against the wildtype group's mean and then log2 transform the value. The resulting matrix was visualized using R software version 3.5.1 (Team, 2017) and "gplots" package (Warnes et al., 2016).

*Immunohistochemical staining of PPP1R1B (DARPP-32)*

In order to further confirm expression alterations of selected proteins, brains from four-week-old wildtype and Dravet mice (n=4 per group) were used for immunohistochemistry. Free-floating sections were washed in PBST (Phosphat-buffered saline, 0.1% Tween 20) at room temperature and heat-induced epitope retrieval (HIER) was performed at 80 °C for 30 minutes using sodium citrate buffer (pH 6.0). Sections were cooled down on ice and rinsed in PBST.

Endogenous peroxidase was inhibited (3 % $H_2O_2$ in TBS for 60 minutes). Slices were rinsed in PBST and a blocking step in 6 % goat serum (60 minutes) was performed to prevent non-specific antibody binding. Sections were then incubated overnight at 4 °C with a monoclonal rabbit DARPP32 primary antibody (Abcam, Berlin, Germany, Cat# ab40801, lot# GR3213231-3) at 1:2500 dilution. The next day, sections were washed in PBST and incubated for 60 minutes at room temperature with biotinylated goat anti-rabbit secondary antibody (Vector laboratories, Cat# BA-1000, lot# 2F0430) at 1:1000 dilutions. After washing steps in TBST, brain sections were incubated at room temperature in VECTASTAIN ABC-Peroxidase Kit (Vector Laboratories Cat# PK-4000, RRID: AB_2336818, lot#2337238, dilution 1:100, 60 minutes). The slices were washed in PBS and stained using SIGMAFAST™ 3,3′-Diaminobenzidine tablets (Sigma-Aldrich, Darmstadt, Germany, Cat# D4418, lot# SLBR2966V) for 1 minute. Brain sections were quickly rinsed in distilled $H_2O$, washed in PBS, mounted on microscope glasses using PBST, and cover slipped with Entellan® (107960, Merck, Darmstadt, Germany). Negative controls were processed in parallel without the primary antibody.

*Immunohistochemical staining of HSD11B1*

The staining protocol for HSD11B1 was identical to the one described above (DARPP-32), with the following exceptions. Inhibition of endogenous peroxidase was done in 3 % $H_2O_2$ in TBS for 15 minutes. A blocking step was performed in 1.5 % goat serum for 120 minutes. The primary antibody was HSD11B1 (Abcam, Berlin, Germany; Cat# ab39364, lot# GR3247054-7) in 1:200 dilution. Slices were stained in SIGMAFAST™ 3,3′-Diaminobenzidine solution for 100 s.

*Microscopy*

Bright field images were captured at 4x, 10x and 40x magnification with an Olympus BH2 microscope with a single chip charge-coupled device (CCD) color camera (Axiocam; Zeiss,

Göttingen, Germany), and an AMD AthlonTM 64 processor based computer with an image capture interface card (Axiocam MR Interface Rev.A; Zeiss, Göttingen, Germany).

*Hyperthermia-induced seizures and threshold determination*

Hyperthermia-induced seizures were analyzed in mice at postnatal day 23, 25, and 32. Mice were transported to the laboratory 30 minutes prior to seizure induction. Temperature and light in the laboratory were adjusted to 22 ± 2˚C and 600 lux. At all experimental days, tests began at 12 p.m. with a randomized order of animals (randomizer.org). Observers were blind to animals' genotype as far as possible. At the early time point blinding proved to be difficult considering the obvious phenotype (lower body weight). The whole procedure was video recorded (Axis communications, Lund, Sweden). Body temperature was measured continuously with a RET-4 rectal probe (Physitemp, Clifton, New Jersey, USA), which was placed in warm saline solution (B. Braun Vet Care GmbH, Tuttlingern, Germany) before use. Subjects were placed in a plexiglass cylinder for 5 minutes to habituate to the environment and to record basal body temperature data. Then, the IR lamp connected to the temperature controller (Physitemp, Clifton, New Jersey, USA) was turned on to slowly increase the body temperature with a ramping of 0.5˚C per 2 minutes (Oakley et al., 2009). Heating was stopped immediately when generalized tonic-clonic seizures were observed or when the body temperature reached 42℃. Animals were allowed to cool down before returning them to their home cage. All equipment was cleaned between subjects with 70 % ethanol (CLN, Langenbach, Germany).

Severity of hyperthermia-induced seizures was assessed based on the Racine scoring system with scores: I (mouth and facial movements), II (head nodding), III (forelimb clonus), IV (rearing with forelimb clonic convulsions) and score V (generalized clonic convulsions followed by rearing and falling) (Racine, 1972).

*Spontaneous seizures*

In order to obtain first information about the onset of spontaneous seizures, their frequency, duration and severity score, a continuous video monitoring was started in all animals in the second postnatal week and continued following weaning with a total monitoring time of 6 weeks. Videos have been carefully reviewed by experienced technicians with maximum 8x speed and all generalized seizures were documented.

Two eight-month-old female mice (one wildtype, one Dravet) and 22 twelve-week-old Dravet mice (11 males, 11 females) underwent survival surgery for telemetry (ETA-F10 or HD-X02, DSI, St. Paul, USA) and EEG electrodes implantation. The order of animals was randomized (randomizer.org). Thirty minutes before anesthesia induction, mice received 1 mg/kg meloxicam s.c. (Metacam®, Boehringer Ingelheim, Germany). For general anesthesia mice received 400 mg/kg chloral hydrate i.p. (Carl Roth, Karlsruhe, Germany) (n=2) or isoflurane (Isofluran CP®, Henry Schein Vet, Hamburg, Germany) with a concentration of 4 % and 1.5 % for anesthesia induction and maintenance, respectively (n=22). The local anesthetic bupivacaine (0.5 %; Jenapharm®, Mibe GmbH, Brehna, Germany) was applied subcutaneously to surgical areas affected by transmitter implants and placement of leads. For intracranial electrode placement, bupivacaine with epinephrine (0.5 % + 0.0005 %; Jenapharm®, Mibe GmbH, Brehna, Germany) was applied subcutaneously.

Firstly, the skin was opened in the dorsocaudal part of the scapula region for placing the telemetric transmitter subcutaneously. Mice were then fixed in a stereotactic frame and three screws were inserted in the skull. The negative EEG lead was connected to the screw over the cerebellum. The positive EEG lead was connected to a bipolar Teflon-isolated stainless-steel electrode, which was implanted into the CA1 region of the hippocampus (ap: - 2,00; lat: + 1,3; dv: - 1,6). The electrode was fixed with Paladur (Heraeus®, Hanau, Germany). The skin over the skull was closed with absorbable sutures, while the initial cut for the transmitter placement was closed with tissue adhesive (Surgibond®, Henry Schein Vet, Hamburg, Germany).

As stated above 22 animals were prepared for additional ECG analysis in the context of another study. Therefore, the negative ECG lead was fixed intramuscularly to the right pectoral muscle, whilst the positive ECG lead was fixed left to xyphoid prior to electrode implantation. Skin over the ECG connections was closed with absorbable sutures (Smi AG, St. Vith, Belgium). Animals were given oxygen until regaining consciousness. On the following day, mice received 1 mg/kg meloxicam s.c. Mice were allowed to recover for full 2 weeks followed by a two-week continuous recording phase. In parallel, animals were video monitored (Axis communications, Lund, Sweden) in order to confirm and analyze behavioral seizure activity. Data were acquired with Ponemah software (Ponemah R, v. 5.2.0, DSI, St. Paul, USA), and seizure activity was detected automatically (Neuroscore$^{TM}$ v. 3.0, DSI, St. Paul, USA).

*Behavioral characterization*

Following hyperthermia-induced seizures, all animals were tested in different behavioral paradigms except for one female Dravet mouse and one female wildtype mouse related to an age difference to the remaining animals. Thus, 22 Dravet mice (11 males; 11 females) and 20 wildtype (11 males; 9 females) mice were used for behavioral assessment.

One male Dravet mouse died following a spontaneous seizure and was therefore not exposed to the elevated plus maze and accelerated rotarod test. Data from one male Dravet mouse were not considered in the saccharin preference test, due to leakage of one of the water bottles. During all behavioral paradigms, animals were single-housed as a presupposition for the social interaction test. Social interaction was analyzed at an age of 7 weeks. The order of the subsequent tests was as follows: open field test, saccharin preference test, elevated plus maze and accelerated rotarod test (Fig. 1B). The testing was completed until an age of 10 weeks. The order of animals for each test was randomized (randomizer.org).

Nest-building activity as well as saccharin preference were assessed in the home cage. All other behavior tests (social interaction, open field test, elevated plus maze, accelerated rotarod test)

were completed in a test room (temperature 22 ± 2 ˚C, humidity 55 ± 5 %) under different light conditions adjusted to the specific paradigm (stated below). All tests were carried out in morning hours (starting from 8 a.m.). All behavioral test runs were documented by photographing (nest complexity) or video-recording (all other tests).

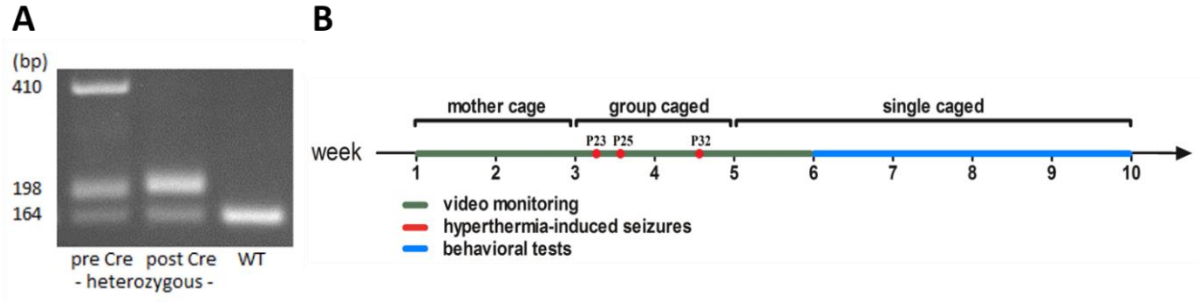


**Fig. 1. A** PCR genotyping for distinguishing Dravet mice with Cre activated A1783V mutation (post Cre heterozygous) and wildtype mice. **B** Experimental timeline.

*Open field test*

The open field paradigm is a widely used test for assessment of exploratory behavior and locomotion in an unfamiliar environment (Carola et al., 2002). Mice were placed in the test room for 1 hour to habituate (lighting 15-20 lux). Two round shaped arenas (Ø 61 cm, height 40 cm) were simultaneously used for the test. Time spend in three different zones (wall, middle and center) was analyzed with Ethovision 8.5 software (EthoVision XT, RRID:SCR_000441). Each mouse was placed in one arena, 10 cm from the wall, and facing the wall. Locomotion was recorded for 30 minutes. Rearing behavior was counted manually. After completing the test, mice were returned to their home cage. The arena was cleaned with 0.1 % acetic acid before continuing with the next animal.

*Saccharin preference test*

The saccharin preference test was used to test anhedonia-associated behavior as one of the symptoms of depressive disorders (Klein et al., 2015). The analysis was conducted at four

consecutive test days in the home cage. Animals were provided with two water bottles. Tests were done in four consecutive 24 hours long periods. First, both bottles were filled with water to determine water intake over 24 hours. Then, the bottle on the left side was filled with a 0.1 % saccharin solution. During the next day, both bottles were again filled with water. At the last day, the right bottle was filled with saccharin solution in order to test for a potential side preference bias. Liquid consumption was measured after each period.

*Nest-building activity*

During postnatal week five, mice were placed individually in type III open cages. The following week animals were as always provided with two new nestlets and nest complexity was assessed on a daily basis. Nests were photographed each morning. The images were later scored by an investigator unaware of the group allocation. Nest complexity was ranked according to the scoring system developed by Jirkof and colleagues (Jirkof et al., 2013): score 0 = nestlet intact, possibly carried around the cage; score 1 = nestlet is poorly manipulated with more than 80% of the nestlet intact; score 3 = evident nest site with most of shreds in the nest site, less than 80% nestlet material intact, nest is hollow in bedding and mice begin to build walls; score 4 = flat nest, hollow in bedding, walls are higher than mice and encasing the nest less than 50%; score 5 = complex, bowl-shaped nest with walls higher than mice and encasing the nest more than 50%.

*Social interaction test*

The social interaction test was performed to assess autism-associated behavioral patterns and affinity towards interaction with another mouse. Mice were kept single in a type III open cage for 2 weeks prior to testing. On the first 2 days, animals were transported to the test room (lighting 15-20 lux) and placed in an empty type III open cage for 10 minutes to habituate. On the test day, animals were transported to the test room 30 minutes prior to testing. Two mice of

the same sex, same genotype and approximately same weight were then simultaneously placed in an empty cage and left for 10 minutes. Active and passive social interaction were measured with a stopwatch by an observer blind to animal genotype and sex. The cage was cleaned with 0.1 % acetic acid between subjects. Sniffing, grooming or following the partner as well as aggressive behavior were considered as active social interaction. Laying or sitting next to each other, without any interaction was classified as passive social interaction (Holter et al., 2015).

*Elevated plus maze*

The elevated plus maze is generally used to assess anxiety-like behavior in rodents (Ben-Hamo et al., 2016). Mice were placed in the test room for 1 hour prior to the experiment. The maze comprises two open arms (40 cm long and 10 cm wide) and two closed arms (same dimensions with walls 15 cm high). The plus maze was elevated 68 cm above the floor. Light was set to approximately 200 lux in open and 60 lux in closed arms. Animals were placed in the center of the maze facing the open arm. Five-minute-long trial was recorded with Ethovision XT. Head-dipping and stretching behavior (exploring open arms with head, while the body stays in closed arms or center part of the maze) were recorded manually by observers blinded to animals' group allocation. The maze was cleaned with 0.1 % acetic acid between animals.

*Accelerated rotarod test*

The accelerated rotarod test is widely used to evaluate motor performance in mice (Shiotsuki et al., 2010). Before experiment onset, mice were placed in the test room for 1 hour to habituate (15-20 lux). A rotarod apparatus (Ugo Basile 47600, Varese, Italy) was used to assess animals' motor coordination. The settings were chosen so that the rotation accelerates from 4 to 40 rpm over 5 minutes. Each animal was subjected to four consecutive trials with approximately 2 minutes break for cleaning the rod (0.1 % acetic acid). Testing was carried out at three subsequent days, first day for training, and second and third days as test sessions. Male animals

were always tested before females. Passive rotations were counted and time staying on rod as well as current speed were noted.

*Statistical analysis*

Statistical analysis was performed with R version 3.5.1. GraphPad Prism (Version 5.04 and 6.01, GraphPad, USA) was used for data visualization, except for heat maps visualized with R and Venn diagrams with an online tool (http://bioinformatics.psb.ugent.be/webtools/Venn/). Spearman correlation matrix was calculated using R version 3.5.2. The significance level for correlation analysis was set at $< -0.5$ or $> 0.5$. Animals with missing data were not considered for the respective correlation analysis.

All data were expressed as mean ± SEM with exception of nest complexity data, for which the median is illustrated in the respective graph. All results were first checked for possible batch effects. If present, batch effects were considered in the statistical analysis.

Two-tailed unpaired t-tests were used for comparison between experimental and control group where indicated. Two-, three-, four- and five-way ANOVAs were used to test the effects of genotype, sex, time, batch and their interaction where appropriate. Comparisons, which included multiple measurements, were tested using repeated measures ANOVA. ANOVA tests were followed by a Bonferroni post-hoc test. Two-tailed Mann-Whitney non-parametric test was used for analyzing nest complexity scores. The significance level was set at $p < 0.05$ for all tests.

*Data availability*

A complete list of abbreviations of significantly regulated proteins mentioned in the manuscript, sorted by their function is provided in *Supplementary Material* (Table A.1).

## *Results*

### *Breeding pattern and outcome*

Twenty-three female mice heterozygous for Cre recombinase (129S1/Sv-*Hprt*$^{tm1(CAG-cre)Mnn}$/J) were bred with 21 conditional knock-in male mice with floxed *Scn1a-1783V* (B6(Cg)-*Scn1a*$^{tm1.1Dsf}$/J) in pairwise and trio matings split in two different batches. Eighteen of them delivered litters with a total of 38 heterozygous mutant mice (Dravet mice) and 41 wildtype littermates. The sex ratio in the offspring was almost balanced with 38 males (19 Dravet; 19 WT) and 41 females (18 Dravet; 23 WT). Due to the 40 % mortality rate around the time of weaning we lost 15 Dravet mice. The remaining 23 Dravet mice and randomly selected 21 wildtype mice (randomizer.org) were used for model characterization.

### *General condition, body weight development, seizure thresholds and spontaneous seizures*

The body weight of Dravet mice proved to be significantly lower at the time point of weaning. However, following weaning affected animals showed a good development of body conditioning scores finally reaching a body weight comparable to wildtype mice (Fig. 2A).

In response to hyperthermia induction all Dravet mice exhibited generalized tonic-clonic seizures at all three testing days. In contrast, their wildtype littermates did not exhibit motor seizure activity despite ramping of the body temperature up to at least 41 °C.

The number of Dravet mice showing running and bouncing behavior increased with repeated hyperthermia induction reaching 18/23 animals on P32. The average threshold temperature for seizure induction on P23, P25 and P32 amounted to 39.7 ± 0.9 °C at P23, 39.7 ± 0.6 °C at P25, and 39.1 ± 0.5 °C at P32 (mean ± SD, Fig. 2B). Seizure duration increased in a significant manner with subsequent stimulations (Fig. 2C). No differences were observed when comparing female and male mice.

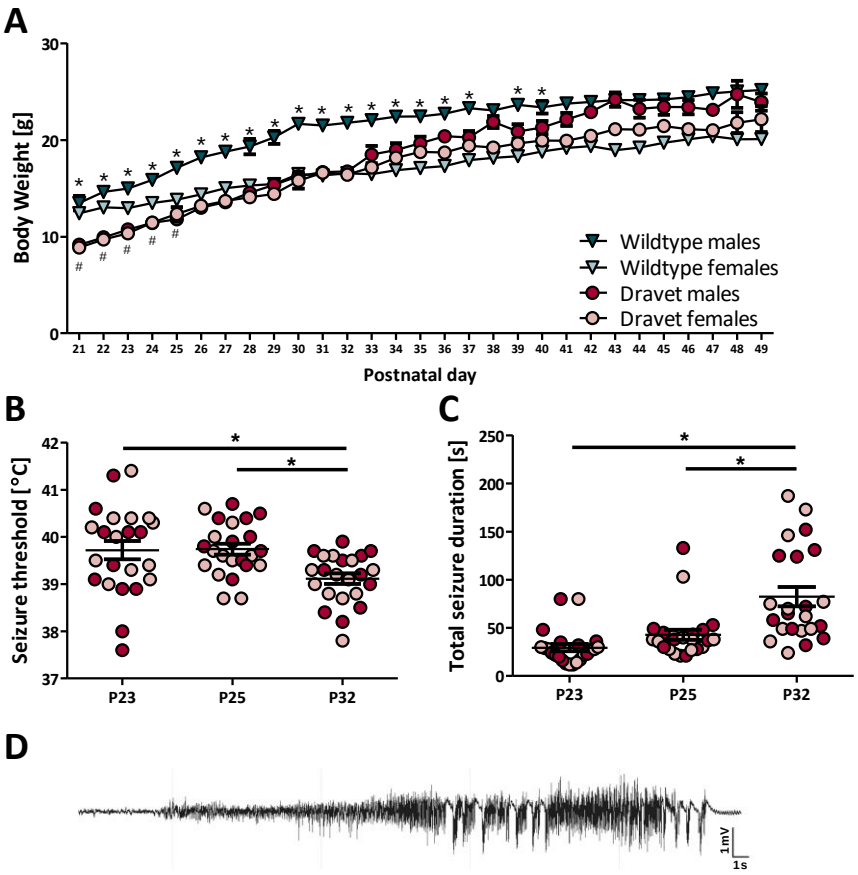


**Fig. 2. Body weight, spontaneous and hyperthermia-induced seizures. A** Body weight development following weaning. Body weight in animals with a Dravet genotype (males n = 11; females n = 11) proved to be significantly lower in the early phase following weaning (females until P25, males until P41) as compared to wildtype mice (males n = 11, females n = 9) (Unpaired t-test; * $p < 0.05$ males, # $p < 0.05$ females, mean ± SEM). **B** Seizure threshold temperature at P23, P25, and P32. The threshold significantly decreased on P32 compared to previous testing. **C** Total duration of hyperthermia-induced seizure activity, calculated as the sum of all motor seizure periods occurring immediately following stimulation. The duration significantly increased with repeated stimulations. **B-C** Data are from 11 male and 12 female animals with a Dravet genotype (Two-way RM ANOVA, Bonferroni post hoc; * $p < 0.05$, mean ± SEM**)**. **D** Representative EEG recording of a generalized tonic-clonic seizure (Racine score V, followed by running und bouncing) in an adult female mouse**.**

Video monitoring of experimental animals in their home cages demonstrated that the animals develop spontaneous motor seizures starting at P16. The seizures observed included generalized tonic-clonic seizures, sometimes associated with running and bouncing indicating seizure spread towards the brain stem. In addition, prolonged phases with behavioral arrest, immobility,

and lack of responsiveness to external stimuli were observed. Between P20 and P23 several Dravet mice died. In several instances video monitoring indicated that death occurred directly associated with a generalized seizure in these animals, thus, indicating that animals died from probable SUDEP. The mortality rate reached 40 %. The remaining 23 Dravet animals were used for behavioral characterization. SUDEP or probable SUDEP seems to be a rare event in older animals as only one animal was found dead in the cage at a later time point following the fourth postnatal week.

To further confirm spontaneous seizure activity, first telemetric EEG recordings were performed in combination with simultaneous video recordings in an adult female Dravet mouse in comparison with a female wildtype mouse. During the one-week recording, a Dravet mouse exhibited multiple generalized tonic-clonic seizures often followed by running and bouncing. Assessment of the EEG recordings confirmed electrographic seizure activity with high amplitude spiking over 500 µV (Fig. 2D). In the wildtype mouse, we did not obtain evidence for electrographic seizure events.

Additional recordings in a group of three-month-old Dravet mice confirmed a high penetrance of the epilepsy phenotype with multiple generalized tonic-clonic seizures in 19/22 mice. On average, mice experienced seven seizures per week (range: two to 16; data not shown). Seizures frequently occurred in clusters with animals often exhibiting seizures at only two subsequent days per week (range: one to four, data not shown). The average seizure duration was 50.19 s (data not shown).

*Phenotype: behavioral alterations*

In the open field paradigm, hyperlocomotion was evident in male and female Dravet mice. Throughout the 30 minutes test, the total distance moved and the rearing frequency reached significantly higher levels in Dravet mice as compared to wildtype animals (Fig. 3A-B). Moreover, immobility time proved to be shorter in Dravet mice (data not shown). Additionally,

thigmotaxis proved to be increased in Dravet mice with more time spent in the wall zone. Time spent in the other zones (middle and center) was not affected by the genotype (Fig. A.1C).

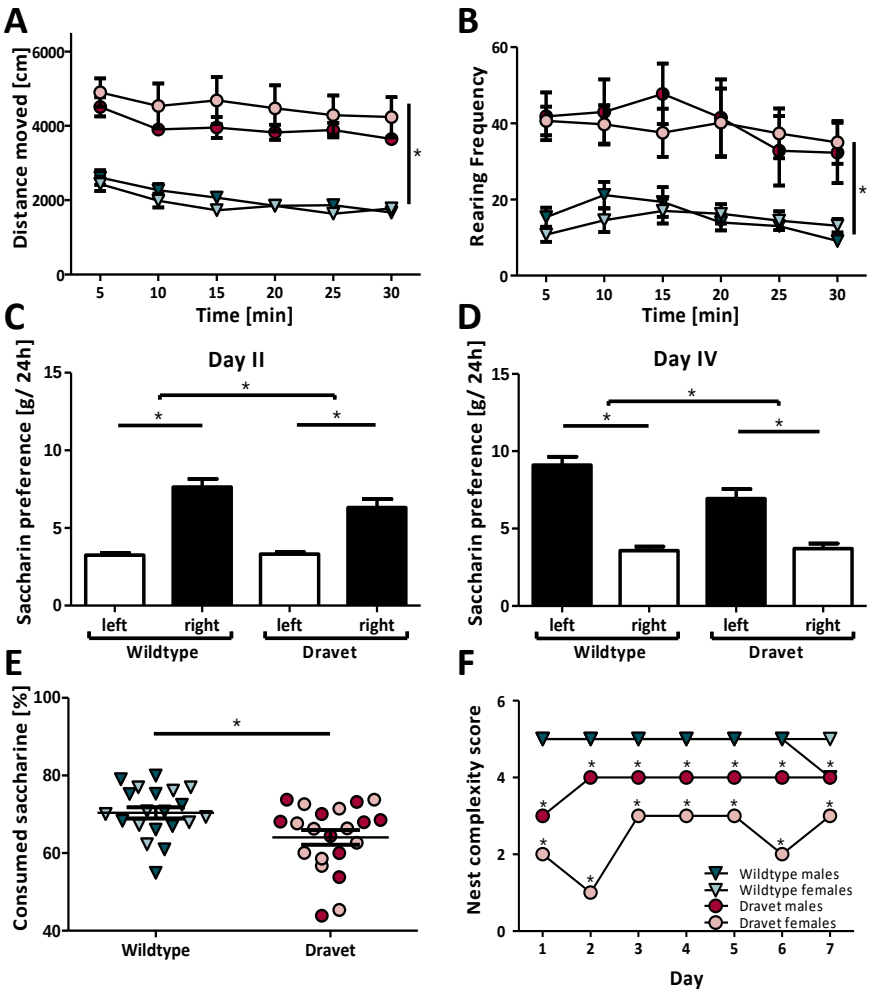


**Fig. 3. Open field test, saccharin preference and nest-building behavior. A** Distance moved in open field test over 30 minutes, divided into mean intervals of 5 minutes. The total distance moved of Dravet mice significantly exceeded that of wildtype mice. **B** Rearing frequency. Dravet mice exhibited more frequent rearing positions than wildtype mice. **A-B** Data are from 22 animals with a Dravet genotype and 20 wildtype animals (Three-way RM ANOVA, Bonferroni post hoc; * $p < 0.05$, mean ± SEM). **C-D** Water or saccharin solution consumption per 24 hours. Both, Dravet mice and wildtype mice preferred saccharin solution over water, independent of a side preference. **E** Total saccharin solution consumption over both days. Dravet mice consumed significantly less saccharin solution as compared to wildtype mice. **C-E** Data shown are from 21 animals with a Dravet genotype and 20 wildtype animals (Three-way ANOVA, Bonferroni post hoc; * $p < 0.05$, mean ± SEM). **F** Nest complexity score over 7 days. As shown in the graph, nests of Dravet mice (n=22) received lower scores as compared to those from wildtype mice (n=20) (Mann-Whitney non-parametric test; * $p < 0.05$, median).

Regardless of the genotype a preference of saccharin solution over water was observed. However, the amount of saccharin consumed by wildtype mice exceeded that in mice with the Dravet genotype. In line with this finding, the percentage of consumed saccharin solution proved to be reduced in Dravet mice (mean ± SD: Dravet mice 64.07 ± 8.64 %; wildtype mice 70.38 ± 6.41 %) (Fig. 3E).

Interestingly, when saccharin consumption was compared between the first and the second exposure, Dravet mice consumed similar amounts, while an increase in the consumption of saccharin solution became evident in wildtype mice (Fig. 3C-D). Findings proved to be comparable in male and female mice.

Assessment of nest-building behavior as a non-essential activity, demonstrated a poorer performance in mice with a Dravet genotype (Fig. 3F).

When analyzing social interaction following a period of social isolation with single-housing, all Dravet mice spent more time engaged in active and less time in passive social interaction, when compared to wildtype littermates (Fig. A.1A-B).

In the elevated plus maze Dravet mice spent an increased time in aversive parts, i.e. the open arms of the maze (Fig. A.1D). In addition, a higher frequency of head dips, as well as a reduction in stretching behavior, was evident in all Dravet mice (Fig. A.1E-F). Sex differences were not observed.

We applied the accelerated rotarod test to address disturbances in motor coordination. During the habituation, animals from both groups showed a “learning” curve with an improvement in the performance with subsequent trials. Thereby, it was evident that the improved performance was related to an increased focus of the animals on the task. When compared to wildtype mice, Dravet mice stayed longer on the rod. Also, females performed better than males in both, control and experimental group (Fig. A.1G-I).

The Spearman correlation coefficients between selected parameters were calculated. Open field test variables including total distance moved showed a significant correlation (all $p<0.001$) with

social interaction (active r=0.69, passive r=-0.52), nest complexity score (r=-0.57), time spent in aversive parts (r=0.58), and number of head-dips in the elevated plus maze test (r=0.76).

*Proteomic profiling*

Proteomic profiling identified over 4000 different proteins in the mouse hippocampus samples. Comparison of protein abundance revealed significant alterations in the expression of 205 and 881 proteins as a consequence of the *Scn1a* genetic deficiency in two- and four-week-old Dravet mice as compared to wildtype littermates, respectively (unpaired t-test, $p<0.05$, Fig. 4A). While the majority of these differentially expressed proteins were up-regulated at the early time point, more proteins proved to be down-regulated at the later time point (Fig. 4B). As a down-regulation of proteins can be a general consequence of neuronal damage and cell loss, we checked the expression of the neuronal marker NeuN, which remained at control level at both time points (data not shown). Moreover, we confirmed that the heterozygous loss-of-function *Scn1a* mutation did not result in changes in $Na_V1.1$ protein abundance regardless of the time point (data not shown). Although one would not necessarily expect changes in protein expression as a consequence of a missense mutation, this finding is of relevance for model characterization as, both, enhanced degradation of a non-functional protein as well as a compensatory up-regulation of expression would have been possible.

A direct comparison of the datasets from both time points revealed an overlap of 67 differentially expressed proteins (Fig. 4A). Most of the proteins maintained the direction of change. However, some proteins were down-regulated at the earlier time point, but later showed an overexpression and vice versa (Fig. 4C).

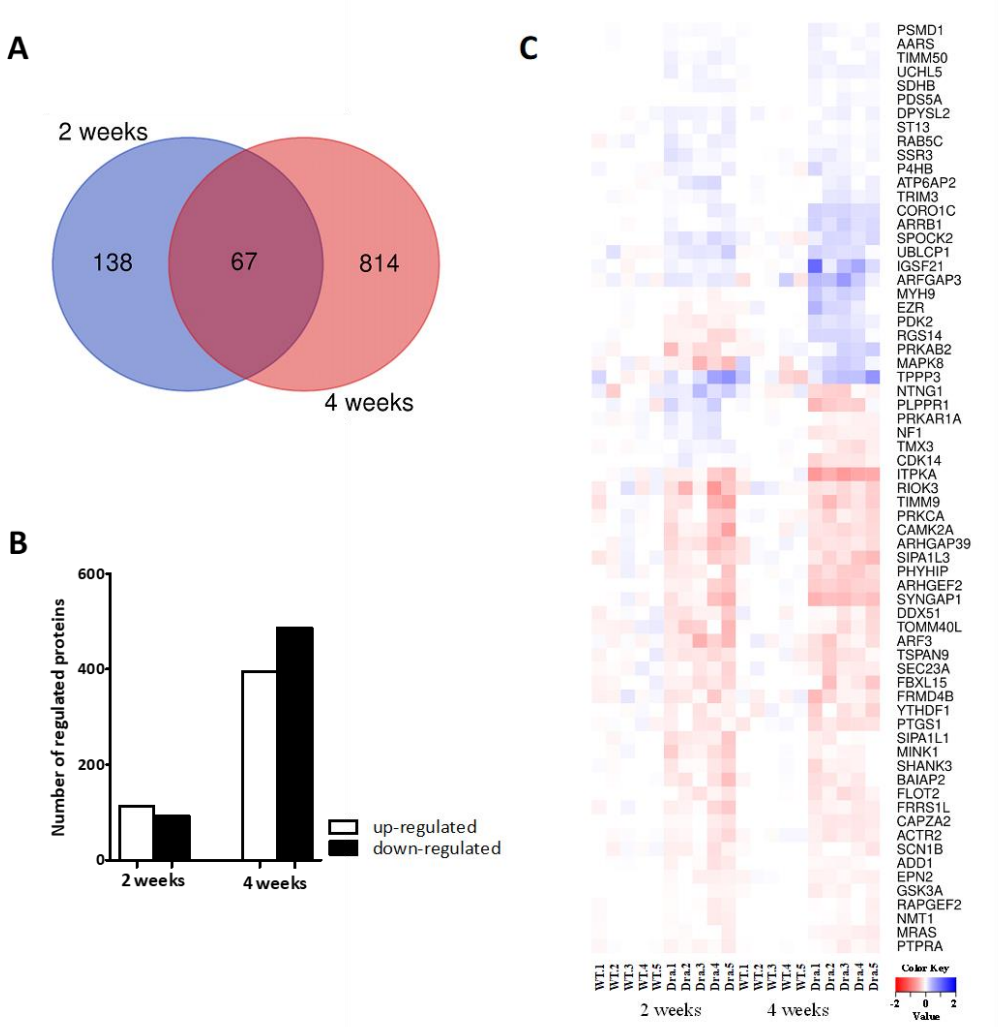


**Fig. 4. Differentially expressed proteins in Dravet mice. A** Overlap in differentially expressed proteins of two- and four-week-old Dravet mice illustrated by Venn diagram. **B** Total number of differentially expressed proteins in two- and four-week-old Dravet mice. **C** Heat map illustrating differential protein expression in in two- and four-week-old Dravet mice.

While a more pronounced proteome alteration was evident at the late time point, the functional annotation of differentially expressed proteins from both time points revealed some similarities in the qualitative pattern of protein regulation with a comparable distribution of regulated proteins to different functional groups (Fig. 5A).

The majority of regulated proteins were classified as nucleic acid binders, enzyme modulators and transferases at the earlier time point, and enzyme modulators, hydrolases and transferases at the later time point. Regarding the molecular function of dysregulated proteins, again a more

pronounced protein regulation was evident at the later time point (Fig. 5B). Proteins associated with catalytic activity and binding exhibited the strongest regulation at both time points.

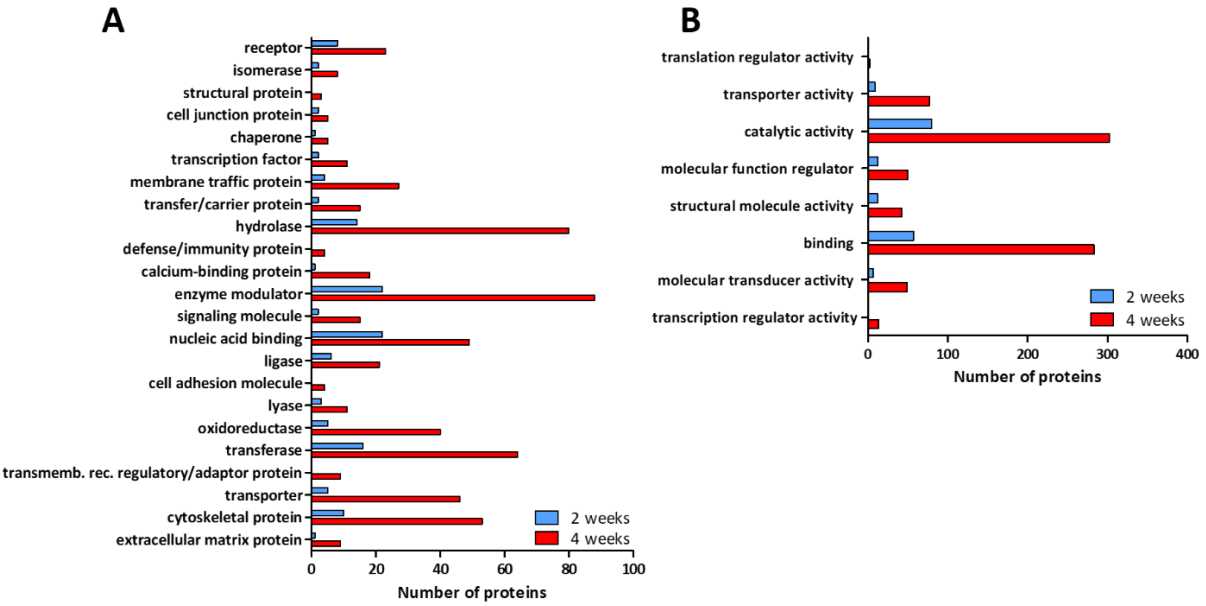


**Fig. 5. Classification of differently expressed proteins.** Functional (**A**) and molecular (**B**) annotation of differentially expressed proteins in two- and four-week-old Dravet mice.

*Differential Protein Expression – early time point*

Proteomic profiling in Dravet mice prior to the occurrence of first spontaneous seizures and epilepsy manifestation can provide information about the process of epileptogenesis as a direct consequence of *Scn1a* genetic deficiency. As mentioned above, a pathway enrichment analysis was completed to obtain general information about the regulation pattern concerning function and neurobiological significance. Pathway enrichment analysis did not identify any significantly regulated pathway ($q<0.01$).

When considering significantly regulated individual proteins in Dravet mice (unpaired t-test, $p<0.05$), the most prominent down-regulation became evident for Ras-specific guanine nucleotide releasing factor 1 (RASGRF1). RASGRF1 is a member of the Ras GTP protein family, which plays a role in synaptic plasticity (Brambilla et al., 1997). RASGRF1 is associated with NMDA receptors (Krapivinsky et al., 2003), and its regulation or dysfunction

has been discussed in the context of epileptogenesis and epilepsy manifestation (Chen et al., 2018; Tonini et al., 2001; Vlaskamp et al., 2019).

Taking the more modest regulation of the majority of significantly regulated proteins into account, we only want to highlight a selection of the remaining list of significantly regulated proteins. These proteins have been chosen considering their putative functional relevance and a minimum change of at least 15 % compared to expression rates in wildtype mice (Fig. 6A).

CAMK2A encodes the alpha subunit of calcium/calmodulin-dependent protein kinase and represents a key player in synaptic plasticity (Lisman et al., 2002). Two-week-old mice exhibited a reduced expression rate that proved to persist at the four-week time point.

Additionally, Dravet mice showed an up-regulation of VEGF receptor KDR (VEGFR2), linked with tight junction disassembly and blood-brain barrier dysfunction, which in turn can contribute to epileptogenesis (Morin-Brureau et al., 2012).

Cytidine triphosphate synthetase 2 (CTPS2) is a protein mediating CTP synthesis from UTP a process that is linked with glutamine deamination to glutamate (Kassel et al., 2010). In two-week-old Dravet mice, we obtained evidence for an increased expression level of CTPS2.

*Differential Protein Expression – later time point*

Proteomic profiling following epilepsy manifestation capturing direct and indirect consequences of *Scn1a* deficiency in Dravet mice revealed 881 regulated proteins (unpaired t-test, $p<0.05$) and 42 regulated pathways ($q<0.01$, Table 1). A heat map, which illustrates the level of individual protein change in relation to the mean of the wildtype group is presented in Fig. 6B.

Pathways functionally linked to synaptic transmission dominated the list of significantly enriched pathways, in total comprising five pathways associated with general synaptic function and its regulation (*Neurotransmitter receptors and postsynaptic signal transmission*; *Transmission across Chemical Synapses*; *Protein-protein interactions at synapses*; *Synaptic*

*adhesion-like molecules* and *Neurexins and neuroligins* with corresponding q-values $4.14e^{-05}$; $4.14e^{-05}$; $2.33e^{-04}$; 0.002; 0.006). The list of differentially expressed proteins linked with these pathways comprised 68 proteins. Several of these proteins proved to be down-regulated as a consequence of the genetic deficiency. These include synaptic adhesion-like molecules such as neurexins and neuroligins (Fig. 6B: NLGN2, NLGN3), which mediate trans-synaptic signaling and facilitate processing of complex signals in neuronal networks (Südhof, 2008), as well as postsynaptic density (PSD) proteins including proteins of the membrane-associated guanylate kinase protein family (Fig. 6B-a), and scaffolding proteins (Fig. 6B-b). Moreover, these pathways included proteins associated with synaptic vesicles (Fig. 6B-c).

Proteins linked with ion channel function showed a complex regulation pattern in Dravet mice. Thereby, the abundance of voltage-gated calcium channels (Fig. 6B-d), voltage-gated potassium channels (Fig. 6B-e) and two inward-rectifier potassium channels (Fig. 6B-f) was reduced in Dravet mice. Another inward-rectifier potassium channel (Fig. 6B: KCNJ10) was up-regulated in Dravet mice.

Interestingly, several neurotransmitter receptor proteins exhibited a differential expression pattern in Dravet mice. The list of these proteins was dominated by glutamatergic receptor proteins (Fig. 6B-g), which all proved to be expressed at lower levels in Dravet mice. In addition, a change in expression of three $GABA_A$ receptor subunits (Fig. 6B-h) and of two $GABA_B$ receptor subunits (Fig. 6B-i) became evident with an induction of GABRA1 and GABBR1, and a down-regulation of GABRB1, GABRB3 and GABBR2.

In the context of neurotransmitter signaling, it is of additional interest that four pathways involved in glutamatergic signaling, specifically AMPA and NMDA receptor activation, binding, and synapses were regulated in Dravet mice (*Glutamatergic synapse*; *Unblocking of NMDA receptor, glutamate binding and activation*; *Trafficking of AMPA receptors*; *Glutamate binding, activation of AMPA receptors and synaptic plasticity* with q-values $1.4e^{-04}$; 0.001; 0.002; 0.002, respectively*)*. Thereby, Dravet mice exhibited a reduced expression of iono- and

metabotropic glutamate receptors, glutamate transporters (Fig. 6B: EAAT1, EAAT2), and glutamine synthetase (Fig 6B: GLUL).

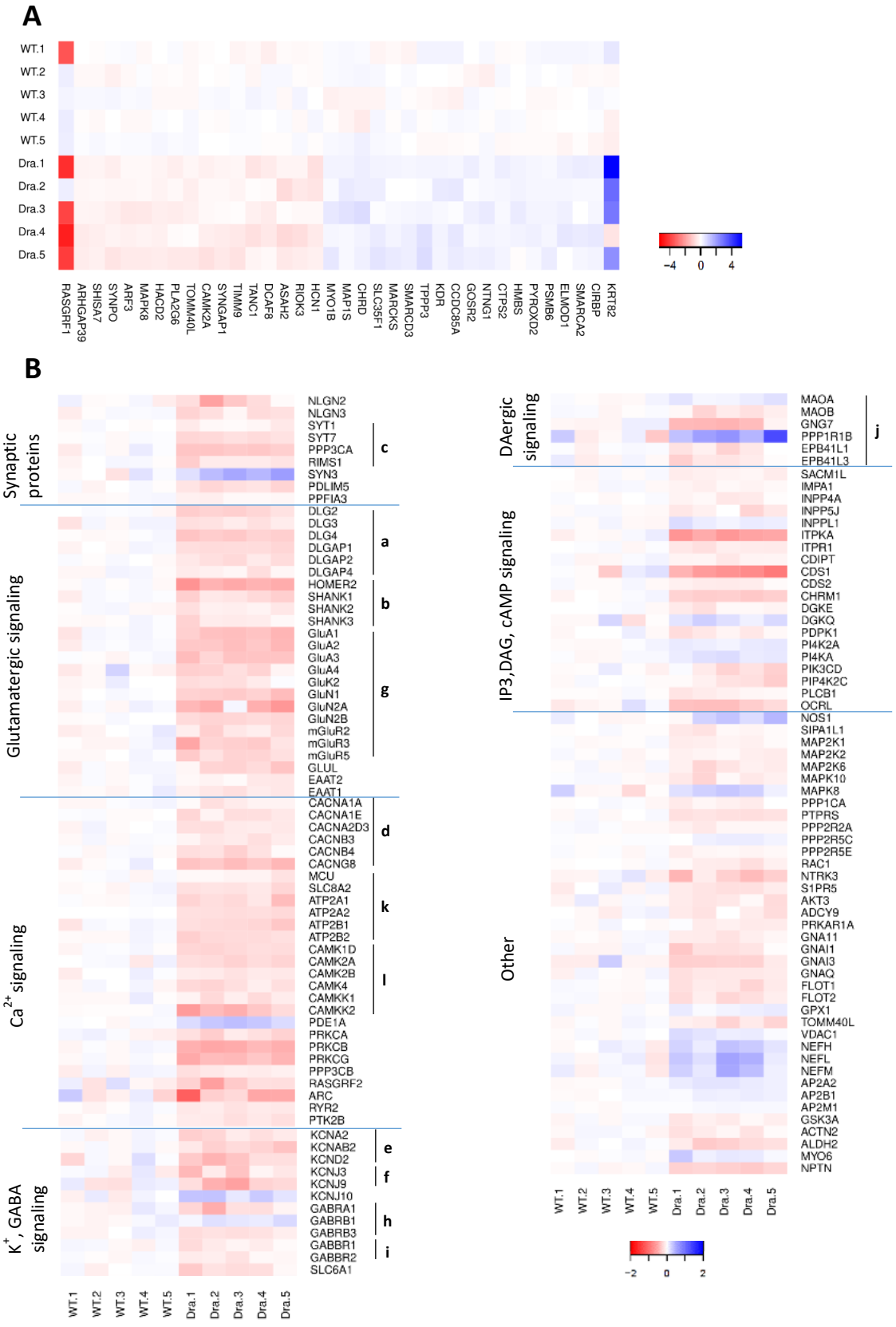

**Fig. 6. Expression analysis of proteins significantly regulated in Dravet mice before and following epilepsy manifestation. A** Expression analysis of proteins significantly regulated in Dravet mice prior to epilepsy manifestation, with a minimum change of at least 15 % compared to expression rates in wildtype mice. R package 'gplots' was used for heat maps and the respective color key is provided next to the heat map. **B** Expression analysis of proteins linked to all significantly enriched pathways in Dravet mice following epilepsy manifestation. R package 'gplots' was used for heat maps. The heat map illustrates the fold change in protein level in relation to the mean of the wildtype group and the respective color key is given under the heat map. **a** PSD membrane-associated guanylate kinase protein family, **b** PSD scaffolding proteins, **c** proteins associated with synaptic vesicles, **d** voltage-gated calcium channel proteins, **e** voltage-gated potassium channel proteins, **f** inward-rectifier potassium channel proteins, **g** glutamatergic receptor proteins**, h** $GABA_A$ receptor subunits, **i** $GABA_B$ receptor subunits**, j** proteins functionally associated with dopaminergic (DAergic) synapse function, **k** calcium transporter proteins, **l** calcium/calmodulin-dependent protein kinases. (Blue cell color indicates an up-regulation, while red cell color stands for a down-regulation).

Pathway enrichment analysis also revealed an overrepresentation of proteins functionally associated with dopaminergic synapse function (q=0.002, Fig. 6B-j). The changes in the pathway were dominated by alterations in the expression of proteins regulating dopamine metabolism or stabilizing D2 and D3 receptors on plasma membranes with MAOA being up-regulated and MAOB, EPB41L1, EPB41L3 being down-regulated. In four-week-old Dravet mice, reduced expression levels were also evident for GNG7, the G protein responsible for $A_{2A}$ adenosine or D1 dopamine receptor-induced neuroprotective responses (Schwindinger et al., 2012). Another protein, which plays a role in synaptic plasticity and can be modulated by both, dopaminergic D1 and glutamatergic NMDA receptors is the neuronal phosphoprotein PPP1R1B. Our data set revealed an overexpression in the hippocampus of four-week-old Dravet mice, which was further confirmed by immunohistochemistry. All Dravet animals demonstrated a marked hippocampal overexpression, particularly evident in CA1 stratum pyramidale neurons (Fig. 7A-B).

In four-week-old mice, pathway enrichment analysis also demonstrated an over-representation of proteins functionally linked to calcium signaling ($q=1.4e^{-04}$). Individual protein changes pointed to a down-regulation of calcium channel proteins and calcium transporters (Fig. 6B-k).

Calcium/calmodulin-dependent protein kinases (Fig. 6B-l) proved to be reduced in Dravet mice.

The list of regulated pathways also included a pathway involved in secondary cell signaling (*Phosphatidylinositol signaling pathway*, q=0.008). Moreover, an over-representation of proteins linked with the *nitric oxide (NO) signaling pathway* (q=0.005) became evident. In this context, the increased level of nitric oxide synthase, the main enzyme responsible for NO synthesis from L-arginine (Knowles et al., 1994), seems to be of interest.

In addition to pathway enrichment analysis, we also identified the proteins with the most prominent regulation pattern. The strongest up-regulation was evident for the intermediate filament proteins glial fibrillary acidic protein (GFAP) and vimentin. The expression of both proteins was elevated by at least two-fold in Dravet mice.

The proteins with the strongest down-regulation were TRIM32 and HSD11B1. Proteomic profiling pointed to a reduction in HSD11B1 expression in Dravet mice, with a two times lower abundance than in wildtype mice. This finding was further confirmed by immunohistochemistry. An apparent down-regulation of the protein was evident in the hippocampus with the most obvious reduction in the hilus (Fig. 7C-D).

*Comparison with published data from models of acquired epilepsy*

Previously, we have completed a proteomic profiling study in an electrical post-status epilepticus (SE) rat model (Bauer et al., 2016; Keck et al., 2017; Keck et al., 2018; Walker et al., 2016). In that study, we analyzed the course of proteome alterations during epileptogenesis focusing on the early post-insult (2 days post SE), latency (10 days post SE) and chronic phase (8 weeks post SE).

In order to compare molecular alterations in a model of acquired and a model of genetic epilepsy, we have directly compared the respective time points before and following epilepsy manifestation. The overlap between the lists of differentially expressed proteins in two-week-

old Dravet mice and in the post-SE latency phase comprised 25 proteins, of which 19 showed the same direction of change (Fig. 7E). In general, these nine up- and ten down-regulated proteins exhibited a more pronounced regulation in the model of acquired epilepsy. This pattern was particularly evident for SHANK3 protein, a scaffold protein of the PSD, and CKAP4, a cytoskeleton-associated protein and cell proliferation promoter.

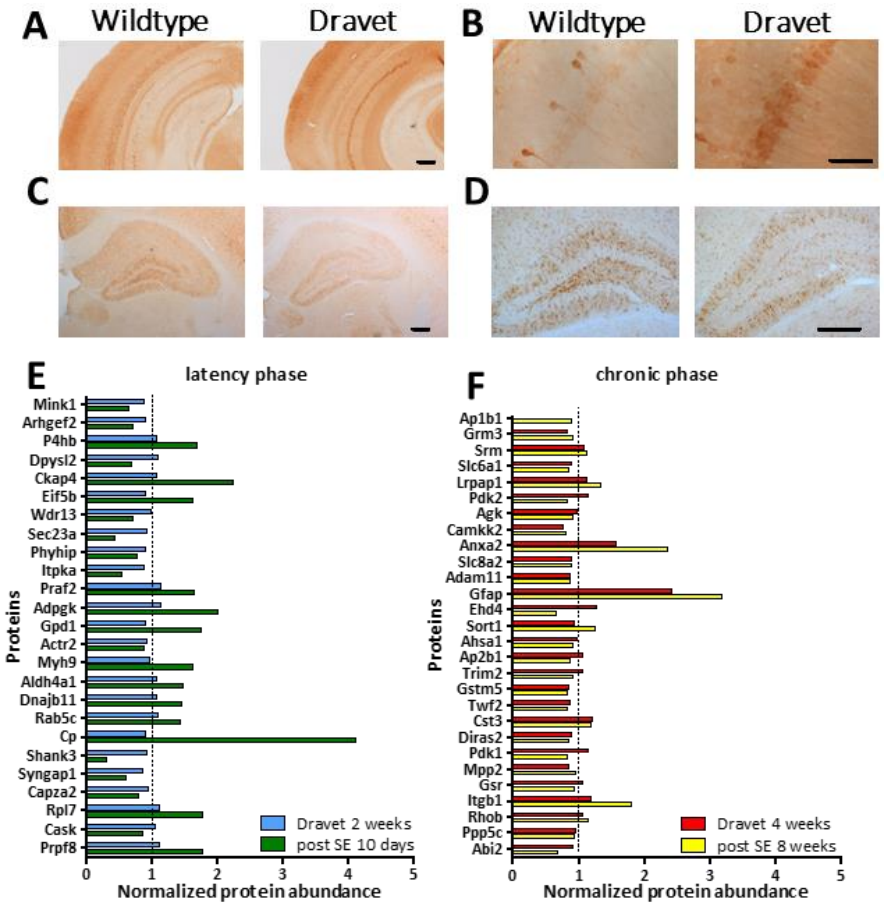


**Fig. 7. Immunohistochemical staining of representative proteins and comparison with electrical post SE induced rat model. A-B** Representative immunohistochemical staining of PPP1R1B protein in the hippocampus (low magnification, **A**) and hippocampal CA1 region (high magnification, **B**). A pronounced protein immunostaining was particularly evident in the CA1 region in Dravet mice. **C-D** Immunohistochemical staining of HSD11B1 protein in the hippocampus (low magnification, **C**) and hippocampal hilar region (higher magnification, **D**). Protein immunoreactivity was reduced in Dravet mice, which was particularly evident in the hilus. Scale bars = 200 µm (A, C, D) and 50 µm (B). **E** Proteins significantly regulated before epilepsy manifestation in two-week-old Dravet mice and 10 days following SE induction in the kainate post-SE model. **F** Proteins significantly regulated during the chronic phase with spontaneous generalized seizures, corresponding to four-week-old Dravet mice and 8 weeks following the SE induction in the kainate post-SE model. GFAP and ANXA2 were the two most up-regulated proteins in both animal models.

Comparison of data sets obtained following epilepsy manifestation confirmed a regulation of 28 proteins in both epilepsy models. Twenty of these proteins showed the same direction of change. A general trend for a stronger regulation in one of models was not evident at this time point. Interestingly, two proteins showed a strong induction in both epilepsy models: GFAP, known as a marker of mature astrocytes, and ANXA2, a pro-angiogenic protein (Fig. 7F).

Considering that species differences may affect the comparison between these data sets, we additionally compared our present data from the mouse Dravet model with published proteomic data from a mouse model of mesiotemporal lobe epilepsy reported by *Bitsika et al.* (Table 2). Comparison of data sets prior to epilepsy manifestation, i.e. from the early time point in the Dravet model and from 3 days following kainate-induced SE, revealed an overlap of four proteins with down-regulation in both epilepsy models. Three of these proteins are functionally linked with synaptic transmission. These comprise one presynaptic (PCLO) and two postsynaptic proteins (SHANK3, BAIAP2). The fourth protein that proved to be regulated in both models is SIPA1L1, involved in regulation of cell processes (Gao et al., 1999).

Following epilepsy manifestation, an interesting overlap has been observed between four-week-old Dravet mice and mice 30 days after the kainic acid injection. This overlap between the lists of differentially expressed proteins comprised 44 proteins with 23 up-regulated and 21 down-regulated in both, genetic and acquired epilepsy. Protein regulation was more prominent in the acquired epilepsy model (data not shown). Among others, the list of co-regulated proteins included cytoskeletal proteins (ARPC1A; DBN1; MAP1A; ADD2; MYO6, PLEC; EZR; CTTNBP2) as well as proteins linked with angiogenesis (ANXA4; VIM; ITGAV) and synaptic plasticity (SYNGAP1; DLG4; BAIAP2; PPP3CA; PPP3CB; PRKCG; RPH3A; SLC6A1).

## *Discussion*

Large-scale proteomic analysis in a novel conditional mouse model of Dravet syndrome with *Scn1a* genetic deficiency provided comprehensive information about molecular alterations characterizing different disease phases. Respective information about the proteomic signature of the Dravet syndrome suggests possible pathophysiological mechanisms that beyond the *Scn1a* haploinsufficiency may be involved in epileptogenesis and ictogenesis in Dravet mice.

As a basis for the proteomic analysis, we initially aimed to validate the novel conditional knock-in mouse model of Dravet syndrome with a heterozygous *Scn1a*-A1783V mutation. A model with this mutation has previously been generated on a pure C57BL/6J background (Ricobaraza et al., 2019) and a mixed (90:10) C57BL/6J and 129S1 background (Kuo et al., 2019) resulting in a more severe phenotype and higher mortality rate. Here, we characterized the model bred on a mixed (50:50) C57BL/6J and 129S1 background with an *Hprt* promoter mediated neuronal knock-in. We confirmed the development of spontaneous seizures and an increased susceptibility for hyperthermia-induced seizures, and demonstrated a mortality rate of 40 %. Besides the seizure phenotype, we also observed behavioral alterations dominated by hyperactivity, which seem to reflect hyperactivity and attention deficits as common behavioral symptoms in patients with Dravet syndrome (Battaglia et al., 2016; Besag, 2004; Dravet, 2011). When compared to other animal models of Dravet syndrome with heterozygous *Scn1a* mutation, our model showed a similar age for onset of spontaneous seizures, increased susceptibility to thermally provoked seizures and notable hyperactivity. The SUDEP rates were relatively low as compared to other models occurring within a short time frame (Table A.2). With the approaches used in this study, we failed to detect motor and social deficits in Dravet mice, which have been reported in selected mouse models (Table A.2). However, an improved performance on accelerated rotarod test was also found in another mouse model (Ito et al., 2013), suggesting the test itself may not be appropriate to assess the Dravet-associated

alterations in motor function and coordination. In this context, it is of interest that we confirmed alterations in gait in a follow-up study based on a catwalk test and a detailed assessment of gait (Miljanovic et al., under revision).

To our knowledge, we were the first ones to report anhedonia-associated behavior in a Dravet mouse model indicating that *SCN1A* deficiency may have an impact on the affective state and may predispose to depression.

Information about body weight development has not been provided for all Dravet mouse models, so that it is not clear for several models whether there was no delay or whether body weight development was not assessed and documented. So, an impact of the genetic deficiency on body weight development has only been reported in selected Dravet mouse models with heterozygous (Ricobaraza et al., 2019) and homozygous mutation (Martin et al., 2010; Ogiwara et al., 2007). In line with these reports, we observed a transient delay in body weight around weaning with animals catching up within five (females) or 20 (males) days following weaning. Taken together, our comprehensive characterization demonstrated an excellent face validity of the Dravet model, thus providing a perfect basis for investigating molecular patterns involved in disease manifestation and its further development.

*GABAergic, glutamatergic, and dopaminergic neurotransmission*

Loss of function of sodium channel subunits encoded by the *SCN1A* gene in GABAergic interneurons is considered as the main source of hyperexcitability and ictogenesis in Dravet patients (Brunklaus and Zuberi, 2014; Catterall, 2018) and animals carrying a respective mutation (Almog et al., 2019; Kalume et al., 2015a; Mantegazza and Broccoli, 2019; Mistry et al., 2014; Rubinstein et al., 2015b; Salgueiro-Pereira et al., 2019; Tai et al., 2014; Tsai et al., 2015; Yu et al., 2006). However, an impact of cellular consequences in excitatory neurons on seizure susceptibility has also been suggested based on experimental findings. For instance, hyperexcitability of dissociated hippocampal pyramidal neurons (Mistry et al., 2014) and

granule cells in dentate gyrus (Tsai et al., 2015) in the period of chronic epilepsy, may promote life-threatening seizures, known to worsen mice phenotype (Dutton et al., 2017; Salgueiro-Pereira et al., 2019). On the other hand, Ogiwara and colleagues demonstrated that *Scn1a* haploinsufficiency in hippocampal excitatory neurons, can ameliorate seizures in Dravet mice (Ogiwara et al., 2013). Interestingly, Almog and colleagues showed how hyperexcitability of CA1 pyramidal neurons during the pre-epileptic state can switch to hypoexcitability during the epileptic state in Dravet mice, suggesting the role of these neurons in seizure propagation (Almog et al., 2019).

Altogether, these data already suggest that, both, inhibitory and excitatory neurotransmission may be directly and indirectly affected by $Na_V1.1$ dysfunction. Interestingly, the proteomic data suggest differential expression of multiple proteins linked with inhibitory and excitatory neurotransmission in *Scn1a*$^{+/-}$ mice.

With changes in the abundance of various $GABA_A$ and $GABA_B$ receptor subunits, our findings indicate that signaling via both GABA receptor systems can be altered as a consequence of an *Scn1a* genetic deficiency with potential consequences for phasic and tonic inhibition. Thereby it needs to be considered that, both, an up- and a down-regulation was observed for the different receptor subunits.

Concerning glutamatergic signaling, proteomic patterns in Dravet mice revealed a comprehensive down-regulation of subunits of NMDA, AMPA, and kainate glutamate receptors. In this context, it is of additional interest that several proteins linked with NMDA receptor function in the post-synaptic density showed a decreased abundance in Dravet mice. In addition, SYNGAP1, a post-synaptic density protein that negatively modulates trafficking of AMPA receptors to the membrane (Jeyabalan and Clement, 2016), also exhibited a dysregulation in the hippocampus as a consequence of the *Scn1a* deficiency.

Concerning the expression patterns of metabotropic glutamate receptor proteins, one needs to take into account that some of these receptors serve as a negative feedback function, with a

limitation of excessive glutamate secretion (Dedeurwaerdere et al., 2015). Along this line, reduced expression of the class two metabotropic glutamate receptor proteins mGluR2 and mGluR3 in Dravet mice might be of functional interest.

In addition to alterations in receptor proteins and PSD proteins, the lowered abundance of glutamine synthase and higher abundance of CTPS2, which contributes to deamination of glutamine to glutamate (Kassel et al., 2010), may imply that changes occur in glutamate metabolism.

Taken together our proteomic data set suggests that complex alterations occur affecting GABA and glutamatergic signaling. The direction of the alterations seems to suggest that some of these changes may contribute to hyperexcitability, whereas others may rather reflect compensatory mechanisms. Further research is necessary to explore the potential functional consequences.

Depending on the receptor subtype, dopaminergic signaling can affect seizure thresholds (Bozzi and Borrelli, 2013). Altered abundance of the dopamine metabolizing enzymes $MAO_A$ and $MAO_B$, of a downstream effector protein of D1 receptors (Bozzi and Borrelli, 2013; O'Sullivan et al., 2008), and of proteins stabilizing D2 and D3 receptors, suggests that it may also be of interest to assess dopamine concentrations in the brain of Dravet mice.

*Voltage-gated ion channels*

Voltage-gated ion channels affect neuronal excitability in different subcellular localizations therefore serving as important target sites for different antiseizure drugs (Sills and Rogawski, 2020).

At the presynaptic level, P/Q- and N-type calcium channels represent important regulators of neurotransmitter release (Kassel et al., 2010). Thus, the extensive down-regulation of voltage-gated calcium channel subunits may constitute a compensatory mechanism counteracting increased neuronal excitability characterizing the Dravet syndrome. In this context, it is of additional interest that various calcium/calmodulin-dependent protein kinases (CaMK)

subtypes proved to be reduced in hippocampal tissue from Dravet mice. CaMK are important regulators, which translate intracellular calcium concentrations into phosphorylation patterns with functional consequences for the targeted proteins (Swulius and Waxham, 2008).

Several potassium channels regulate outward potassium currents, thereby affecting membrane polarization and neuronal excitability (Villa and Combi, 2016). Proteomic data revealed a reduction of three potassium channel subunits (Kv1.2, Kv2.1 and Kv4.2), that attenuate back-propagating action potentials and prevent highly repetitive neuronal firing as one of the pathophysiological hallmarks of epileptic seizures (Niday and Tzingounis, 2018).

In summary, various changes in voltage-gated ion channel proteins occur in the Dravet mouse model. The reduction of calcium channel subunits and of potassium channel subunits may have contrasting consequences, which, however, need to be further assessed in follow-up investigations.

While previous studies also suggested alterations in sodium channel subunits with an up-regulation of $Na_V1.3$ in hippocampal interneurons in a different Dravet mouse model (Yu et al., 2006), our data did not detect this protein in the *Scn1a*-A1783V mouse model.

*Astrogliosis, angiogenesis and NO signaling*

Reactive astrogliosis can promote hyperexcitability, affect inflammatory signaling, and disrupt integrity of the blood–brain barrier (Devinsky et al., 2013). Increased GFAP abundance provides evidence for astrogliosis in the *Scn1a*-A1783V mouse model. This finding is in line with previous reports describing astrogliosis in other mouse models of Dravet syndrome (Alonso Gómez et al., 2018; Hawkins et al., 2019). Alterations in the astrocytic functional state are further supported by evidence for a reduction of astroglial excitatory amino acid transporters (EAAT1 and EAAT2) and for an overexpression of the inward rectifying potassium channel Kir4.1 (KCNJ10). These findings may imply contrasting functional consequences, which, however, need to be confirmed by further investigations.

Following seizure onset, we observed an additional regulation of ANXA2 and vimentin, which both act as modulators of VEGF signaling and angiogenesis (Dave and Bayless, 2014; Liu and Hajjar, 2016), previously discussed as a pro-epileptogenic factor and as a potential target for antiepileptogenesis (Morin-Brureau et al., 2012; Rigau et al., 2007).

Proteomic profiling also revealed a dysregulation of nitric oxide (NO) signaling in Dravet mice with an increased expression of neuronal nitric oxide synthase (nNOS) following onset of spontaneous recurrent seizures. Considering that NO can induce reactive glial proliferation and promote angiogenesis (Arhan et al., 2011; Morbidelli et al., 2004), it is discussed that it might play a role during epileptogenesis and for hyperexcitability in the epileptic brain.

*Proteomic alterations before epilepsy manifestation*

While rather limited alterations were evident before epilepsy manifestation, these changes may be of interest as they might provide information about molecular mechanisms that occur as an early consequence of the *SCN1A* genetic deficiency and that may contribute to disease onset. In this context, the down-regulation of RASGRF1 might be of functional relevance considering the fact that a contribution of RASGRF1 to epileptogenesis has been suggested based on a study with genetic and pharmacological targeting (Bao et al., 2018). Thus, it might be of interest to further explore a potential contribution of early RASGRF1 down-regulation to disease manifestation and seizure onset in Dravet mice.

*Shared and common pathophysiological mechanisms: Dravet model versus models of acquired epilepsy*

The molecular perspective taken in the present study revealed, both, differences to and commonalities with mechanisms reported for acquired epilepsies following an initial brain insult. Our proteomic data set provides evidence that astrogliosis, enhanced angiogenesis and NO signaling might be mechanisms that do not only characterize pathophysiology of acquired

epilepsy, but may also contribute to hyperexcitability states in Dravet syndrome. However, the findings rather argue against a relevant induction of pro-inflammatory signaling pathways, which characterizes epileptogenesis and disease manifestation of acquired epilepsies (Fabene et al., 2010; Klein et al., 2018; Terrone et al., 2017; Vezzani, 2014).

The *Scn1a* deficiency in the *Scn1a*-A1783V mouse model triggers complex alterations, which may affect GABAergic, glutamatergic and dopaminergic signaling at multiple levels including synaptogenesis, synaptic vesicle trafficking, neurotransmitter release, receptor subunit expression and composition, and post-synaptic density modulation of receptor function. Synaptic plasticity and more specifically plasticity of GABAergic and glutamatergic mechanisms has been repeatedly described in different models of acquired epilepsy and in the brain of patients with temporal lobe epilepsy (Joshi and Kapur, 2012; Klein et al., 2018; Scharfman and Brooks-Kayal, 2014).

*Study limitations*

Considering the whole proteome approach applied to hippocampal samples and the characteristics of the mouse model, one also needs to take respective limitations into account. Firstly, disease manifestation occurs early on in Dravet mice resulting in a delayed postnatal bodyweight development, which in itself may also impact molecular alterations in the brain. Moreover, considering that untargeted proteomic studies are limited to screening proteins in the entire sample, further studies investigating the expression patterns in different hippocampal sub-regions and cell types along with studies addressing the functional consequences are needed to provide more specific information allowing conclusion about the functional relevance of the findings. The present findings provide a perfect basis to design respective studies applying targeted proteomic approaches. Finally, one needs to consider that bulk approaches imply the risk to miss relevant changes in a selected cell population due to a dilution effect.

As a matter of course interpretation needs to take into account that molecular alterations can be a mere consequence of repeated seizure activity or disease-associated alterations without functional implications. Thus, as repeatedly pointed out, it is of utmost relevance to further assess functional implications in future studies.

## *Conclusions*

In conclusion, the whole proteome analysis in a mouse model of Dravet syndrome demonstrated complex molecular alterations in the hippocampus as a consequence of the genetic deficiency. Some of these alterations may have an impact on excitability or may serve as a compensatory function, which, however, needs to be further confirmed by future investigations.

The findings provide evidence that genetic epilepsy due to *Scn1a* haploinsufficiency may share pathophysiological mechanisms with acquired epilepsies developing following brain insults.

Moreover, the proteomic data indicate that due to molecular consequences of the genetic deficiency the pathophysiological mechanisms become more complex during the course of the disease, and that the management of Dravet syndrome may need to consider further molecular and cellular alterations. Along this line, based on functional follow-up studies the data sets may provide valuable guidance for future development of novel therapeutic approaches.

## *Acknowledgements*

The authors thank Sarah Driebusch, Verena Buchecker, Fabio Wolf, Sieglinde Fischlein, Katharina Gabriel and Katharina Schönhoff for their excellent technical assistance.

We are very grateful to Ana Mingorance and the Dravet Syndrome Foundation from Spain for their efforts and investment to generate a commercially available Dravet mouse line in collaboration with the Jackson laboratory. Moreover, we thank Ana Mingorance for all her further support and the discussions about our plannings and data.

This research is supported by a grant of the Deutsche Forschungsgemeinschaft (DFG, FOR 2591, GZ: PO681/9-1).

## *Declarations of Interest*

None.

## *Tables*

**Table 1. Overrepresented pathways in four-week-old mice (q<0.01, ConsensusPathDB)**

| p-value | q-value | Pathway | Source | Overlap members |
|---|---|---|---|---|
| 0.000 | 0.000 | *Neuronal System* | Reactome | SLC6A1; CACNG8; PDLIM5; GLUA2; GLUA3; GLUA1GLUA1; GLUA4; CACNA1E; CAMKK1; GLUL; KCND2; CACNA2D3; GABBR1; GABBR2; CACNB4; KCNA2; AP2B1; GNAI1; DLGAP2; DLG3; DLG2; GNAI3; PPFIA3; GABRA1; CACNB3; CACNA1A; CAMK4; NTRK3; AP2M1; ADCY9; DLGAP1; GRIK2; DLGAP4; SIPA1L1; MGLUR5; GLUN1; HOMER2; RIMS1; EPB41L1; PLCB1; EPB41L3; KCNJ10; NLGN2; NLGN3; NPTN; PRKCA; PRKCB; CAMK2A; CAMK2B; KCNAB2; PRKCG; AP2A2; GABRB1; GABRB3; SHANK3; SHANK2; SHANK1; DLG4; KCNJ3; ACTN2; PTPRS; RASGRF2; SYT1; KCNJ9; MYO6; ALDH2; SYT7; GLUN2B; GNG7; MAOA; GLUN2A; FLOT1; FLOT2; NEFL; PDPK1; SYN3; EAAT2; EAAT1 |
| 0.000 | 0.000 | *Neurotransmitter receptors and postsynaptic signal transmission* | Reactome | GLUA2; GLUA3; GLUA1; GLUA4; ADCY9; GABBR1; GABBR2; GABRA1; AP2B1; GNAI1; CACNG8; DLG3; NPTN; DLG4; NEFL; CAMK4; GNAI3; AP2M1; GLUN1; EPB41L1; PLCB1; KCNJ10; PRKCA; PRKCB; CAMK2A; CAMK2B; PRKCG; AP2A2; GABRB1; GABRB3; KCNJ3; ACTN2; RASGRF2; KCNJ9; MYO6; GLUN2B; GNG7; CAMKK1; GLUN2A; PDPK1; GRIK2 |
| 0.000 | 0.000 | *Transmission across Chemical Synapses* | Reactome | SLC6A1; GLUA2; GLUA3; GLUA1GLUA1; GLUA4; ADCY9; CAMKK1; GLUL; CACNA2D3; GABBR1; GNAI3; GABRA1; |

| | | | | |
|---|---|---|---|---|
| | | | | AP2B1; GNAI1; CACNG8; DLG3; NPTN; DLG4; CACNB3; CACNA1A; CACNA1E; CAMK4; CACNB4; AP2M1; GRIK2; GLUN1; RIMS1; EPB41L1; PLCB1; KCNJ10; PRKCA; PRKCB; CAMK2A; CAMK2B; PRKCG; GABBR2; AP2A2; GABRB1; GABRB3; PPFIA3; KCNJ3; ACTN2; RASGRF2; SYT1; KCNJ9; MYO6; ALDH2; GLUN2B; GNG7; MAOA; GLUN2A; NEFL; PDPK1; SYN3; EAAT2; EAAT1 |
| 0.000 | 0.000 | *Amphetamine addiction - Homo sapiens (human)* | KEGG | GLUN2B; PPP1R1B; PPP1CA; PRKCA; GLUA3; GLUA1; CAMK4; CAMK2B; CAMK2A; GLUA2; MAOB; MAOA; ARC; GLUA4; PRKCB; GLUN2A; PPP3CA; PPP3CB; GLUN1; PRKCG |
| 0.000 | 0.000 | *Calcium signaling pathway - Homo sapiens (human)* | KEGG | CAMK1D; ATP2A2; NOS1; PRKCG; CACNA1E; PTK2B; VDAC1; ATP2A1; ATP2B2; CACNA1A; PDE1A; RYR2; CAMK4; ITPKA; MGLUR5; GLUN1; SLC8A2; PLCB1; PRKCA; PRKCB; CAMK2A; CHRM1; CAMK2B; ATP2B1; ITPR1; MCU; GNAQ; ADCY9; GLUN2A; GNA11; PPP3CA; PPP3CB |
| 0.000 | 0.000 | *Glutamatergic synapse - Homo sapiens (human)* | KEGG | GLUA2; GLUA3; GLUA1; GLUA4; GLUL; GNAI3; GNAI1; DLG4; CACNA1A; DLGAP1; MGLUR5; GLUN1; HOMER2; MGLUR2; MGLUR3; PLCB1; PRKCA; PRKCB; PRKCG; ITPR1; SHANK3; SHANK2; SHANK1; KCNJ3; GNAQ; GRIK2; ADCY9; GLUN2B; GNG7; GLUN2A; PPP3CA; PPP3CB; EAAT2; EAAT1 |
| 0.000 | 0.000 | *Protein-protein interactions at synapses* | Reactome | GLUA3; GLUA1; GLUA4; DLG3; DLG2; PPFIA3; NTRK3; DLGAP2; DLGAP1; DLGAP4; SIPA1L1; MGLUR5; GLUN1; HOMER2; EPB41L1; PDLIM5; EPB41L3; NLGN2; NLGN3; SHANK3; SHANK2; SHANK1; DLG4; PTPRS; |

| | | | | |
|---|---|---|---|---|
| | | | | SYT1; SYT7; GLUN2B; GLUN2A; FLOT1; FLOT2 |
| 0.000 | 0.001 | *Unblocking of NMDA receptor. glutamate binding and activation* | Reactome | ACTN2; DLG4; GLUA2; GLUA3; GLUA1; CAMK2A; GLUA4; GLUN2B; GLUN2A; CAMK2B; NEFL; GLUN1 |
| 0.000 | 0.002 | *Dopaminergic synapse - Homo sapiens (human)* | KEGG | GLUA2; GLUA3; GLUA1; GLUA4; AKT3; MAPK10; GNAI3; GNAI1; PPP1R1B; MAOB; CACNA1A; MAPK8; PLCB1; PRKCA; PRKCB; PPP2R2A; CAMK2A; CAMK2B; PRKCG; PPP3CA; ITPR1; KCNJ3; GNAQ; PPP1CA; KCNJ9; GSK3A; GLUN2B; GNG7; MAOA; GLUN2A; PPP2R5E; PPP3CB; PPP2R5C |
| 0.000 | 0.002 | *Trafficking of AMPA receptors* | Reactome | EPB41L1; CACNG8; PRKCB; DLG4; PRKCA; GLUA3; GLUA1; CAMK2B; CAMK2A; PRKCG; MYO6; AP2M1; GLUA2; GLUA4; AP2A2; AP2B1 |
| 0.000 | 0.002 | *Glutamate binding. activation of AMPA receptors and synaptic plasticity* | Reactome | EPB41L1; CACNG8; PRKCB; DLG4; PRKCA; GLUA3; GLUA1; CAMK2B; CAMK2A; PRKCG; MYO6; AP2M1; GLUA2; GLUA4; AP2A2; AP2B1 |
| 0.000 | 0.002 | *Synaptic adhesion-like molecules* | Reactome | DLG3; PTPRS; DLG4; GLUA3; GLUA1; GLUA4; GLUN2B; GLUN2A; FLOT1; FLOT2; GLUN1 |
| 0.000 | 0.003 | *Neuroactive ligand-receptor interaction - Homo sapiens (human)* | KEGG | GLUA2; GLUA3; GRIK2; GLUA1; S1PR5; GLUN2B; GLUN2A; GLUA4; CHRM1; GABBR1; MGLUR5; GABRB1; GABBR2; GABRB3; GABRA1; GLUN1; MGLUR2; MGLUR3 |
| 0.000 | 0.003 | *Amyotrophic lateral sclerosis (ALS) - Homo sapiens (human)* | KEGG | GPX1; TOMM40L; RAC1; NEFM; NEFL; GLUA1; NEFH; GLUN2B; GLUA2; NOS1; GLUN2A; MAP2K6; PPP3CA; PPP3CB; GLUN1; EAAT2 |

| | | | | |
|---|---|---|---|---|
| 0.000 | 0.005 | *nitric oxide signaling pathway* | BioCarta | NOS1; DLG4; PRKCA; PRKCB; CAMK2B; GLUN2B; GLUN2A; PRKAR1A; PPP3CA; PPP3CB; GLUN1 |
| 0.000 | 0.006 | *Neurexins and neuroligins* | Reactome | DLG3; DLG2; DLG4; DLGAP2; DLGAP1; DLGAP4; SIPA1L1; MGLUR5; GLUN1; HOMER2; EPB41L1; PDLIM5; EPB41L3; NLGN2; NLGN3; SHANK3; SHANK2; SHANK1; SYT1; SYT7; GLUN2B; GLUN2A |
| 0.000 | 0.008 | *Cocaine addiction - Homo sapiens (human)* | KEGG | PPP1R1B; DLG4; GLUA2; GLUN2B; MAOB; MAOA; GLUN2A; GLUN1; MGLUR3; GNAI3; MGLUR2; GNAI1 |
| 0.000 | 0.008 | *Fmlp induced chemokine gene expression in hmc-1 cells* | BioCarta | PLCB1; RAC1; PRKCA; PRKCB; MAP2K1; CAMK2B; MAP2K2; CAMKK2; CAMKK1; MAP2K6; PPP3CA; PPP3CB |
| 0.000 | 0.008 | *Phosphatidylinositol signaling system - Homo sapiens (human)* | KEGG | OCRL; PLCB1; PRKCB; PI4KA; INPPL1; PRKCA; CDS1; CDS2; DGKQ; PIK3CD; SACM1L; INPP4A; ITPKA; IMPA1; PRKCG; DGKE; PI4K2A; ITPR1; INPP5J; PIP4K2C; CDIPT |

**Table 2. An overlap in differentially expressed proteins with a kainic acid mouse model of mesiotemporal lobe epilepsy reported by *Bitsika et al., 2016*.**

| | | |
|---|---|---|
| Dravet 2 weeks | 3 days post KA | PCLO; BAIAP2; SIPA1L; SHANK3 |
| Dravet 4 weeks | 30 days post KA | ARPC1A; CYB5R3; SNAP91; CAMKV; HRSP12; NPTX1; ADD2; BAIAP2; RPH3A; SYNGAP1; PRMT1; ITGAV; VIM; MYO6; MAP1A; CST3; EPB41L1; MYH9; PPP3CB; SUCLG1; CTTNBP2; OXR1; PRRT1; PRKCG; CD44; APRT; ANXA4; SNX5; GFAP; RAPGEF2; DLG4; PPP3CA; MLC1; EZR; ENDOD1; PLEC; P4HB; SCG2; CYB5A; DBN1; DLG2; PSD3; SLC6A1; CLIC1; SLC2A13; PADI2; YWHAB; MAP2K1 |

## *References*


Almog, Y., et al., 2019. Early hippocampal hyperexcitability followed by disinhibition in a mouse model of Dravet syndrome. bioRxiv. 790170.

Alonso Gómez, C., et al., 2018. P.2.029 - Characterisation of a Dravet syndrome knock-in mouse model useful for investigating cannabinoid-based treatments. European Neuropsychopharmacology. 28**,** S41.

Arhan, E., et al., 2011. Effects of epilepsy and antiepileptic drugs on nitric oxide, lipid peroxidation and xanthine oxidase system in children with idiopathic epilepsy. Seizure. 20**,** 138-42.

Bao, Y., et al., 2018. RASgrf1, a Potential Methylatic Mediator of Anti-epileptogenesis? Neurochem Res. 43**,** 2000-2007.

Battaglia, D., et al., 2016. Outlining a core neuropsychological phenotype for Dravet syndrome. Epilepsy Res. 120**,** 91-7.

Bauer, A., et al., 2016. Identification of cyclins A1, E1 and vimentin as downstream targets of heme oxygenase-1 in vascular endothelial growth factor-mediated angiogenesis. Scientific reports. 6**,** 29417.

Ben-Hamo, M., et al., 2016. Differential effects of photoperiod length on depression- and anxiety-like behavior in female and male diurnal spiny mice. Physiol Behav. 165**,** 1-6.

Besag, F. M., 2004. Behavioral aspects of pediatric epilepsy syndromes. Epilepsy Behav. 5 Suppl 1**,** S3-13.

Bitsika, V., et al., 2016. High-throughput LC–MS/MS proteomic analysis of a mouse model of mesiotemporal lobe epilepsy predicts microglial activation underlying disease development. Journal of proteome research. 15**,** 1546-1562.

Bozzi, Y., Borrelli, E., 2013. The role of dopamine signaling in epileptogenesis. Front Cell Neurosci. 7**,** 157.

Brambilla, R., et al., 1997. A role for the Ras signalling pathway in synaptic transmission and long-term memory. Nature. 390**,** 281-286.

Brunklaus, A., Zuberi, S. M., 2014. Dravet syndrome--from epileptic encephalopathy to channelopathy. Epilepsia. 55**,** 979-84.

Carola, V., et al., 2002. Evaluation of the elevated plus-maze and open-field tests for the assessment of anxiety-related behaviour in inbred mice. Behav Brain Res. 134**,** 49-57.

Catterall, W. A., 2018. Dravet Syndrome: A Sodium Channel Interneuronopathy. Curr Opin Physiol. 2**,** 42-50.

Chen, H., et al., 2018. RASGRF1 hypermethylation, a putative biomarker of colorectal cancer. Annals of Clinical & Laboratory Science. 48**,** 3-10.

Danış, Ö., et al., 2011. Changes in intracellular protein expression in cortex, thalamus and hippocampus in a genetic rat model of absence epilepsy. Brain research bulletin. 84**,** 381-388.

Dave, J. M., Bayless, K. J., 2014. Vimentin as an integral regulator of cell adhesion and endothelial sprouting. Microcirculation. 21**,** 333-44.

Dedeurwaerdere, S., et al., 2015. In the grey zone between epilepsy and schizophrenia: alterations in group II metabotropic glutamate receptors. Acta Neurol Belg. 115**,** 221-32.

Devinsky, O., et al., 2013. Glia and epilepsy: excitability and inflammation. Trends Neurosci. 36**,** 174-84.

Dravet, C., 2011. The core Dravet syndrome phenotype. Epilepsia. 52 Suppl 2**,** 3-9.

Dravet, C., Oguni, H., 2013. Dravet syndrome (severe myoclonic epilepsy in infancy). Handb Clin Neurol. 111**,** 627-33.

Dugger, S. A., et al., 2018. Drug development in the era of precision medicine. Nature Reviews Drug Discovery. 17**,** 183.

Dutton, S. B. B., et al., 2017. Early-life febrile seizures worsen adult phenotypes in Scn1a mutants. Exp Neurol. 293**,** 159-171.

Fabene, P. F., et al., 2010. The emerging role for chemokines in epilepsy. J Neuroimmunol. 224**,** 22-7.

Gao, Q., et al., 1999. The E6 oncoproteins of high-risk papillomaviruses bind to a novel putative GAP protein, E6TP1, and target it for degradation. Molecular and cellular biology. 19**,** 733-744.

Hawkins, N. A., et al., 2019. Gene expression profiling in a mouse model of Dravet syndrome. Exp Neurol. 311**,** 247-256.

Holter, S. M., et al., 2015. Tests for Anxiety-Related Behavior in Mice. Curr Protoc Mouse Biol. 5**,** 291-309.

Jeyabalan, N., Clement, J. P., 2016. SYNGAP1: Mind the Gap. Front Cell Neurosci. 10**,** 32.

Jirkof, P., et al., 2013. Assessment of postsurgical distress and pain in laboratory mice by nest complexity scoring. Lab Anim. 47**,** 153-61.

Joshi, S., Kapur, J., GABA(A) Receptor Plasticity During Status Epilepticus. In: J. L. Noebels, et al., (Eds.), Jasper's Basic Mechanisms of the Epilepsies. National Center for Biotechnology Information (US)



Kalume, F., 2013. Sudden unexpected death in Dravet syndrome: respiratory and other physiological dysfunctions. Respir Physiol Neurobiol. 189**,** 324-8.

Kalume, F., et al., 2015. Sleep impairment and reduced interneuron excitability in a mouse model of Dravet Syndrome. Neurobiol Dis. 77**,** 141-54.

Kamburov, A., et al., 2009. ConsensusPathDB—a database for integrating human functional interaction networks. Nucleic acids research. 37**,** D623-D628.

Kassel, K. M., et al., 2010. Regulation of human cytidine triphosphate synthetase 2 by phosphorylation. Journal of Biological Chemistry. 285**,** 33727-33736.

Keck, M., et al., 2017. A systems level analysis of epileptogenesis-associated proteome alterations. Neurobiology of disease. 105**,** 164-178.

Keck, M., et al., 2018. Proteomic profiling of epileptogenesis in a rat model: Focus on cell stress, extracellular matrix and angiogenesis. Neurobiol Dis. 112**,** 119-135.

Klein, P., et al., 2018. Commonalities in epileptogenic processes from different acute brain insults: Do they translate? Epilepsia. 59**,** 37-66.

Klein, S., et al., 2015. Sucrose consumption test reveals pharmacoresistant depression-associated behavior in two mouse models of temporal lobe epilepsy. Exp Neurol. 263**,** 263-71.

Krapivinsky, G., et al., 2003. The NMDA receptor is coupled to the ERK pathway by a direct interaction between NR2B and RasGRF1. Neuron. 40**,** 775-784.

Kuo, F.-S., et al., 2019. Disordered breathing in a mouse model of Dravet syndrome. Elife. 8**,** e43387.

Lepper, M. F., et al., 2018. Proteomic landscape of patient-derived CD4+ T cells in recent-onset type 1 diabetes. Journal of proteome research. 17**,** 618-634.

Li, A., et al., 2010. Proteomic profiling of the epileptic dentate gyrus. Brain pathology. 20**,** 1077-1089.

Liao, L., et al., 2008. Quantitative proteomic analysis of primary neurons reveals diverse changes in synaptic protein content in fmr1 knockout mice. Proceedings of the National Academy of Sciences. 105**,** 15281-15286.

Lisman, J., et al., 2002. The molecular basis of CaMKII function in synaptic and behavioural memory. Nature Reviews Neuroscience. 3**,** 175-190.

Liu, W., Hajjar, K. A., 2016. The annexin A2 system and angiogenesis. Biol Chem. 397**,** 1005-16.

Liu, X. Y., et al., 2008. Comparative proteomics and correlated signaling network of rat hippocampus in the pilocarpine model of temporal lobe epilepsy. Proteomics. 8**,** 582-603.

Lossin, C., 2009. A catalog of SCN1A variants. Brain Dev. 31**,** 114-30.

Mantegazza, M., Broccoli, V., 2019. SCN 1A/NaV1. 1 channelopathies: Mechanisms in expression systems, animal models, and human iPSC models. Epilepsia. 60**,** S25-S38.

Martin, M. S., et al., 2010. Altered function of the SCN1A voltage-gated sodium channel leads to gamma-aminobutyric acid-ergic (GABAergic) interneuron abnormalities. J Biol Chem. 285**,** 9823-34.

Mistry, A. M., et al., 2014. Strain- and age-dependent hippocampal neuron sodium currents correlate with epilepsy severity in Dravet syndrome mice. Neurobiol Dis. 65**,** 1-11.

Molin, S., et al., 2015. The hand eczema proteome: imbalance of epidermal barrier proteins. British Journal of Dermatology. 172**,** 994-1001.

Morbidelli, L., et al., 2004. Role of nitric oxide in tumor angiogenesis. Cancer Treat Res. 117**,** 155-67.

Morin-Brureau, M., et al., 2012. Why and how to target angiogenesis in focal epilepsies. Epilepsia. 53 Suppl 6**,** 64-8.

Niday, Z., Tzingounis, A. V., 2018. Potassium Channel Gain of Function in Epilepsy: An Unresolved Paradox. Neuroscientist. 24**,** 368-380.

O'Sullivan, G. J., et al., 2008. Dopamine D1 vs D5 receptor-dependent induction of seizures in relation to DARPP-32, ERK1/2 and GluR1-AMPA signalling. Neuropharmacology. 54**,** 1051-61.

Oakley, J. C., et al., 2009. Temperature- and age-dependent seizures in a mouse model of severe myoclonic epilepsy in infancy. Proc Natl Acad Sci U S A. 106**,** 3994-9.

Ogiwara, I., et al., 2013. Nav1.1 haploinsufficiency in excitatory neurons ameliorates seizure-associated sudden death in a mouse model of Dravet syndrome. Hum Mol Genet. 22**,** 4784-804.

Ogiwara, I., et al., 2007. Nav1.1 localizes to axons of parvalbumin-positive inhibitory interneurons: a circuit basis for epileptic seizures in mice carrying an Scn1a gene mutation. J Neurosci. 27**,** 5903-14.

Racine, R. J., 1972. Modification of seizure activity by electrical stimulation. II. Motor seizure. Electroencephalogr Clin Neurophysiol. 32**,** 281-94.

Ricobaraza, A., et al., 2019. Epilepsy and neuropsychiatric comorbidities in mice carrying a recurrent Dravet syndrome SCN1A missense mutation. Scientific reports. 9**,** 1-15.

Rigau, V., et al., 2007. Angiogenesis is associated with blood-brain barrier permeability in temporal lobe epilepsy. Brain. 130**,** 1942-56.

Rubinstein, M., et al., 2015. Genetic background modulates impaired excitability of inhibitory neurons in a mouse model of Dravet syndrome. Neurobiol Dis. 73**,** 106-17.

Salgueiro-Pereira, A. R., et al., 2019. A two-hit story: Seizures and genetic mutation interaction sets phenotype severity in SCN1A epilepsies. Neurobiol Dis. 125**,** 31-44.

Scharfman, H. E., Brooks-Kayal, A. R., 2014. Is plasticity of GABAergic mechanisms relevant to epileptogenesis? Adv Exp Med Biol. 813**,** 133-50.

Schwindinger, W. F., et al., 2012. Synergistic roles for G-protein γ3 and γ7 subtypes in seizure susceptibility as revealed in double knock-out mice. Journal of Biological Chemistry. 287**,** 7121-7133.

Shiotsuki, H., et al., 2010. A rotarod test for evaluation of motor skill learning. J Neurosci Methods. 189**,** 180-5.

Sills, G. J., Rogawski, M. A., 2020. Mechanisms of action of currently used antiseizure drugs. Neuropharmacology. 168**,** 107966.

Südhof, T. C., 2008. Neuroligins and neurexins link synaptic function to cognitive disease. Nature. 455**,** 903-911.

Swulius, M. T., Waxham, M. N., 2008. Ca(2+)/calmodulin-dependent protein kinases. Cell Mol Life Sci. 65**,** 2637-57.

Tai, C., et al., 2014. Impaired excitability of somatostatin- and parvalbumin-expressing cortical interneurons in a mouse model of Dravet syndrome. Proc Natl Acad Sci U S A. 111**,** E3139-48.

Tang, S. H. E., et al., 2002. A Cre/loxP-deleter transgenic line in mouse strain 129S1/SvImJ. genesis. 32**,** 199-202.

Team, R. C., 2017. R Core Team (2017). R: A language and environment for statistical computing. R Found. Stat. Comput. Vienna, Austria.

Terrone, G., et al., 2017. Inflammation and Epilepsy: Preclinical Findings and Potential Clinical Translation. Curr Pharm Des. 23**,** 5569-5576.

Tonini, R., et al., 2001. Involvement of CDC25Mm/Ras-GRF1-dependent signaling in the control of neuronal excitability. Molecular and Cellular Neuroscience. 18**,** 691-701.

Tsai, M. S., et al., 2015. Functional and structural deficits of the dentate gyrus network coincide with emerging spontaneous seizures in an Scn1a mutant Dravet Syndrome model during development. Neurobiol Dis. 77**,** 35-48.

Vezzani, A., 2014. Epilepsy and inflammation in the brain: overview and pathophysiology. Epilepsy Curr. 14**,** 3-7.

Villa, C., Combi, R., 2016. Potassium Channels and Human Epileptic Phenotypes: An Updated Overview. Front Cell Neurosci. 10**,** 81.

Vlaskamp, D. R., et al., 2019. SYNGAP1 encephalopathy: a distinctive generalized developmental and epileptic encephalopathy. Neurology. 92**,** e96-e107.

Walker, A., et al., 2016. Proteomic profiling of epileptogenesis in a rat model: Focus on inflammation. Brain Behav Immun. 53**,** 138-158.

Wallace, A., et al., 2016. Pharmacotherapy for Dravet Syndrome. Paediatr Drugs. 18**,** 197-208.

Warnes, M. G. R., et al., 2016. Package 'gplots'. Various R Programming Tools for Plotting Data.

Xu, B., et al., 2018. Proteomic profiling of brain and testis reveals the diverse changes in ribosomal proteins in fmr1 knockout mice. Neuroscience. 371**,** 469-483.

Yu, F. H., et al., 2006. Reduced sodium current in GABAergic interneurons in a mouse model of severe myoclonic epilepsy in infancy. Nature Neuroscience. 9**,** 1142.

*Supplementary Information*

**Table A.1. List of abbreviations (left column) and full names (right column) of all regulated proteins mentioned in the manuscript and their general function.**

| | |
|---|---|
| ***GABAergic signaling*** | |
| GABBR1 | Gamma-aminobutyric acid type B receptor subunit 1 |
| GABBR2 | Gamma-aminobutyric acid type B receptor subunit 2 |
| GABRA1 | Gamma-aminobutyric acid receptor subunit alpha-1 |
| GABRB1 | Gamma-aminobutyric acid receptor subunit beta-1 |
| GABRB3 | Gamma-aminobutyric acid receptor subunit beta-3 |
| SLC6A1 | Sodium- and chloride-dependent GABA transporter 3 |
| ***Glutamatergic signaling*** | |
| CTPS2 | Cytidine triphosphate synthetase 2 |
| GluA1 | Glutamate ionotropic receptor AMPA subunit 1 |
| GluA2 | Glutamate ionotropic receptor AMPA subunit 2 |
| GluA3 | Glutamate ionotropic receptor AMPA subunit 3 |
| GluA4 | Glutamate ionotropic receptor AMPA subunit 4 |
| GluK2 | Glutamate ionotropic receptor kainate type subunit 2 |
| GLUL | Glutamine synthetase |
| GluN1 | Glutamate ionotropic receptor NMDA type subunit 1 |
| GluN2A | Glutamate ionotropic receptor NMDA type subunit 2A |
| GluN2B | Glutamate ionotropic receptor NMDA type subunit 2B |
| mGluR2 | Metabotropic glutamate receptor type 2 |
| mGluR3 | Metabotropic glutamate receptor type 3 |
| mGluR5 | Metabotropic glutamate receptor type 5 |
| ***Synaptic transmission*** | |
| DLG2 | Disks large homolog 2 |
| DLG3 | Disks large homolog 3 |
| DLG4 | Disks large homolog 4 |
| DLGAP1 | Disks large-associated protein 1 |
| DLGAP2 | Disks large-associated protein 2 |
| DLGAP4 | Disks large-associated protein 4 |
| HOMER2 | Homer Scaffold Protein 2 |
| NLGN2 | Neuroligin 2 |
| NLGN3 | Neuroligin 3 |
| PCLO | Protein piccolo |
| PPP3CA | Serine/threonine-protein phosphatase 2B catalytic subunit alpha isoform |
| PPP3CB | Serine/threonine-protein phosphatase 2B catalytic subunit beta isoform |
| PRKCG | Protein kinase C gamma type |
| RASGRF1 | Ras-specific guanine nucleotide releasing factor 1 |
| RIMS1 | Regulating Synaptic Membrane Exocytosis 1 |
| SHANK1 | SH3 and multiple ankyrin repeat domains protein 1 |
| SHANK2 | SH3 and multiple ankyrin repeat domains protein 2 |
| SHANK3 | SH3 and multiple ankyrin repeat domains protein 3 |
| SYNGAP1 | Ras/Rap GTPase-activating protein SynGAP |
| SYT | Synaptotagmin |

| | |
|---|---|
| RPH3A | Rabphilin-3A |
| BAIAP2 | Brain-specific angiogenesis inhibitor 1-associated protein 2 |
| ***Dopaminergic signaling*** | |
| EPB41L1 | Band 4.1-like protein 1 |
| EPB41L3 | Band 4.1-like protein 3 |
| GNG7 | Guanine nucleotide-binding protein G(I)/G(S)/G(O) subunit gamma-7 |
| MAOA | Monoamine oxidase A |
| MAOB | Monoamine oxidase B |
| PPP1R1B | Protein phosphatase 1 regulatory subunit 1B |
| ***Calcium signaling*** | |
| CACNA1A | Calcium voltage-gated channel subunit alpha1 A |
| CACNA1E | Calcium voltage-gated channel subunit alpha1 E |
| CACNA2D3 | Calcium voltage-gated channel auxiliary subunit alpha2delta 3 |
| CACNB3 | Calcium voltage-gated channel auxiliary subunit beta 3 |
| CACNB4 | Calcium voltage-gated channel auxiliary subunit beta 4 |
| CACNG8 | Calcium voltage-gated channel auxiliary subunit gamma 8 |
| CAMK1D | Calcium/calmodulin-dependent protein kinase type 1D |
| CAMK2A | Calcium/calmodulin-dependent protein kinase type II subunit alpha |
| CAMK2B | Calcium/calmodulin-dependent protein kinase type II subunit beta |
| CAMK4 | Calcium/calmodulin-dependent protein kinase type IV |
| CAMKK1 | Calcium/calmodulin-dependent protein kinase kinase 1 |
| CAMKK2 | Calcium/calmodulin-dependent protein kinase kinase 2 |
| ***Potassium channels*** | |
| KCNA2 | Potassium voltage-gated channel subfamily A member 2 |
| KCNAB2 | Voltage-gated potassium channel subunit beta-2 |
| KCND2 | Potassium voltage-gated channel subfamily D member 2 |
| KCNJ10 | ATP-sensitive inward rectifier potassium channel 10 |
| KCNJ3 | G protein-activated inward rectifier potassium channel 1 |
| KCNJ9 | G protein-activated inward rectifier potassium channel 3 |
| ***Reactive astrogliosis*** | |
| GFAP | glial fibrillary acidic protein |
| EAAT1 | Excitatory amino acid transporter 1 |
| EAAT2 | Excitatory amino acid transporter 2 |
| ***Angiogenesis*** | |
| ANXA2 | Annexin A2 |
| ANXA4 | Annexin A4 |
| ITGAV | Integrin alpha-V |
| KDR | Vascular endothelial growth factor receptor 2 |
| VIM | Vimentin |
| ***Nitric oxide signaling*** | |
| NOS1 | Neuronal nitric oxide synthase |
| ***Cytoskeletal proteins*** | |
| ADD2 | Beta-adducin |
| ARPC1A | Actin-related protein 2/3 complex subunit 1A |
| CKAP4 | Cytoskeleton-associated protein 5 |
| CTTNBP2 | Cortactin-binding protein 2 |
| DBN1 | Drebrin |

| | |
|---|---|
| EZR | Ezrin |
| MAP1A | Microtubule-associated protein 1A |
| MYO6 | Unconventional myosin-VI |
| PLEC | Plectin |

**Table A.2. A comparison between here characterized mouse model of Dravet syndrome (*Scn1a*-A1873V, first row) and other available mouse models with a heterozygous *Scn1a* mutation.** The arrow indicates increased or reduced behavior characteristic. Minus (-) indicates no significant changes in evaluated tests. P – postnatal day, PW – postnatal week, M – months, n.a. - not available. A grey horizontal line was used between mouse models carrying the same *Scn1a* mutation, while a black horizontal line was used between mouse models carrying a different *Scn1a* mutation. [1](Ricobaraza et al., 2019); [2](Kuo et al., 2019); [3](Ogiwara et al., 2007); [4](Ito et al., 2013); [5](Dutton et al., 2013); [6](Han et al., 2012; Kalume, 2013; Oakley et al., 2009); [7](Yu et al., 2006); [8](Cheah et al., 2012); [9](Ogiwara et al., 2013); [10](Miller et al., 2014); [11](Mistry et al., 2014); [12](Tsai et al., 2015); [13](Martin et al., 2010); [14](Dutton et al., 2017; Sawyer et al., 2016).

| Mouse model | BL/6:129S1 background [~%] | Mortality rate [%] | Spontaneous seizures onset | HIS threshold, test day (P) | Activity level | Anxiety-like behavior | Social behavior | Cognition | Anhedonia-related behavior | Motor coordination | Body weight |
|---|---|---|---|---|---|---|---|---|---|---|---|
| *Scn1a*-A1783V | 50:50 | 40 | P16 | 39.4 (P23) | ↑ | ↓ | ↑ | - | ↑ | ↓ | ↓ |
| [1]*Scn1a*$^{WT/A1783V}$ | 100:0 | 75 | PW3 | 38.2 (1-6 M) | ↑ | ↑ | - | ↓ | n.a. | ↓ | ↓ |
| [2]*Scn1a*$^{\Delta E26}$ | 90:10 | 100 | P14 | 41.1 (P12-14) | n.a | n.a. | n.a. | n.a. | n.a. | n.a. | - |
| [3] *Scn1a*$^{RX/+}$ | 75:25 | 40 | P18 | n.a. | n.a. | n.a. | n.a. | n.a. | n.a. | - | - |
| [4]*Scn1a*$^{RX/+}$ | 100:0 | 40 | P18 | n.a. | ↑ | ↓ | ↓ | ↓ | n.a. | - | - |
| [5]*Scn1a*$^{Flox/+}$Cre$^{+/-}$ | 100:0 | 100 | P21 | 40.7 (P22) | ↑ | ↑ | ↓ | ↓ | n.a. | n.a. | n.a. |
| [6]*Scn1a*$^{+/-}$ | 99.9:0.1 | 40 | P21 | 39.5 (P20-46) | ↑ | ↑ | ↓ | ↓ | n.a. | ↓ | n.a. |
| [7]*Scn1a*$^{+/-}$ | 0:100 | 10 | P21 | n.a. | n.a. | n.a. | n.a. | n.a. | n.a. | n.a. | n.a. |
| [7]*Scn1a*$^{+/-}$ | 100:0 | 80 | P21 | n.a. | n.a. | n.a. | n.a. | n.a. | n.a. | n.a. | n.a. |
| [8]*Scn1a*$^{fl/+}$ | 100:0 | 70 | P18 | 39 (P35) | ↑ | n.a. | ↓ | ↓ | n.a. | n.a. | n.a. |
| [9]*Scn1a*$^{d/+}$ | 97:3 | 25 | PW3 | n.a. | n.a. | n.a. | n.a. | n.a. | n.a. | - | n.a. |
| [10]*Scn1a*$^{tm1Kea}$ | 75:25 | 54 | P24 | n.a. | n.a. | n.a. | n.a. | n.a. | n.a. | n.a. | n.a. |
| [11]*Scn1a*$^{tm1Kea}$ | 50:50 | 50 | P18 | n.a. | n.a. | n.a. | n.a. | n.a. | n.a. | n.a. | n.a. |
| [12]*Scn1a*$^{E1099X/+}$ | 75:25 | 46 | P20 | 40.2 (PW3-5) | n.a. | n.a. | n.a. | n.a. | n.a. | n.a. | n.a. |
| [13]*Scn1a*$^{RH/+}$ | 100:0 | 5 | n.a. | 41.3 (P14-15) | ↑ | - | ↓ | ↓ | n.a. | ↓ | - |
| [14]*Scn1a*$^{RH/+}$ | mix | 5 | n.a. | 43.1 (P14-15) | n.a. | n.a. | n.a. | n.a. | n.a. | n.a. | - |

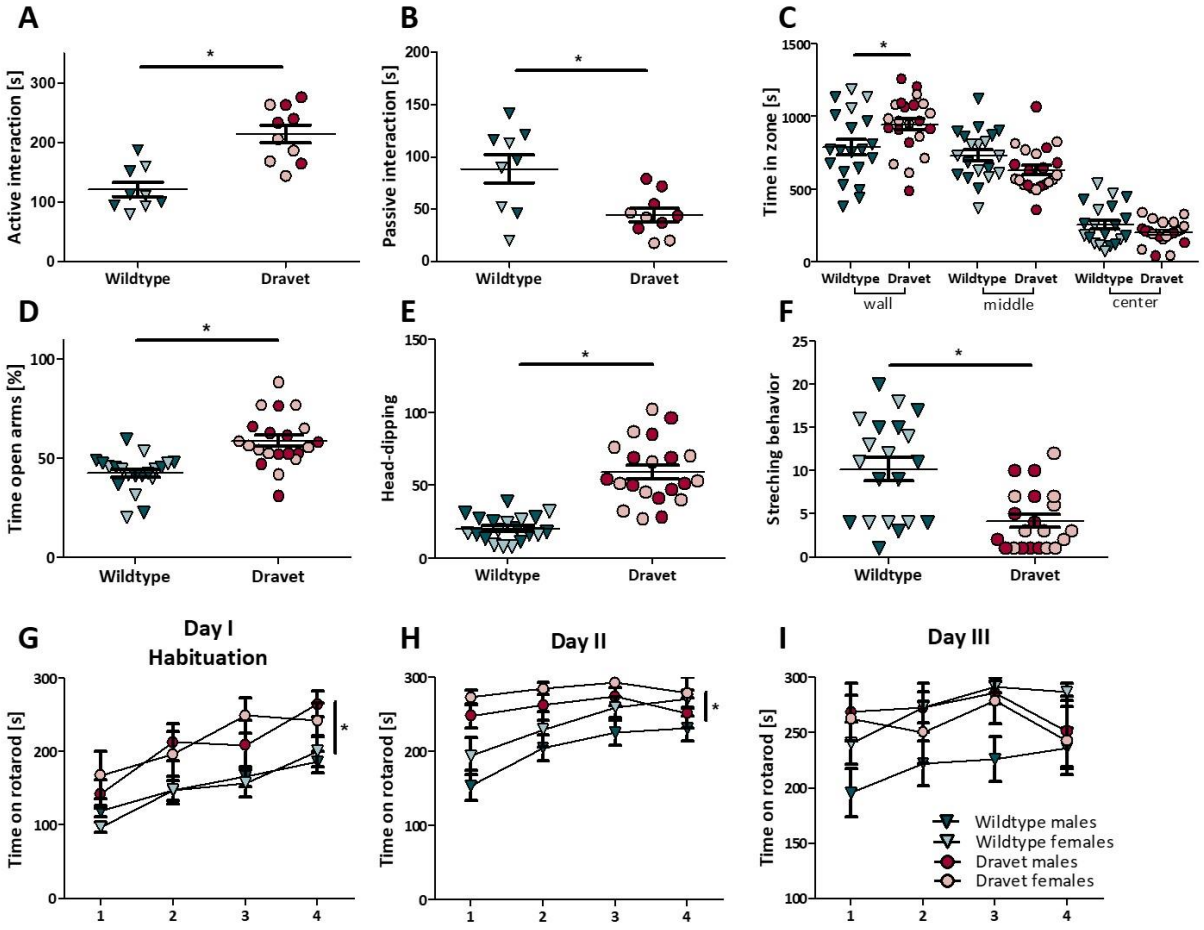


**Fig. A.1. Social interaction, thigmotaxic behavior, elevated plus maze and accelerated rotarod test. A** Time spent in active social interaction. Dravet mice engaged more in active interaction than their wildtype littermates. **B** Time spent in passive social interaction. Dravet mice spent less time than wildtype animals engaged in passive interaction. **A-B** Data shown are from 10 animal pairs with a Dravet genotype vs 9 wildtype animal pairs (Two-way ANOVA, Bonferroni post hoc; * $p < 0.05$, mean ± SEM). **C** Time spent in wall, middle and center zone over 30 minutes. Dravet mice spent more time in the wall zone than wildtype mice, while no significant difference was observed in the time spent in the middle or center zone (Three-way RM ANOVA, Bonferroni post hoc; * $p < 0.05$, mean ± SEM). **D** Time spent exploring open arms of elevated plus maze. Dravet mice exhibited a significantly higher preference towards open arms of the maze as compared to wildtype group. **E** Frequency to dip head over the maze. Dravet animals made significantly more head dips than wildtype mice. **F** Stretching postures to explore open arms of EPM. Dravet animals showed significantly lower number of stretching positions as compared to wildtype mice (Three-way ANOVA, Bonferroni post hoc; * $p < 0.05$, mean ± SEM). **G-I** Time on accelerated rod on three consecutive test days. Dravet mice performed better on rotarod comparing to wildtype mice. Females performed better than males (Five-way RM ANOVA, Bonferroni post hoc; * $p < 0.05$, mean ± SEM). C-I Data shown are from 21 (**D-F**) or 22 (**C, G-I**) animals with a Dravet genotype (n = 10 or 11 males, n = 11 females) vs 20 wildtype (n = 11 males, n = 9 females) animals.

## *References*

Cheah, C. S., et al., 2012. Specific deletion of NaV1.1 sodium channels in inhibitory interneurons causes seizures and premature death in a mouse model of Dravet syndrome. Proc Natl Acad Sci U S A. 109**,** 14646-51.

Dutton, S. B., et al., 2013. Preferential inactivation of Scn1a in parvalbumin interneurons increases seizure susceptibility. Neurobiol Dis. 49**,** 211-20.

Dutton, S. B. B., et al., 2017. Early-life febrile seizures worsen adult phenotypes in Scn1a mutants. Exp Neurol. 293**,** 159-171.

Han, S., et al., 2012. Autistic-like behaviour in Scn1a+/- mice and rescue by enhanced GABA-mediated neurotransmission. Nature. 489**,** 385-90.

Ito, S., et al., 2013. Mouse with Nav1.1 haploinsufficiency, a model for Dravet syndrome, exhibits lowered sociability and learning impairment. Neurobiol Dis. 49**,** 29-40.

Kalume, F., et al., 2007. Reduced sodium current in Purkinje neurons from Nav1.1 mutant mice: implications for ataxia in severe myoclonic epilepsy in infancy. J Neurosci. 27**,** 11065-74.

Martin, M. S., et al., 2010. Altered function of the SCN1A voltage-gated sodium channel leads to gamma-aminobutyric acid-ergic (GABAergic) interneuron abnormalities. J Biol Chem. 285**,** 9823-34.

Miller, A. R., et al., 2014. Mapping genetic modifiers of survival in a mouse model of Dravet syndrome. Genes Brain Behav. 13**,** 163-72.

Mistry, A. M., et al., 2014. Strain- and age-dependent hippocampal neuron sodium currents correlate with epilepsy severity in Dravet syndrome mice. Neurobiol Dis. 65**,** 1-11.

Ogiwara, I., et al., 2013. Nav1.1 haploinsufficiency in excitatory neurons ameliorates seizure-associated sudden death in a mouse model of Dravet syndrome. Hum Mol Genet. 22**,** 4784-804.

Ogiwara, I., et al., 2007. Nav1.1 localizes to axons of parvalbumin-positive inhibitory interneurons: a circuit basis for epileptic seizures in mice carrying an Scn1a gene mutation. J Neurosci. 27**,** 5903-14.

Ricobaraza, A., et al., 2019. Epilepsy and neuropsychiatric comorbidities in mice carrying a recurrent Dravet syndrome SCN1A missense mutation. Scientific reports. 9**,** 1-15.

Tsai, M. S., et al., 2015. Functional and structural deficits of the dentate gyrus network coincide with emerging spontaneous seizures in an Scn1a mutant Dravet Syndrome model during development. Neurobiol Dis. 77**,** 35-48.

Yu, F. H., et al., 2006. Reduced sodium current in GABAergic interneurons in a mouse model of severe myoclonic epilepsy in infancy. Nature Neuroscience. 9**,** 1142.

## *2. Manuscript II*

This chapter contains a manuscript submitted to the journal *Epilepsia* (doi: 10.1111/epi.16976). The manuscript aimed to identify metabolic consequences of *Scn1a* genetic deficiency in the hippocampus and plasma of Dravet mice. In addition, we intended to examine the impact of the ketogenic diet on the epileptic phenotype and metabolome in these mice.

# Metabolomic signature of the Dravet syndrome: a genetic mouse model study.

**Miljanovic N., van Dijk RM., Buchecker V., Potschka H.**

The author of the present thesis is the first author of this manuscript. **N.M**. designed and performed all experiments, completed statistical analysis and provided the original manuscript draft. **R.M.v.D.** contributed to study design and statistical analysis. **V.B.** contributed to experiments execution. **H.P.** provided conception and funding for the study, wrote sections of the manuscript. All authors contributed to the manuscript revision and approved the submitted version.

# Metabolomic signature of the Dravet syndrome: a genetic mouse model study

Nina Miljanovic[a,b], R. Maarten van Dijk[a,c], Verena Buchecker[a], Heidrun Potschka[a]

[a]Institute of Pharmacology, Toxicology & Pharmacy, Ludwig-Maximilians-University (LMU), Munich, Germany

[b]Graduate School of Systemic Neurosciences (GSN), Ludwig-Maximilians-University (LMU), Munich, Germany

[c]current address: Staburo GmbH, München, Germany.

*Correspondence: Dr. H. Potschka, Institute of Pharmacology, Toxicology, and Pharmacy, Ludwig-Maximilians-University, Koeniginstr. 16, D-80539 Munich, Germany;

Phone: +49-89-21802662; Fax: +49-89-218016556;

e-mail: potschka@pharmtox.vetmed.uni-muenchen.de

Declarations of interest: none

## *Abstract*

**Objective**: Alterations in metabolic homeostasis can contribute to neuronal hyperexcitability and seizure susceptibility. While the pivotal role of impaired bioenergetics is obvious in metabolic epilepsies, there is a gap-of-knowledge regarding secondary changes in metabolite patterns as a result of genetic *Scn1a* deficiency and ketogenic diet in the Dravet syndrome.

**Methods**: A comprehensive untargeted metabolomics analysis along with assessment of spontaneous seizure activity and behavioral tests, were completed in a Dravet mouse model. Data sets were compared between animals on a control and a ketogenic diet and metabolic alterations associated with Dravet mice phenotype and ketogenic diet were identified.

**Results**: Hippocampal metabolomic data revealed complex alterations in energy metabolism with an effect of the genotype on several glycolysis and tricarboxylic acid (TCA) cycle intermediates. While low glucose, lactate, malate, and citrate concentrations became evident, the increase of several intermediates suggested a genotype-associated activation of catabolic processes with enhanced glycogenolysis and glycolysis. Moreover, we observed an impact on the glutamate/GABA-glutamine cycle with reduced levels of all components along with a shift towards an increased GABA:glutamate ratio. Further alterations in metabolic patterns comprised a reduction in hippocampal levels of noradrenaline, corticosterone and of two bile acids.

**Significance**: Considering that energy depletion can predominantly compromise the function of GABAergic interneurons, the changes in energy metabolism may contribute to seizure susceptibility and ictogenesis. They may also explain the therapeutic potential of the ketogenic diet, which aims to shift energy metabolism towards a more fat-based energy supply. Conversely, the increased GABA:glutamate ratio might serve as an endogenous compensatory mechanism, which can be further supported by GABAergic drugs, the mainstay of therapeutic management of Dravet syndrome. In view of a possible neuroprotective function of bile acids,

it might be of interest to explore a possible therapeutic potential of bile-acid mediated therapies, which are already in discussion for neurodegenerative disorders.

**Keywords**: metabolomics, epileptic encephalopathy, ketogenic diet, *Scn1a*, mice.

## *Key points box:*

- Metabolomic analysis in a mouse model demonstrated that Dravet syndrome can be associated with complex alterations in the metabolome.
- Pronounced alterations in glucose and TCA cycle metabolism may contribute to seizure susceptibility and ictogenesis in Dravet mice.
- The findings may explain the potential of dietary approaches including KD aiming to shift metabolism towards a fat-based energy supply.
- The increased GABA:glutamate ratio may represent an endogenous compensatory mechanism, which can be further supported by GABAergic drugs.
- Ketogenic diet improved motor function in Dravet mice.

## *Introduction*

Changes in metabolic homeostasis and dysmetabolic states have a major impact on neuronal excitability and seizure susceptibility (Masino and Rho, 2019; McDonald et al., 2018; Patel, 2018). Experimental and clinical research in epileptology has so far focused on energy fueling of the brain and its links with hyperexcitability, epileptogenesis and ictogenesis (Kovács et al., 2018; Oyarzabal and Marin-Valencia, 2019). The fact that permanent neuroglycopenia can affect seizure thresholds has been convincingly proven by the characterization of the glucose transporter-1 (GLUT1) deficiency syndrome (Pong et al., 2012). The identification of further genetic epilepsies related to variance in metabolic pathways has resulted in an integration of the term 'metabolic epilepsies' in the etiological classification suggested by the International League against Epilepsy (Scheffer et al., 2017).

While the pivotal role of impaired bioenergetics is obvious in metabolic epilepsies, evidence exists that relevant alterations in the metabolic state also occur in other genetic epilepsies as well as acquired epilepsies (Patel, 2018; Reid et al., 2014; Waldbaum and Patel, 2010). The functional relevance of perturbed brain bioenergetics received indirect confirmation by the therapeutic success of the ketogenic diet (KD) and alternate dietary approaches aiming to shift the energy metabolism from glucose-based towards fat-based energy generation (Barañano and Hartman, 2008; McDonald et al., 2018; Youngson et al., 2017). While it is an established first line therapeutic concept for GLUT1 deficiency syndrome, the list of possible indications comprises different genetic epilepsy syndromes including the Dravet syndrome, which is characterized by a severe clinical phenotype and a poor pharmacoresponsiveness (Dravet, 2011). For Dravet syndrome a recent meta-analysis has suggested an improvement of seizure control and behavioral symptoms in response to the KD (Wang et al., 2020). This finding supports the recommendation of KD for Dravet patients with failure to respond to three or four different antiseizure drugs (Cross et al., 2019). Therapeutic success of the ketogenic diet provides indirect evidence that the metabolic and bioenergetics state might be altered in patients

with Dravet syndrome rendering it a valuable target for therapeutic intervention. Further evidence for changes in brain bioenergetics came from a limited number of $^{18}$F-labelled fluorodeoxyglucose positron emission tomography (FDG-PET) studies reporting alterations in glucose uptake in a Dravet mouse model and in patients with Dravet syndrome (Haginoya et al., 2018; Kumar et al., 2018; Ricobaraza et al., 2019).

Despite the use of dietary approaches, there is a surprising gap in knowledge when it comes to the metabolic consequences of epilepsy syndromes. A gain-in-knowledge will provide a basis for a more rational application of dietary approaches, for the identification of potential biomarkers predicting responsiveness guiding individualized therapeutic decisions, and information for the design and development of small molecule compounds targeting metabolic pathways as an alternate to dietary approaches. Alternate metabolism-targeting pharmacological approaches are of particular interest considering that KD is characterized by a relatively poor tolerability and a high adverse effect potential.

Thus, there is a particular interest to improve the knowledge about the metabolic state developing following *SCN1A* deficiency as the most frequent clinical cause of Dravet syndrome. Therefore, we have completed a metabolomics analysis in a genetic Dravet mouse model with animals exposed to a control diet or a KD. Among other findings, the data set revealed pronounced alterations in energy metabolism and in the glutamate/GABA-glutamine cycle in Dravet mice. The metabolic patterns are of particular interest in the context of pathophysiological mechanisms of seizure susceptibility and ictogenesis and of possible endogenous compensatory mechanisms.

## *Material and methods*

### *Animals*

Parental breeding lines, B6(Cg)-*Scn1a*$^{tm1.1Dsf}$/J (#026133 (Kuo et al., 2019; Ricobaraza et al., 2019)) and 129S1/Sv-*Hprt*$^{tm1(CAG-cre)Mnn}$/J (#004302 (Tang et al., 2002)), were purchased from the Jackson Laboratory (Bar Harbor, Maine, USA). Heterozygous A1783V-*Scn1a* Dravet (mutant) and wildtype (control) mice were generated by crossing female mice heterozygous for Cre recombinase (X-linked to *Hprt* gene) with male mice with floxed *Scn1a*. The resulting offspring was generated on a mixed (50:50) C57BL/6J and 129S1 genetic background and genotyped as previously described (Miljanovic et al., under revision). In a parallel study, we demonstrated that Dravet mice exhibit first spontaneous tonic-clonic seizures from P16 on, followed by recurrent seizure with a high seizure frequency, a transient delay in body weight development and a SUDEP rate of 40 % around the time of weaning. Moreover, a pronounced hyperactivity became evident in Dravet mice (Miljanovic et al., under revision).

All experiments were approved by the government of Upper Bavaria (license number 55.2-1-54-2532-168-2016) and conducted in line with the EU directive 2010/63/EU for animal experiments and the German Animal Welfare act. Experiments were designed and executed in line with ARRIVE guidelines and Basel declaration (http://www.basel.declaration.org) including the 3R concept.

A pilot study designed to determine an adequate duration of ketogenic diet exposure was performed in five Dravet (2 males; 3 females) and five wildtype (2 males; 3 females) mice (Fig. S6). For the main study, 35 heterozygous Dravet and 28 wildtype mice were generated. Nine Dravet mice died due to probable SUDEP resulting in a mortality rate of 25.7 %. From remaining animals, twenty-two heterozygous (11 males; 11 females) and 20 wildtype mice (10 males; 10 females) were selected for the experiment and split in two cohorts with 2 weeks apart, based on their day of birth.

Please note that baseline data from video-EEG recordings in heterozygous mice have already previously been presented in the context of a study characterizing the line (Miljanovic et al., under revision; Table S1).

*Experiment timeline*

Twelve-week-old wildtype and Dravet mice were implanted with telemetric transmitters (HD-X02, DSI, St. Paul, USA) and depth electrodes in the hippocampus. Recordings were initiated after a two-week recovery phase. Following a one-week baseline video-EEG-ECG recording, animals were allocated to four groups considering genotype and treatment: wildtype control diet (WT CD, n=10), wildtype ketogenic diet (WT KD, n=10), Dravet control diet (Dra CD, n=10) and Dravet ketogenic diet (Dra KD, n=11) group. When allocating Dravet mice to groups, the number of convulsive seizures was used as a relevant parameter for stratified randomization (R software). One male and two female Dravet mice with no seizures during the baseline recording, were excluded for the second recording session. Animals were provided with CD or KD for a period of 3 weeks, following which the mice had a second week of continuous video-EEG-ECG recordings. For the next 2 weeks animals were exposed to different behavioral tests comprising nest building activity, saccharin preference test, open field test, novel object recognition and gait assessment. Mice were fasted for 6 hours prior to euthanasia, and plasma and hippocampal tissue were collected for metabolomic analysis (metaSysX GmbH). The experimental timeline is sketched in Fig. S1A. All experimental procedures are described in detail in *Supporting Information* (Fig. S1B).

*Statistical analysis*

R software (version 3.6.1.) was used for statistical analysis. GraphPad Prism (Version 5.04, GraphPad, USA) and R software (version 3.6.1.) were used for data visualization. Spearman correlation matrix was calculated and visualized using R software (R package “gplots”(Warnes

et al., 2016)) and the significance level was set at < -0.5 or > 0.5. Missing data from individual animals were not considered for the respective correlation analysis.

All data were expressed as mean ± SEM except for nest complexity score and body weight, for which the median and mean are illustrated in respective graphs. Smoothing of body weight graph line in Fig. S7 is based on a Loess regression. All results were firstly checked for possible batch and sex effects. If present, they were considered in the statistical analysis.

Two-tailed paired t-test was used for comparison between baseline and post diet seizure data in Dravet mice where indicated. Two-tailed unpaired t-test was used for a comparison between wildtype and Dravet mice CD fed where indicated. Two-way ANOVAs were used for testing the genotype and diet effect where appropriate, followed by a Bonferroni post-hoc test. In addition, false discovery rate (FDR) correction was applied to metabolome analysis to minimize multiple comparisons error. Next complexity score was analyzed with Friedman non-parametric test, Dunn's Multiple Comparison Test. The significance level was set at $p < 0.05$ for all tests.

## *Results*

### *Metabolomics*

Metabolomic screening detected 118 and 120 different metabolites in plasma and hippocampal samples, respectively. Genotype differences between Dravet and wildtype mice were identified for 72 metabolites in the hippocampus and for none of the metabolites in the plasma (Two-way ANOVA, FDR corrected).

The KD affected metabolite levels in both, plasma (18 metabolites) and hippocampus (14 metabolites) samples of wildtype and Dravet mice (Two-way ANOVA, FDR corrected). No relevant difference between sexes were observed.

### *Genotype associated alteration in hippocampus and plasma metabolites in Dravet*

Following entry into cells, glucose is phosphorylated to glucose-6-phosphate to prevent its diffusion out of the cell and create a pool that draws more glucose into the cell (Mergenthaler et al., 2013). Interestingly, a decrease in glucose and an increase of phosphorylated glucose (D-glucose-6-phosphate and α-D-glucose-6-phosphate) were noted in the hippocampus of Dravet mice when compared to wildtype mice (Fig. 1, S2A-C). Additionally, α-D-glucose-1-phosphate was up-regulated in the hippocampus of Dravet mice (Fig. S2D). Depending of the energetic state, it can act as glycogen precursor or as the main product of glycogen degradation, which next converts to glucose-6-phosphate and enters glycolysis (Obel et al., 2012). Furthermore, β-hydroxybutyrate (BHB), a ketone body and alternative brain fuel, was neither regulated in plasma nor in the hippocampus of Dravet mice fed CD (Fig. 1, 3D-E).

Several intermediate metabolites in glycolysis proved to be up-regulated in the hippocampus of Dravet mice. These included D-fructose-6-phosphate, D-fructose-1,6-biphosphate, D-fructose-1-phosphate, dihydroxyacetone-phosphate and pyruvic acid (Fig. 1, S3). Pyruvate can enter the tricarboxylic acid (TCA) cycle. Some intermediates of the TCA cycle were down-regulated in hippocampal tissue of Dravet mice, including malic acid and citric acid (Fig. 1, S4A-E). (S)-

lactate is one of the favored brain fuels produced from pyruvate (Smith et al., 2003). Recently, its significance in shuttle between astrocytes and neurons and microglia, revealed a pivotal role in neuroenergetics (Mason, 2017). Interestingly, Dravet mice displayed a reduced level of (S)-lactate in the hippocampus in comparison with wildtype controls (Fig. 1, S4F).

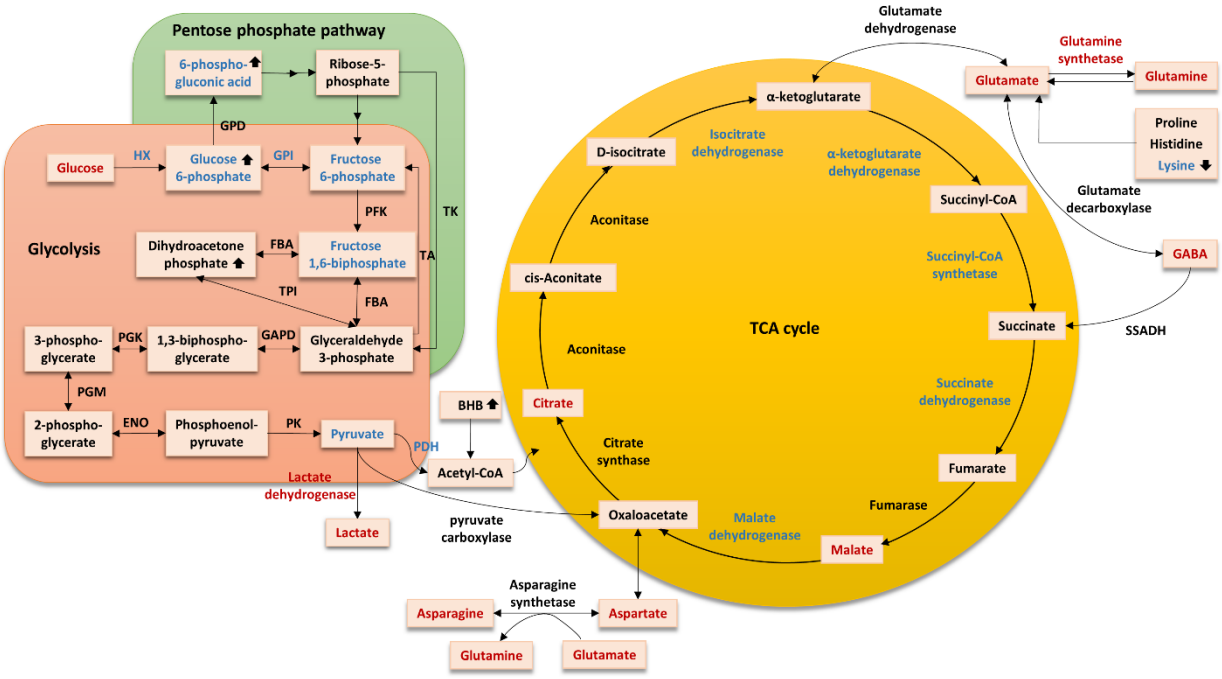


**Fig. 1 Hippocampal glycolysis, the pentose phosphate pathway and tricarboxylic acid (TCA) cycle in mice with Dravet mice.** This sketch illustrates metabolites (presented in blocks) and proteins detected in the previous study (only text; Miljanovic et al., under revision). Changes in metabolite or protein abundance in Dravet mice as compared to wildtype mice are indicated by text color (blue = up-regulation, red = down-regulation). Ketogenic diet effects on selected metabolites in Dravet mice are indicated with an arrow (up = up-regulation, down = down-regulation). HX – hexokinase, GPD - glucose-6-phosphate dehydrogenase, GPI - glucose-6-phosphate isomerase, PFK – phosphofructokinase, TA – transaldolase, TK – transketolase, FBA - fructose-bisphosphate aldolase, GAPD – glyceraldehyde 3-phosphate dehydrogenase, TPI - triose-phosphate isomerase, PGK - phosphoglycerate kinase, PGM - phosphoglycerate mutase, ENO – enolase, PK – pyruvate kinase, PDH – pyruvate dehydrogenase, BHB – β-hydroxybutyrate, SSADH - succinic semialdehyde dehydrogenase.

Glucose-6-phosphate can be processed in the pentose phosphate pathway (Mergenthaler et al., 2013). Some of the intermediate metabolites were up-regulated in Dravet mice (Fig. 1). These comprised 6-phosphogluconic acid (Fig. S4G) as well as D-fructose-6-phosphate (Fig. S3A),

an intermediate which can enter glycolysis. In contrast, ribose-5-phosphate remained unchanged in Dravet mice (Fig. S4H).

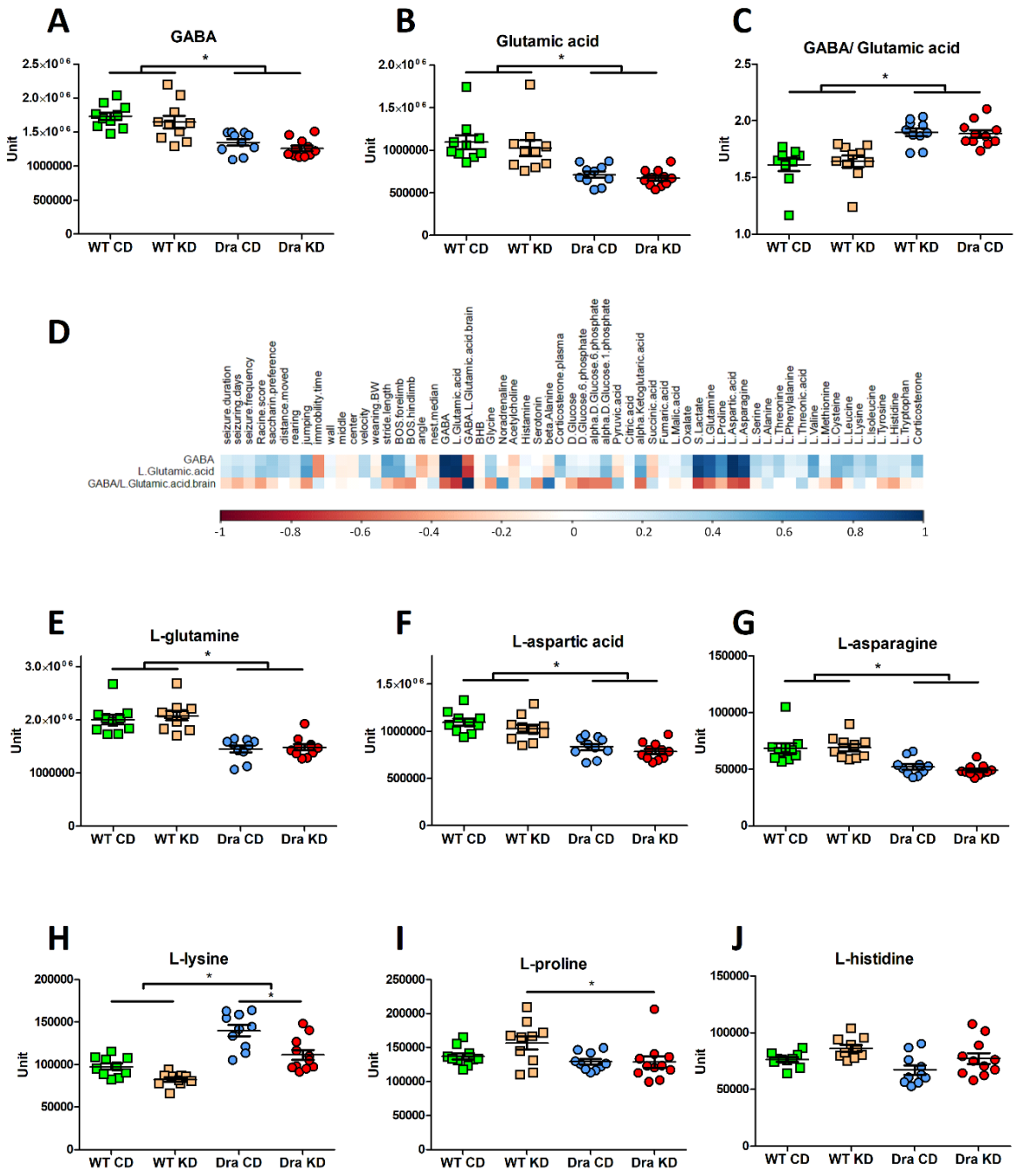


**Fig. 2 Hippocampal levels of GABA, glutamic acid and its amino acids precoursors. A** Hippocampal abundance of GABA. Hippocampal levels of GABA were significantly reduced in mice with the Dravet genotype. **B** Hippocampal level of glutamic acid. Dravet mice exhibited a reduced abundance of glutamic acid when compared to wildtype mice. **C** GABA:glutamic acid ratio in the hippocampus. This ratio was higher in Dravet mice as compared to wildtype mice. **D** Spearman correlation matrix between GABA, glutamic acid, GABA:glutamic acid ratio, and behavioral parameters, selected hippocampal metabolites and plasma corticosterone. The heat map represents individual Spearman correlations between selected parameters in

Dravet mice. The color scale is shown below the matrix with blue and red indicating positive and negative correlations, respectively. GABA:glutamic acid ratio showed a strong positive correlation with levels of noradrenaline and β-alanine, and a negative correlation with levels of phosphorylated forms of glucose, lactate and glutamic acid precursors in the hippocampus. **E-J** Hippocampal abundance of L-glutamine (**E**), L-aspartic acid (**F**), L-asparagine (**G**), L-lysine (**H**), L-proline (**I**) and L-histidine (**J**). **E-G** The level of L-glutamine, L-aspartic acid and L-asparagine was reduced in Dravet mice regardless of the applied diet. **H** Hippocampal abundance of L-lysine was enhanced in Dravet mice. In addition, KD significantly reduced the metabolite level only in Dravet mice. **I** The level of L-proline in the hippocampus of KD fed mice was significantly lower in Dravet, as compared to wildtype mice. **J** The hippocampal level of L-histidine remained constant in all four groups. Data shown are from 20 wildtype mice (10 CD, 10 KD) and 21 Dravet mice (10 CD, 11 KD). (Two-way ANOVA, FDR correction, Bonferroni post-hoc test, * = $p<0.05$, mean±SEM).

The balance between GABA and glutamate in the brain resembles one of the most important mechanisms contributing to hyperexcitability in epilepsies. Hippocampal levels of both, GABA and glutamate (glutamic acid), were reduced in Dravet mice (Fig. 1, 2A-B). Yet, the GABA:glutamate ratio was significantly increased in Dravet mice, implying a more pronounced reduction of glutamate levels (Fig. 2C). Interestingly, the ratio showed a negative correlation with D-glucose-6-phosphate, α-D-glucose-6-phosphate, α-D-glucose-1-phosphate, α-ketoglutarate, (S)-lactate, L-glutamine, L-asparagine and L-aspartic acid (R=-0.55; -0.53; -0.53, -0.56, -0.69, -0.55, -0,64, -0.69, respectively) and a positive correlation with noradrenaline and β-alanine (R=0.58, 0.74, respectively) (Fig. 2D).

Since glutamate can be synthesized from L-glutamine through the glutamate/GABA-glutamine cycle, it is of interest that Dravet mice showed a pronounced L-glutamine down-regulation in the hippocampus (Fig. 1, 2E). Other amino acids known as glutamate precursors were also regulated in mice with *Scn1a* deficiency with aspartic acid and asparagine showing a down-regulation and lysine showing an up-regulation (Fig. 1, 2F-H). On the other hand, proline and histidine were not regulated in the hippocampus of mutant mice (Fig. 1, 2I-J). Lastly, no changes in the level of α-ketoglutarate, an TCA cycle intermediator and important glutamate precursor, were noted in Dravet mice.

Several neurotransmitters were detected in hippocampal tissue. Noradrenaline was reduced and beta-alanine, which has been suggested to act as an amino acid neurotransmitter(Tiedje et al., 2010), was increased in the hippocampus of Dravet mice. Further neurotransmitters including serotonin, acetylcholine, histamine and glycine were not affected by the genotype (Fig. S5).

Analysis of the plasma metabolome in CD fed mice, pointed towards a down-regulation of corticosterone, allocholic and cholic bile acid and an up-regulation of malic acid in Dravet mice (Fig. 3A-C; unpaired t-test, FDR corrected). Deoxycholic and hyodeoxycholic acid plasma levels remained unaffected (data not shown).

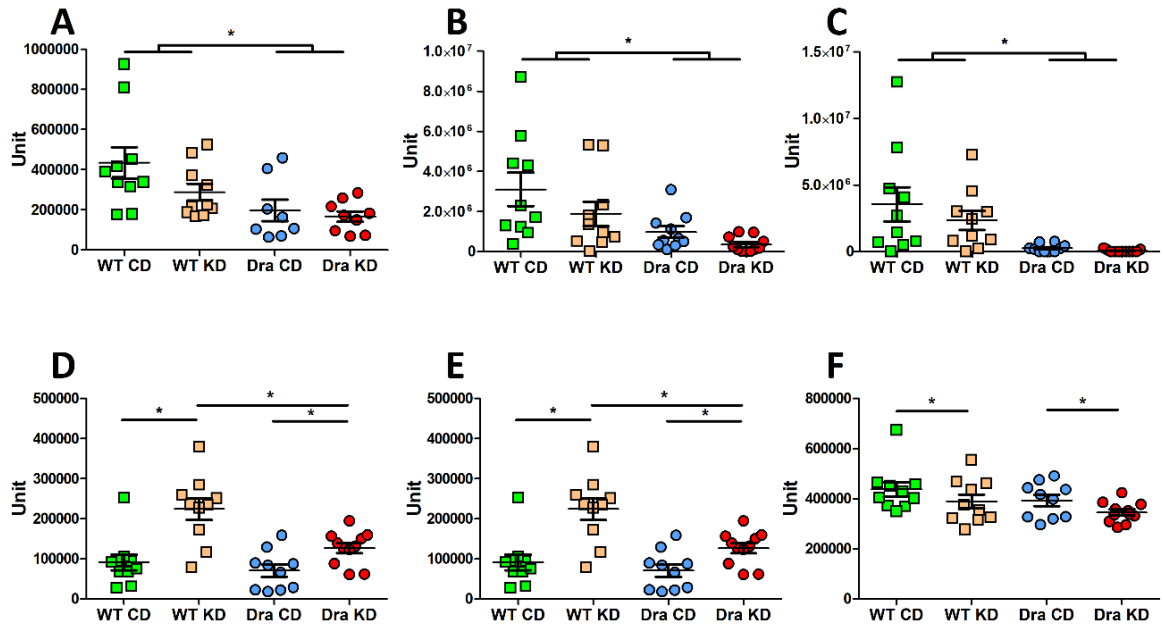


**Fig. 3 Plasma metabolites and ketosis confirmation. A** Plasma level of corticosterone. The metabolite level was reduced in mice with the Dravet genotype, regardless of the diet. **B-C** Plasma levels of allocholic (**B**) and cholic acid (**C**). Allocholic and cholic acids were reduced in Dravet mice, regardless of the diet. **D-E** β-hydroxybutyrate (BHB) level in the hippocampus (**D**) and plasma (**E**). KD increased hippocampal and plasma BHB in both wildtype and Dravet mice. In addition, the BHB level was higher in wildtype mice consuming KD, as compared to Dravet mice in both the hippocampus and plasma. **F** Plasma level of glucose. KD decreased plasma glucose in both wildtype and Dravet mice. Data shown are from 20 wildtype mice (10 CD, 10 KD) and 21 Dravet mice (10 CD, 11 KD). (Two-way ANOVA, FDR correction, Bonferroni post-hoc test, * = $p<0.05$, mean±SEM).

*Ketogenic diet effect on hippocampus and plasma metabolome*

An increased BHB in wildtype and Dravet animals, confirmed that KD exposure induced ketosis in both genotypes. However, hippocampus and plasma BHB levels in wildtype mice exceeded the respective levels in Dravet mice (Fig. 3D-E). As KD is poor in carbohydrates, it was no surprise that exposure was associated with lowered plasma glucose levels (Fig. 3F). Yet, hippocampal glucose levels remained unaffected (Fig. S2A). Intracellular glucose forms (D-glucose-6-phosphate, α-D-glucose-6-phosphate) were increased only in Dravet mice fed KD, as compared to those fed CD (Fig. 1, S2B-C). Additionally, a mild KD effect on glucose metabolism was observed. An increase of two glycolysis intermediates was noted, with D-fructose-1-phosphate increased only in wildtype and dihydroxyacetone-phosphate increased only in Dravet mice (Fig. 1, S3C-D). An intermediate metabolite of the phosphate pentose cycle, 6-phosphogluconic acid, was increased in Dravet mice fed KD, as compared to those fed CD (Fig. 1, S4G). Concerning the TCA cycle, levels of α-ketoglutarate and succinic acid in wildtype mice fed KD exceeded those in Dravet mice with KD exposure (Fig. S4A, D).

*Effect of KD on food intake and body weight development*

Over the period of 7 weeks, wildtype and Dravet mice fed CD consumed a higher amount of diet than mice fed KD. Additionally, the amount of KD consumption in Dravet mice, exceeded the amount consumed by wildtype mice (Fig. S7A). In this context it needs to be considered that the caloric value of the KD was higher than that of the CD (KD: 6.7 kcal/g; CD: 3.8 kcal/g). Mice fed KD had an overall higher caloric intake. Additionally, Dravet mice fed KD exhibited the highest overall caloric intake exceeding that in all other groups (Fig. S7B).

As expected body weight increased in all groups during the experimental course. However, body weight of Dravet mice fed KD exceeded that from all other groups in both, males and females (Fig. S7C).

*Effect of KD on spontaneous generalized tonic-clonic seizures and behavior*

Dravet mice had two video-EEG recording sessions, and the diet effect was examined by analyzing a relative change of motor seizure parameters. The diet did not affect any of the motor seizure parameters including: total seizure duration, seizure frequency, number of days with seizures within a week and Racine score (Fig. 4A, Table S2). Electrographic seizure activity was confirmed with EEG recordings and high amplitude spiking over 500 μV (Fig. 4B).

However, in Dravet mice fed CD seizures were prolonged and more frequent in animals with lower levels of D-glucose-6-phosphate and higher levels of citric acid, L-glutamine and other amino acids (Fig. 4C-up). Following KD exposure of Dravet mice a positive correlation between seizure parameters and metabolites was restricted to α-D-glucose-6-phosphate, α-D-glucose-1-phosphate and the TCA cycle intermediates α-ketoglutarate and malic acid (Fig. 4C-down).

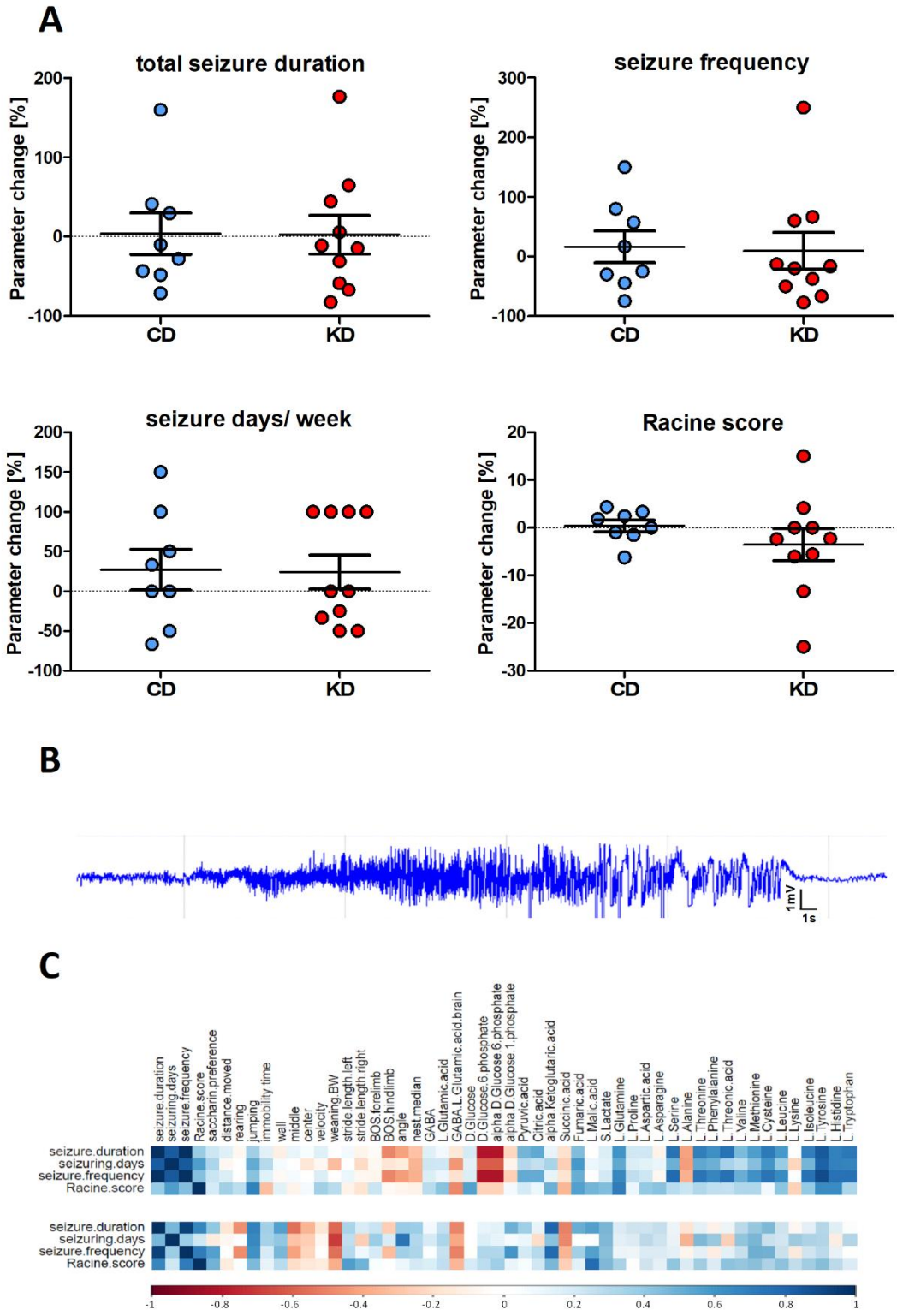


**Fig. 4 Generalized tonic-clonic seizure parameters. A** Total seizure duration, seizure frequency, number of days with seizures within a week and Racine score in Dravet mice. KD did not affect any of the assessed seizure parameters. Data shown are from 17 Dravet mice (8 CD, 9 KD). (Unpaired t-test, * = $p<0.05$, mean±SEM). **B** A representative EEG recording of a spontaneous, generalized tonic-clonic seizure in a Dravet mouse. **C** Spearman correlation matrix between seizure parameters, behavioral parameters, selected hippocampal metabolites, and plasma corticosterone. The heat map represents individual Spearman correlations between

selected parameters in Dravet mice fed control diet (CD, upper band) and Dravet mice fed KD (lower band). The color scale is shown below the matrix with blue and red indicating positive and negative correlations, respectively. Seizure severity (total seizure frequency and duration) showed a strong positive correlation with levels of citric acid, L-glutamine and other amino acids and a negative correlation with the level of D-glucose-6-phosphate in Dravet mice fed CD (upper band). In Dravet mice fed KD, a positive correlation between seizure severity and α-D-glucose-6-phosphate, α-D-glucose-1-phosphate, α-ketoglutarate and malic acid was observed (lower band).

Assessment of gait revealed no differences in stride length, regardless of the genotype and diet (Fig. 5A). The angle between forelimb paw orientation and body direction proved to be wider in Dravet mice (Fig. 5B) without an influence of the diet. The forelimb base of support (BOS) was neither affected by genotype nor diet (Fig. 5C). However, hindlimb BOS proved to be shorter in Dravet mice. Interestingly, exposure to the KD in Dravet mice, reversed hindlimb BOS to wildtype values (Fig. 5D). Notably, an improvement of gait with an increase of hindlimb BOS in Dravet mice, showed a strong positive correlation with glucose, D-glucose-6-phosphate, α-D-glucose-6-phosphate and acetylcholine, and a negative correlation with β-alanine in the hippocampus (Fig. 5E-up). Moreover, when analyzing data from Dravet mice on KD, the hindlimb BOS parameter positively correlated with glucose, lactate, GABA, glutamate, acetylcholine, glutamine, aspartic acid, threonine, phenylalanine, lysine and histidine concentrations in the hippocampus. Lastly, a negative correlation with fumaric acid was noted (Fig. 5E-down). No differences between sexes were detected in any of the gait parameters.

The impact of genotype and KD on open field test, novel object recognition, saccharin preference test and nest-building activity is reported in *Supporting Information* (Fig. S8).

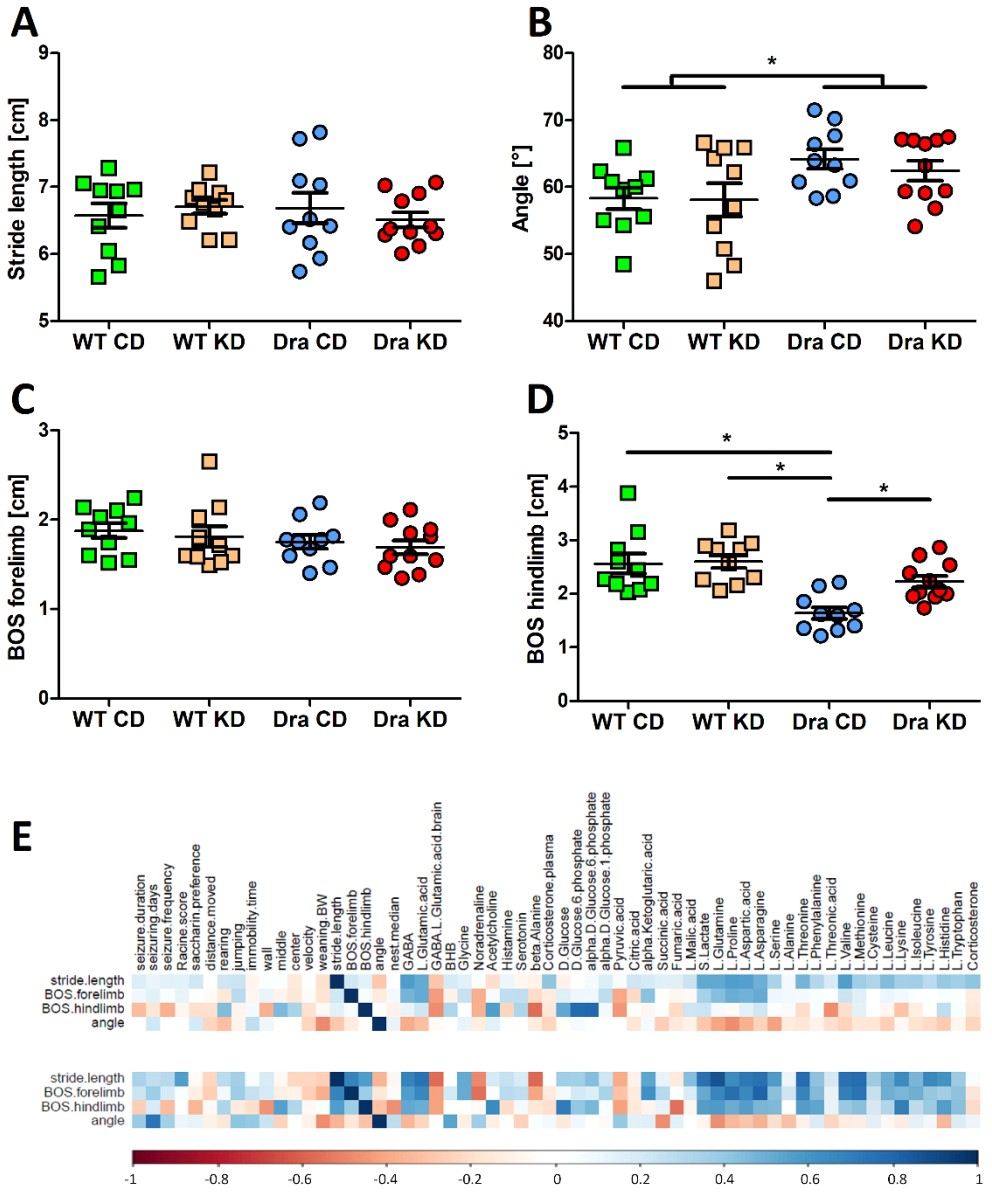


**Fig. 5 Gait analysis. A** Stride length. Dravet and wildype mice had a comparable length of stride, regardless of the consumed diet. **B** Angle between forelimb paw and body direction. Mice with the Dravet genotype had a significantly wider angle than wildtype mice. **C-D** Base of support (BOS) between forelimbs (**C**) and hindlimbs (**D**). No differences in forelimb BOS were noted between all four groups. Hindlimb BOS was reduced in mice with the Dravet genotype. Application of KD in Dravet mice, restored this parameter to the values of wildtype mice, thus improving the gait. Data shown are from 20 wildtype mice (10 CD, 10 KD) and 21 Dravet mice (10 CD, 11 KD). (Two-way ANOVA, Bonferroni post hoc test, * = $p<0.05$, mean±SEM). **E** Spearman correlation matrix between assessed gait parameters, other behavioral parameters and selected hippocampal metabolites (except for corticosterone, measured in plasma). The heat map represents individual Spearman correlations between selected parameters in Dravet mice (upper band) and Dravet mice fed KD (lower band). The color scale is shown below the matrix with blue and red indicating positive and negative correlations, respectively. Hindlimb BOS showed a positive correlation with levels of glucose, D-glucose-6-phosphate, α-D-glucose-6-phosphate and acetylcholine, and a negative correlation

with levels of β-alanine in the hippocampal tissue of Dravet mice (upper band). In Dravet mice fed KD, hindlimb BOS showed a positive correlation with levels of glucose, lactate, GABA, L-glutamic acid, acetylcholine, L-glutamine, L-aspartic acid, L-threonine, L-phenylalanine, L-lysine and L-histidine, and a negative correlation with the level of fumaric acid in the hippocampus (lower band).

## *Discussion*

Hippocampal metabolomic analysis in a Dravet mouse model revealed complex alterations in energy metabolism. Moreover, we obtained evidence for a direct and indirect impact of *Scn1a* deficiency on the glutamate/GABA-glutamine cycle, on concentrations of noradrenaline and two bile acids concentrations. A previous large-scale proteomic analysis gave us the opportunity to interpret the present findings in the context of alterations in enzymes or transporter molecules.

Alterations in glucose metabolism point to a genotype-associated activation of catabolic processes with enhanced glycogenolysis and glycolysis. A shift in brain glucose transport and metabolism in Dravet syndrome with *Scn1a* deficiency has previously been suggested by experimental and clinical FDG-PET data (Haginoya et al., 2018; Ricobaraza et al., 2019). As intracellular FDG accumulation largely depends on glucose uptake at the blood-brain barrier and its metabolism to glucose-6-phosphate by hexokinase, it is of interest that we observed a lowered expression of glucose-1 transporter responsible for astrocytic uptake of glucose and an increased expression of hexokinase in the proteomic analysis (Table S1).

While we obtained evidence for an enhanced supply of pyruvate and increased expression of several enzymes contributing to TCA cycle activity, reduced concentrations of lactate and of the TCA cycle intermediates malate and citrate indicate that there might be a failure to adequately fulfil increased neuronal energy demands related to enhanced synaptic activity. Along this line, the up-regulation of glycogenolysis and glycolysis might reflect the cellular attempt to compensate for energetic failure. In this context, it is of particular interest that the neuronal transporter, glucose transporter 3 and the lactate transporter monocarboxylate transporter 1, are up-regulated in Dravet mice (Table S1). Thus, the metabolic coupling between astrocytes and neurons, with predominant regulation of glycolysis in astrocytes, shuttling of lactate to neurons, and predominant regulation of the TCA cycle in neurons (Turner and

Adamson, 2011), seems to be significantly altered in Dravet mice with genetic deficiency (Fig. 6).

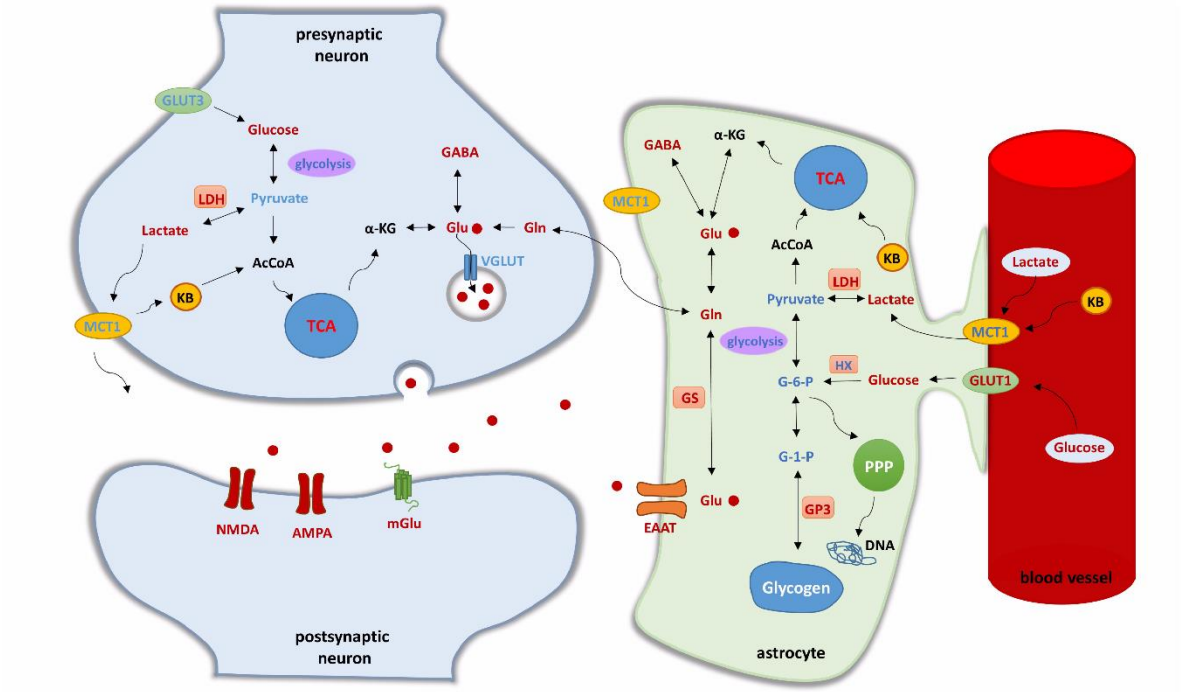


**Fig. 6 Hippocampal glucose metabolism in Dravet mice.** This sketch illustrates detected metabolites (presented with text) and proteins detected in the previous study (enzymes, receptors and transporters; Miljanovic et al., under revision). Changes in metabolite or protein abundance in Dravet mice are indicated by text color (blue = up-regulation, red = down-regulation). Glu – glutamate, Gln – glutamine, α-KG - α-ketoglutarate, G-6-P – glucose-6-phosphate, G-1-P – glucose-1-phosphate, KB – ketone bodies, GLUT – glucose transporter, VGLUT - vesicular glutamate transporter, MCT1 - monocarboxylate transporter 1, EAAT – excitatory amino acid transporter, GS - glutamine synthetase, HX – hexokinase, LDH – lactate dehydrogenase, GP3 - glycogen phosphorylase 3a., PPP – pentose phosphate pathway, TCA - tricarboxylic acid cycle.

In the epileptic brain, energy depletion occurring during seizures is considered an important contributor to seizure termination (Yang et al., 2013b). In the interictal phase, enhanced spiking activity of neurons is associated with enhanced energy consumption related to ion channel activity as well as synaptic neurotransmitter processing (Ivanov et al., 2015). Our present findings provide evidence that Dravet syndrome can also be associated with a significantly altered energy metabolism. This finding might at least partly be related to enhanced interictal activity and associated increases in neuronal energy demand. In this context, it needs to be taken

into account that alterations in glucose metabolism and TCA cycle activity should not only be considered as a consequence of seizures and interictal activity, but can also contribute to an enhanced seizure susceptibility and ictogenesis. The pathophysiological relevance has been convincingly demonstrated by the characterization of genetic epilepsies with primary failure of energy supply related to a genetic deficiency of glucose transporter 1 or the sodium-dependent citrate transporter NaCT encoded by the *SLC13A5* gene (Henke et al., 2020; Pong et al., 2012). In the context of *SLC13A5* deficiency the interneuron energy hypothesis has been formulated (Bhutia et al., 2017), which is based on the fact that inhibitory interneurons are characterized by a higher energy consumption than excitatory principal neurons (Kann, 2016). As discussed previously (Henke et al., 2020), energy deficits in inhibitory interneurons may result in disinhibition of excitatory neurons causing hyperexcitability. Thus, cumulative neuronal energy depletion as a consequence of increased interictal spiking may actually pave the way for a continuous lowering of the seizure threshold and generation of the next seizure event. Along this line, changes in TCA cycle activity can reduce ATP and adenosine concentrations with an impact on adenosine $A_1$ receptors subsequently affecting inwardly-rectifying potassium channels and neuronal excitability (Boison, 2017; Boison and Steinhäuser, 2018; Henke et al., 2020; Masino and Rho, 2019). Our data therefore suggest that the complex alterations in energy metabolism may contribute to the high seizure frequency often characterizing the clinical phenotype of Dravet syndrome. This conclusion received further confirmation by the fact that we identified a correlation between seizure duration and frequency, and glucose metabolism and TCA cycle intermediates.

Another key finding of the broad-scale metabolic analysis was the down-regulation of the entire glutamate/GABA-glutamine cycle. Considering that TCA cycle activity is linked to glutamate formation via its intermediate α-ketoglutarate (Wu et al., 2016; Youngson et al., 2017), lowered concentrations of glutamate, GABA, and glutamine might be related to decreased TCA cycle-mediated supply of the glutamate precursor α-ketoglutarate. Alterations in the concentrations

of the major excitatory and inhibitory neurotransmitters glutamate and GABA will likely affect neuronal excitability. Thereby, the increased GABA:glutamate ratio indicates a shift favoring GABA synthesis from glutamate. Thus, the alterations affecting the glutamate/GABA-glutamine cycle may actually reflect a mechanism that may partially compensate the *Scn1a*-deficiency related limitations in GABAergic interneuron function that seems to drive network hyperexcitability in Dravet syndrome according to experimental findings in different mouse models (Dutton et al., 2013; Oakley et al., 2011; Tran et al., 2020; Yu et al., 2006). However, it needs to be considered that proteomic analysis revealed a down-regulation of excitatory amino acid transporters and of glutamine synthetase responsible for astrocytic uptake of glutamate and its conversion of glutamine (Table 1). Thus, it is possible that an accumulation of extracellular glutamate concentrations triggering neuronal hyperexcitability might occur despite an overall decrease of the total glutamate concentration (Fig. 6). However, this greater decrease in glutamate may also be related to the age of animals, which is why it would be of interest to assess GABA and glutamate levels in younger mice.

Interestingly, further neurotransmitters comprising aspartate and noradrenaline exhibited lowered concentrations in hippocampal samples from Dravet mice. Considering their role in neuronal excitability (Dingledine and McBain, 1999; Giorgi et al., 2004; O'Donnell et al., 2012; Patri, 2019), these changes might additionally affect seizure susceptibility. However, further studies would be necessary to explore a potential functional relevance.

While it is common knowledge that highly increased levels of bile acids can exert toxic effects on neuronal function, we just more recently started to develop a more differentiated perspective about the impact of bile acids in the healthy and diseased brain (Grant and DeMorrow, 2020; Kiriyama and Nochi, 2019; McMillin and DeMorrow, 2016). This resulted in a discussion about the potential of bile-acid mediated therapies in neurodegenerative disorders(Grant and DeMorrow, 2020). Along this line, reduced levels of two bile acids in Dravet mice suggest that future studies should further explore the disease-associated regulation of bile acids and its

consequences in order to provide information about a potential pathophysiological role and possible basis for therapeutic intervention.

Despite ongoing research efforts, the mechanisms of the KD diet still remain to be incompletely understood at this point of time. Among other mechanisms, a shift in energy supply and in catabolic pathway activities, with a reduction of glycolysis and an enhanced oxidation of fatty acids and ketone bodies, may represent one key mechanism. This shift might help to provide more ATP resulting in adenosine increases, and related to alternate fueling of the TCA cycle might provide more α-ketoglutarate as a precursor for glutamate and subsequent GABA synthesis (Youngson et al., 2017). Interestingly, the fact that the level of ketosis in wildtype mice exceeded that in Dravet mice, provides evidence that related to a different metabolic baseline situation, it can be more difficult to increase ketone body levels in individuals with Dravet syndrome.

Despite the confirmation of ketosis, the alterations in energy metabolism were rather limited. While we observed an increase of different glycolysis intermediates, we failed to confirm a direct effect on TCA cycle activity in both genotypes. Thus, our data do not confirm the energy shift with a down-regulation of glycolytic activity and enhanced TCA cycle activity suggested by previous studies (D'Andrea Meira et al., 2019; Puchalska and Crawford, 2017; Youngson et al., 2017). However, in clinical practice KD is in the majority of patients applied as an adjunctive therapy in combination with antiseizure drugs (Cross et al., 2019). Therefore, we cannot exclude that additional therapy with antiseizure drugs results in an at least partial control of interictal neuronal activity resulting in a better metabolic initial situation, which is then easier to influence by a dietary approach. This assumption is further confirmed by the failure to control seizure activity by the exposure to KD as a monotherapy in the present study. Considering these findings, it would be of interest to assess the impact of different antiseizure drugs on the metabolomic signature of Dravet syndrome. In this context, it is of particular interest that stiripentol, an orphan drug licensed for therapy of Dravet syndrome, can exert direct effects on

metabolism based on an inhibition of lactate dehydrogenase (Sada et al., 2015). Lastly, we cannot exclude the possibility that it might be easier to demonstrate an effect of KD in a mouse model with a more severe seizure phenotype.

The clinical manifestation of Dravet syndrome is also characterized by the development of ataxia, motor deficits and gait disturbance (Gataullina and Dulac, 2017). The latter is partly explained by the fact that $Na_v1.1$ encoded by the *SCN1A* gene is also expressed in cerebellar Purkinje cells and in nodes of Ranvier of motor neurons (Duflocq et al., 2008; Gataullina and Dulac, 2017). KD exposure in Dravet mice resulted in partial normalization of one of the main outread parameters of gait assessment. This finding demonstrates that the metabolic consequences of KD were sufficient to affect the clinical phenotype and that glucose, glucose-6-phosphate, acetylcholine and β-alanine may be relevant markers for gait improvement. Moreover, this result draws attention to a potential beneficial impact of dietary approaches such as the KD on motor dysfunction. So far, there is only very limited clinical information providing first evidence that KD can improve coordination and gait in patients with Dravet syndrome (Tian et al., 2019). Concerning the beneficial effect on gait disturbance, it is recommended to additionally assess the impact of KD on metabolomics in the cerebellum and in peripheral motor neurons.

In conclusion, the comprehensive metabolomic analysis revealed substantial alterations in energy metabolism in mice with the *Scn1a* genetic deficiency. These complex changes might contribute to seizure susceptibility and ictogenesis. In response to KD exposure a beneficial effect on motor dysfunction became evident suggesting that metabolic changes contribute to ataxia and gait disturbances developing during the course of Dravet syndrome.

Interestingly, we also demonstrated alterations in the glutamate/GABA-glutamine cycle, which might serve as an endogenous compensatory mechanism, which can be further supported by GABAergic drugs recommended for management of Dravet syndrome.

## *Acknowledgements*

The authors thank Sarah Glisic, Sieglinde Fischlein, Katharina Gabriel, Sabine Vican and Uwe Roßberg for their excellent technical assistance.

We are also very grateful to Prof. Dr. Jerzy Adamski for his support in the initial discussion of the study planning.

## *Disclosure of Conflicts of Interest*

None of the authors has any conflict of interest to disclose.

## *Ethical Publication Statement*

We confirm that we have read the Journal's position on issues involved in ethical publication and affirm that this report is consistent with those guidelines.

## *References*


Barañano, K. W., Hartman, A. L., 2008. The ketogenic diet: uses in epilepsy and other neurologic illnesses. Curr Treat Options Neurol. 10**,** 410-9.

Bhutia, Y. D., et al., 2017. Plasma Membrane $Na^+$-Coupled Citrate Transporter (SLC13A5) and Neonatal Epileptic Encephalopathy. Molecules. 22.

Boison, D., 2017. New insights into the mechanisms of the ketogenic diet. Curr Opin Neurol. 30**,** 187-192.

Boison, D., Steinhäuser, C., 2018. Epilepsy and astrocyte energy metabolism. Glia. 66**,** 1235-1243.

Cross, J. H., et al., 2019. Dravet syndrome: Treatment options and management of prolonged seizures. Epilepsia. 60 Suppl 3**,** S39-S48.

D'Andrea Meira, I., et al., 2019. Ketogenic Diet and Epilepsy: What We Know So Far. Front Neurosci. 13**,** 5.

Dingledine, R., McBain, C., 1999. Glutamate and aspartate are the major excitatory transmitters in the brain. Basic Neurochemistry: Molecular, Cellular and Medical Aspects. Ed. GJ Siegel, BW Agranoff, RW Albers, SK Fisher, MD Uhler. Philadelphia.

Dravet, C., 2011. The core Dravet syndrome phenotype. Epilepsia. 52 Suppl 2**,** 3-9.

Duflocq, A., et al., 2008. Nav1.1 is predominantly expressed in nodes of Ranvier and axon initial segments. Mol Cell Neurosci. 39**,** 180-92.

Dutton, S. B., et al., 2013. Preferential inactivation of Scn1a in parvalbumin interneurons increases seizure susceptibility. Neurobiol Dis. 49**,** 211-20.

Gataullina, S., Dulac, O., 2017. From genotype to phenotype in Dravet disease. Seizure. 44**,** 58-64.

Giorgi, F. S., et al., 2004. The role of norepinephrine in epilepsy: from the bench to the bedside. Neurosci Biobehav Rev. 28**,** 507-24.

Grant, S. M., DeMorrow, S., 2020. Bile Acid Signaling in Neurodegenerative and Neurological Disorders. Int J Mol Sci. 21.

Haginoya, K., et al., 2018. [(18)F]fluorodeoxyglucose-positron emission tomography study of genetically confirmed patients with Dravet syndrome. Epilepsy Res. 147**,** 9-14.

Henke, C., et al., 2020. Disruption of the sodium-dependent citrate transporter SLC13A5 in mice causes alterations in brain citrate levels and neuronal network excitability in the hippocampus. Neurobiol Dis. 143**,** 105018.

Ivanov, A. I., et al., 2015. Metabolic responses differentiate between interictal, ictal and persistent epileptiform activity in intact, immature hippocampus in vitro. Neurobiol Dis. 75**,** 1-14.

Kann, O., 2016. The interneuron energy hypothesis: Implications for brain disease. Neurobiol Dis. 90**,** 75-85.

Kiriyama, Y., Nochi, H., 2019. The Biosynthesis, Signaling, and Neurological Functions of Bile Acids. Biomolecules. 9.

Kovács, R., et al., 2018. Bioenergetic Mechanisms of Seizure Control. Front Cell Neurosci. 12**,** 335.

Kumar, A., et al., 2018. Evolution of Brain Glucose Metabolic Abnormalities in Children With Epilepsy and SCN1A Gene Variants. J Child Neurol. 33**,** 832-836.

Kuo, F.-S., et al., 2019. Disordered breathing in a mouse model of Dravet syndrome. Elife. 8**,** e43387.

Masino, S. A., Rho, J. M., 2019. Metabolism and epilepsy: Ketogenic diets as a homeostatic link. Brain Res. 1703**,** 26-30.

Mason, S., 2017. Lactate Shuttles in Neuroenergetics-Homeostasis, Allostasis and Beyond. Front Neurosci. 11**,** 43.

McDonald, T., et al., 2018. Impairments in Oxidative Glucose Metabolism in Epilepsy and Metabolic Treatments Thereof. Front Cell Neurosci. 12**,** 274.

McMillin, M., DeMorrow, S., 2016. Effects of bile acids on neurological function and disease. Faseb j. 30**,** 3658-3668.

Mergenthaler, P., et al., 2013. Sugar for the brain: the role of glucose in physiological and pathological brain function. Trends Neurosci. 36**,** 587-97.

O'Donnell, J., et al., 2012. Norepinephrine: a neuromodulator that boosts the function of multiple cell types to optimize CNS performance. Neurochem Res. 37**,** 2496-512.

Oakley, J. C., et al., 2011. Insights into pathophysiology and therapy from a mouse model of Dravet syndrome. Epilepsia. 52 Suppl 2**,** 59-61.

Obel, L. F., et al., 2012. Brain glycogen-new perspectives on its metabolic function and regulation at the subcellular level. Front Neuroenergetics. 4**,** 3.

Oyarzabal, A., Marin-Valencia, I., 2019. Synaptic energy metabolism and neuronal excitability, in sickness and health. J Inherit Metab Dis. 42**,** 220-236.

Patel, M., 2018. A Metabolic Paradigm for Epilepsy. Epilepsy Curr. 18**,** 318-322.

Patri, M., Synaptic Transmission and Amino Acid Neurotransmitters. Neurochemical Basis of Brain Function and Dysfunction. IntechOpen, 2019.

Pong, A. W., et al., 2012. Glucose transporter type I deficiency syndrome: epilepsy phenotypes and outcomes. Epilepsia. 53**,** 1503-10.

Puchalska, P., Crawford, P. A., 2017. Multi-dimensional Roles of Ketone Bodies in Fuel Metabolism, Signaling, and Therapeutics. Cell Metab. 25**,** 262-284.

Reid, C. A., et al., 2014. Epilepsy, energy deficiency and new therapeutic approaches including diet. Pharmacol Ther. 144**,** 192-201.

Ricobaraza, A., et al., 2019. Epilepsy and neuropsychiatric comorbidities in mice carrying a recurrent Dravet syndrome SCN1A missense mutation. Scientific reports. 9**,** 1-15.

Sada, N., et al., 2015. Epilepsy treatment. Targeting LDH enzymes with a stiripentol analog to treat epilepsy. Science. 347**,** 1362-7.

Scheffer, I. E., et al., 2017. ILAE classification of the epilepsies: Position paper of the ILAE Commission for Classification and Terminology. Epilepsia. 58**,** 512-521.

Smith, D., et al., 2003. Lactate: a preferred fuel for human brain metabolism in vivo. J Cereb Blood Flow Metab. 23**,** 658-64.

Tang, S. H. E., et al., 2002. A Cre/loxP-deleter transgenic line in mouse strain 129S1/SvImJ. genesis. 32**,** 199-202.

Tian, X., et al., 2019. The Efficacy of Ketogenic Diet in 60 Chinese Patients With Dravet Syndrome. Front Neurol. 10**,** 625.

Tiedje, K. E., et al., 2010. Beta-alanine as a small molecule neurotransmitter. Neurochem Int. 57**,** 177-88.

Tran, C. H., et al., 2020. Interneuron Desynchronization Precedes Seizures in a Mouse Model of Dravet Syndrome. J Neurosci. 40**,** 2764-2775.

Turner, D. A., Adamson, D. C., 2011. Neuronal-astrocyte metabolic interactions: understanding the transition into abnormal astrocytoma metabolism. J Neuropathol Exp Neurol. 70**,** 167-76.

Waldbaum, S., Patel, M., 2010. Mitochondrial dysfunction and oxidative stress: a contributing link to acquired epilepsy? J Bioenerg Biomembr. 42**,** 449-55.

Wang, Y. Q., et al., 2020. Efficacy of the ketogenic diet in patients with Dravet syndrome: A meta-analysis. Seizure. 81**,** 36-42.

Warnes, M. G. R., et al., 2016. Package 'gplots'. Various R Programming Tools for Plotting Data.

Wu, N., et al., 2016. Alpha-Ketoglutarate: Physiological Functions and Applications. Biomol Ther (Seoul). 24**,** 1-8.

Yang, H., et al., 2013. Glycolysis in energy metabolism during seizures. Neural Regen Res. 8**,** 1316-26.

Youngson, N. A., et al., 2017. The mechanisms mediating the antiepileptic effects of the ketogenic diet, and potential opportunities for improvement with metabolism-altering drugs. Seizure. 52**,** 15-19.

Yu, F. H., et al., 2006. Reduced sodium current in GABAergic interneurons in a mouse model of severe myoclonic epilepsy in infancy. Nature Neuroscience. 9**,** 1142.

## *Supporting information*

## *Methods*

### *Housing of animals*

From birth until weaning time (P19-21), each litter was housed in individually ventilated cages (Tecniplast, Hohenpeißenberg, Germany). Following weaning, animals were kept in groups of 3-5 animals per standard Makrolon type III cage (Ehret, Emmendingen, Germany). Following surgery, mice were kept single-housed.

Once per week, each cage was provided with fresh sawdust as a bedding material (Lignocel, Rosenberg, Germany), one animal house (Tecniplast, Hohenpeißenberg, Germany; Zoonlab GmbH, Castrop-Rauxel, Germany), and 7 g of Enviro-dri® nest material (Claus GmbH, Neuwied Germany). Animal housing was maintained under standard conditions (temperature 22 ± 2˚C, humidity 40-60 %, regular 12-hour light/dark cycle).

All animals received ad libitum tap water and food (ssniff® R/M-H, Sniff, Soest, Germany). Between postnatal day P14 and P26 animals had additional access to a Dietgel76A as a supplement (Sniff, Soest, Germany).

Following group allocation, animals were provided either with 6:1 fat:protein ketogenic diet (KD; #TD07797, Envigo, Italy), or a vitamin and mineral balanced control diet (CD; #TD150300, Envigo, Italy). CD or KD were provided to animals over a period of 41-42 days (depending on the day of sacrifice). The amount of consumed food was measured daily. Since the food had a consistency of paste, animals were provided with wooden popsicles as an enrichment (Pura Sticks, Labodia AG, Niederglatt, Switzerland).

### *Ketosis confirmation*

A pilot study with five wildtype and five Dravet mice was conducted in order to determine the duration of KD exposure sufficient to guarantee development of ketosis in all animals. A drop

of blood was sampled from the facial vein with a lancet (Cat# GR-5MM, BioSebLab, Vitrolles, France), and beta-hydroxybutyrate (BHB) was measured with ß-ketone test stripes and Glucomen Areo 2K device (GlucoMen® Areo, Berlin, Germany. Due to the circadian nature of BHB concentrations, onset and end of the light phase (6 a.m. and 6 p.m.) were chosen as the two time points for measurement. Before the exposure to KD, mice were fed a standard chow and baseline blood BHB was measured. Then, mice were fed KD for 3 weeks and blood BHB was measured weekly. Blood BHB from three wildtype and three Dravet mice was not measured at 6 a.m. for the baseline and 1 week after the initiation of KD. One wildtype female mouse died in the context of blood sampling after one-week exposure to the KD. Once ketosis was confirmed, KD was replaced with standard chow and animals were euthanized with 600 mg/kg pentobarbital.

*Surgery and video-EEG recordings*

Twelve-week-old wildtype and Dravet mice underwent a survival surgery for telemetric transmitter (HD-X02, DSI, St. Paul, USA) and electrode implantation preparing the animals for EEG-ECG recordings. Wildtype mice were used as controls and were therefore implanted with a dummy transmitter with no recording opportunity. Each cohort was implanted within 1 week, and the order of animals during the day was randomized (R software).

Mice received 1 mg/kg meloxicam s.c. (Metacam®, Boehringer Ingelheim, Germany) for analgesia 30 minutes before the anesthesia induction and 24 hours afterwards. Isoflurane (Isofluran CP®, Henry Schein Vet, Hamburg, Germany) was used as a general anesthetic: 4 % for induction and 1.5 % for maintenance of anesthesia. Bupivacaine was applied subcutaneously as a local anesthetic: 0.25 % (Jenapharm®, Mibe GmbH, Brehna, Germany) to surgical areas affected by transmitter implant and placement of leads; and 0.5 % + 0.0005 % epinephrine (Jenapharm®, Mibe GmbH, Brehna, Germany) for intracranial electrode placement.

For the subcutaneous placement of telemetric transmitter, the skin was opened in the dorsocaudal part of the scapula region. ECG leads were fixed intramuscularly: negative lead to the right pectoral muscle, and positive lead to xyphoid. Skin was closed over the ECG lead with absorbable sutures (Smi AG, St. Vith, Belgium) and animals were fixed in the stereotactic surgical frame. Three screws were fixed into the scull and the negative EEG lead was connected to the screw placed over the cerebellum. The positive EEG lead was connected to a bipolar Teflon-isolated stainless-steel electrode, before implanting it in the hippocampal CA1 region (ap: - 2.00; lat: + 1.3; dv: - 1.6).

Paladur (Heraeus®, Hanau, Germany) was used for fixation of the electrode and absorbable sutures for closing the skin around the skull. A tissue adhesive (Surgibond®, Henry Schein Vet, Hamburg, Germany) was applied to close the initial cut for placing the transmitter.

Mice were provided with oxygen (Oxyboy oxygen generator, Hugo Sacks Electronic, March-Hugstetten, Germany) until regaining consciousness. Following a recovery time of 2 weeks, a one-week continuous video-EEG-ECG baseline recordings was completed using Ponemah software (Ponemah R, v. 5.2.0, DSI, St. Paul, USA). Spontaneous seizure activity was detected automatically (NeuroscoreTM v. 3.0, DSI, St. Paul, USA) and further confirmed and analyzed using acquired videos (Axis communications, Lund, Sweden). The amplitude threshold for seizure spikes was set to 500 µV. Seizure duration, frequency, severity, and number of days with seizures within a week were evaluated. Seizure severity was scored based on the adapted Racine scoring system: (Dutton et al., 2017; Racine, 1972): I (orofacial movements), II (head nodding), III (forelimb myoclonus), IV (forelimb clonic convulsions with rearing), V (generalized motor convulsions followed by rearing and falling) and score VI (generalized motor convulsions followed by running and bouncing).

*Behavioral assessment*

Behavior tests were completed in morning hours starting from 8 a.m. Nest-building activity and saccharin preference were conducted in the home cage during the first week of behavior tests. In the second week of behavioral testing, the open field test, the novel object recognition test and gait assessment were completed and video documented in a test room under standard conditions (temperature 22 ± 2˚C, humidity 40-60 %, lighting 15-20 lx).

*Nest-building activity*

Following the second week of continuous video-EEG recording, nest building activity was assessed. For seven consecutive days, nests were photographed each morning. The images were used for nest complexity scoring by an investigator blinded to animals' genotype and treatment. Nest complexity was scored based on a scoring system adapted from Jirkof and colleagues (Jirkof et al., 2013): score 0 = nesting material is intact; score 1 = nesting material is noticeably manipulated and possibly spread around the cage; score 2 = nest site is evident with over 50 % of nesting material at nest site or animals starting to build walls (one to two sides) and nest is hollow in bedding; score 3 = a flat nest with visible walls, can be hollow in bedding; score 4 = a complex, bowl-shaped nest with walls higher than mice, surrounding the nest in more than 50 %.

*Saccharin Preference Test*

In parallel with the nest building assessment, the saccharin preference test was completed. The aim of the test is to assess anhedonia-associated behavior used for detection of depressive-like behavior in mice (Klein et al., 2015). The test was carried out at four consecutive days (24-hour periods). On each day, mice were provided with two water bottles and liquid consumption was measured at the end of each period. On the first day, animals were provided two bottles of water in order to determine baseline water intake. On the following day, the right bottle was replaced

with 0.1 % saccharin solution to assess preference for sweet solution. On the third day, both bottles were filled with water. During the last period, the left bottle was filled with 0.1 % saccharin solution, aiming to check for possible side preference. Saccharin is an artificial sweetener with no effective calories, meaning it could not interfere with the composition of provided diet.

*Open Field Test*

The open field test is frequently used to examine locomotion and exploratory behavior in an unfamiliar surrounding (Carola et al., 2002). One hour prior to testing, mice were placed in the test room to habituate. The order of animals was randomized. Two white cylinders (diameter 61 cm, height 40 cm) were used simultaneously, in order to test two mice in parallel. Mice were placed individually into the cylinder, facing the wall at a distance of 10 cm from the wall. Ten-minute-long trials were recorded with Ethovision 8.5 Software (EthoVision XT, Noldus, Wageningen, The Netherlands). The software was used for automatic analysis of locomotion and time spent in different zones (wall, middle, center). Rearing behavior was scored manually by an observer unaware of animals' group allocation. Following the end of the trial, mice were returned to their home cage. Cylinders were cleaned with 0.1 % acetic acid between trials.

*Novel Object Recognition*

Novel object recognition test is a common test for assessing learning and memory in mice, performed over three consecutive days (Lueptow, 2017). The open field test was used as the first test day (habituation phase). On the second and third day of testing, all conditions were replicated with the exception of providing two objects in the open field arena. On the second day (training phase), mice were introduced to two identical objects (grey, textured pyramid or white, smooth cylinder; diameter 4 cm, height 10 cm) placed 15 cm apart and 12 cm from the wall, with the same lighting conditions. On the next day (test phase), one of the objects was

replaced with an unfamiliar object. The order of the animals, the object for the training phase (pyramid or cylinder) and the position of the novel object in the test phase were randomized. Over the 10-minute session, the time sniffing at and exploring the familiar (TF) and novel object (TN) was automatically measured with Ethovision 8.5 Software and the nose point tracking tool. Mice were considered to sniff an object once their nose point was up to 2 cm away from the object and/or mice were touching the object with the nose or forepaws. Sitting on the object was not counted as active object exploration. Discrimination index was calculated using following formula: TN/(TN+TF) x100 %.

*Gait analysis*

A transparent plexiglas runway (length 100 cm, width 10 cm) surrounded by white walls (height 10 cm), was placed 1 m over the ground and used for gait assessment. An entrance to a covered black box (15x15 cm), a dark shelter, was placed at the end of the runway. Each animal was placed on the runway, 80 cm from the black-box entrance, and their gait was recorded with a camera (Bastler acA1300-60gm, Noldus, Wageningen, The Netherlands) positioned under the runway and Ethovision 12.0 Software (Ethovision XT, Noldus, Wageningen, The Netherlands). The lighting from the ground was adjusted to ensure sufficient lighting for camera and was around 20 lx on the runway surface. For each animal, five trials were completed. Only a straight walk without any interruptions was considered for gait analysis. Thus, the second trial was chosen for analysis, excluding the first and last 10 cm of the walk. Video frames (60/s) were extracted using VLC 2.2.4. “Weatherwax” media player (VideoLan Organization) and merged for analysis with GIMP 2.10.14 software. The two consecutive strides per animal were selected and the following parameters were measured: stride length, forelimb and hindlimb base of support (horizontal stride width), and the angle between forelimb paw and body direction (Fig. S1B).

*Euthanasia, plasma and hippocampus sampling*

Prior to sacrifice, all mice were fasted for 6 hours during the light cycle phase in order to eliminate direct effects of diet consumption. Mice were euthanized between 12 and 3:30 p.m. with 600 mg/kg Pentobarbital i.p. in 10 ml/kg injection volume. In order to minimize circadian effects on metabolites, animals were randomly divided into groups euthanized at two separate days.

Following the stop of breathing, the thorax was opened and blood was collected from the heart into 1.3 ml K3 EDTA micro tubes (SARSTEDT AG & Co. KG, Nümbrecht, Germany). The tubes were gently shaken and then centrifuged on 3500 rpm (Hettich® MIKRO 200/200R, Andreas Hettich GmbH & Co. KG, Tuttlingen, Germany) for 10 minutes at room temperature. Plasma was pipetted into 1.5 ml Protein LoBind Tubes (Eppendorf, Wesseling-Berzdorf, Germany) and fresh frozen in liquid nitrogen (Besamungsstation München-Grub, Poing, Germany). Hippocampal tissue was dissected from both hemispheres, fresh frozen in liquid nitrogen using 1.5 ml Protein LoBind Tubes and stored at -80 °C until analysis. Tail samples were collected for PCR genotype confirmation. Plasma and hippocampus samples were sent to metaSysX GmbH for analysis. Firstly, all samples were prepared in line with metaSysX standard procedure. Metabolites were extracted from the whole grounded hippocampus samples and 100 µl of the plasma samples. Polar and semi-polar primary and secondary metabolites were measured with a Waters ACQUITY Reversed Phase Ultra Performance Liquid Chromatography (RP-UPLC; C18 column) coupled to a Thermo-Fisher Exactive mass spectrometer which consists of an ElectroSpray Ionization source (ESI) and an Orbitrap mass analyzer. Extraction of the data was accomplished with the software REFINER MS® 11.1 (GeneData, http://www.genedata.com), after which it was annotated using the in-house metaSysX database of chemical compounds (database query of m/z and the retention time).

In addition, primary metabolites were measured on an Agilent Technologies Gas Chromatography (column: 30 m, DB-35; starting temperature 85 °C for 2 minutes; gradient: 15

°C/minute up to 360 °C) coupled to a Leco Pegasus High Throughput mass spectrometer, which consists of an electron ionization source and a time-of-flight mass analyzer. Samples were measured in splitless (injection of full volume) and split mode (injection of 1/5 of full volume) to allow the selection of the proper mode for the compounds of interest. The compound annotation was done by comparing the spectra and the retention index to the Fiehn Library and to a user created library. Lastly, the hippocampal data were normalized first to the weight of the samples and then to the median of intensities of each sample and plasma data were normalized to the median of intensities of each sample.

*Data availability*

The raw data of this study are available from the corresponding author, upon reasonable request.

## *Results*

### *Ketosis confirmation*

A pilot study has been completed to determine the duration of KD exposure sufficient to ensure ketosis in the majority of animals. The blood level of BHB increased over the time of exposure to KD. In the evening samples one, 2 and 3 weeks following KD onset, BHB blood levels were significantly higher as compared to baseline (Fig. S6). In contrast, there was no significant change in BHB levels in the morning samples, when compared to baseline. However, at 2 and 3 weeks following KD introduction, BHB levels in blood were higher in the morning than in the evening, implying a pronounced effect of nocturnal feeding. Based on the pilot data 3 weeks were selected as a sufficient duration for KD exposure.

### *Genotype and diet effect on behavioral parameters*

The open field paradigm revealed a pronounced hyperlocomotion with total distance moved and mean velocity significantly increased in Dravet mice, regardless of the diet (Fig. S8A-B). Immobility time was significantly reduced in all Dravet animals (Fig. S8C). Rearing behavior and jumping on the walls proved to be significantly increased in all Dravet mice (Fig. S8D-E). An impact of the diet on rearing behavior became evident with Dravet mice fed KD exhibiting more rearing behavior as compared to Dravet mice fed CD. Thigmotaxis was evident in all Dravet mice regardless of the diet, with an increase in time spent in wall zone and decrease in time spent in middle and center zones as compared to wildtype mice (Fig. S8F). Sex differences were not observed.

Assessment of novel object recognition test did not show any effect of genotype or diet on cognitive performance in mice (Fig. S8H).

Wildtype mice consuming CD or KD, and Dravet mice consuming CD showed a preference of saccharin solution over water. However, the amount of consumed saccharin was significantly

reduced in Dravet mice, when compared to wildtypes. Moreover, KD reduced the preference for saccharin in both genotypes (Fig. S8G). Findings proved to be comparable in males and females.

Nest-building activity assessment revealed a strong genotype effect, with a significantly poorer performance in Dravet mice when compared to wildtype mice fed CD (Fig. S8I). Diet and sex effects were not observed.

## *References*

Carola, V., et al., 2002. Evaluation of the elevated plus-maze and open-field tests for the assessment of anxiety-related behaviour in inbred mice. Behav Brain Res. 134**,** 49-57.

Dutton, S. B. B., et al., 2017. Early-life febrile seizures worsen adult phenotypes in Scn1a mutants. Exp Neurol. 293**,** 159-171.

Jirkof, P., et al., 2013. Assessment of postsurgical distress and pain in laboratory mice by nest complexity scoring. Lab Anim. 47**,** 153-61.

Klein, S., et al., 2015. Sucrose consumption test reveals pharmacoresistant depression-associated behavior in two mouse models of temporal lobe epilepsy. Exp Neurol. 263**,** 263-71.

Lueptow, L. M., 2017. Novel Object Recognition Test for the Investigation of Learning and Memory in Mice. J Vis Exp.

Racine, R. J., 1972. Modification of seizure activity by electrical stimulation. II. Motor seizure. Electroencephalogr Clin Neurophysiol. 32**,** 281-94.

*Tables and figures:*

**Table S1.** Abundances of selected proteins detected in the hippocampus of Dravet mice following the disease manifestation. The fold change is provided in relation to wildtype controls along with the level of significance (p). Please note that the data are from a study focused on a broad scale proteomic analysis presented in a manuscript by Miljanovic et al., under revision.

| Genes | Protein names | fold change Dravet/ WT | p-value |
|---|---|---|---|
| Hk3 | Hexokinase-3 | 1.34 | 0.1155 |
| Ldha | L-lactate dehydrogenase A chain | 1.00 | 0.8912 |
| Ldhb | L-lactate dehydrogenase B chain | 0.87 | 0.0008 |
| Pdha1 | Pyruvate dehydrogenase E1 component subunit alpha, somatic form, mitochondrial | 1.04 | 0.0006 |
| Pdhb | Pyruvate dehydrogenase E1 component subunit beta, mitochondrial | 1.04 | 0.1901 |
| Pdhb | Pyruvate dehydrogenase E1 component subunit beta, mitochondrial | 1.04 | 0.1901 |
| Slc2a1 | Solute carrier family 2, facilitated glucose transporter member 1 | 0.93 | 0.0601 |
| Slc2a3 | Solute carrier family 2, facilitated glucose transporter member 3 | 1.13 | 0.0009 |
| Slc16a1 | Monocarboxylate transporter 1 | 1.20 | 0.0150 |
| Gpi | Glucose-6-phosphate isomerase | 1.04 | 0.0209 |
| Taldo1 | Transaldolase | 0.98 | 0.4335 |
| Tkt | Transketolase | 0.99 | 0.4577 |
| Aldoa | Fructose-bisphosphate aldolase A | 1.05 | 0.0697 |
| Aldoc | Fructose-bisphosphate aldolase C | 0.92 | 0.0854 |
| Gapdh | Glyceraldehyde-3-phosphate dehydrogenase | 0.95 | 0.4178 |
| Tpi1 | Triosephosphate isomerase | 1.03 | 0.6351 |
| Pgk1 | Phosphoglycerate kinase 1 | 1.01 | 0.7376 |
| Pgam2 | Phosphoglycerate mutase 2 | 1.04 | 0.5814 |
| Pgam1 | Phosphoglycerate mutase 1 | 1.03 | 0.1903 |
| Eno1 | Alpha-enolase | 0.97 | 0.3230 |
| Eno3 | Beta-enolase | 0.93 | 0.1477 |
| Eno2 | Gamma-enolase | 0.99 | 0.8365 |
| Pkm | Pyruvate kinase PKM | 1.00 | 0.9063 |
| Aldh5a1 | Succinate-semialdehyde dehydrogenase, mitochondrial | 0.96 | 0.0769 |
| Idh2 | Isocitrate dehydrogenase [NADP], mitochondrial | 1.07 | 0.1822 |
| Idh1 | Isocitrate dehydrogenase [NADP] cytoplasmic | 1.05 | 0.0571 |
| Idh3a | Isocitrate dehydrogenase [NAD] subunit alpha, mitochondrial | 1.06 | 0.0279 |
| Idh3g | Isocitrate dehydrogenase [NAD] subunit gamma 1, mitochondrial | 1.03 | 0.0773 |
| Cs | Citrate synthase, mitochondrial | 1.03 | 0.0899 |
| Acly | ATP-citrate synthase | 1.06 | 0.0099 |
| Aco2 | Aconitate hydratase, mitochondrial | 1.00 | 0.9506 |

| | | | |
|---|---|---|---|
| Aco1 | Cytoplasmic aconitate hydratase | 0.98 | 0.0842 |
| Sdhd | Succinate dehydrogenase [ubiquinone] cytochrome b small subunit, mitochondrial | 1.04 | 0.2673 |
| Sdha | Succinate dehydrogenase [ubiquinone] flavoprotein subunit, mitochondrial | 1.04 | 0.0072 |
| Sdhc | Succinate dehydrogenase cytochrome b560 subunit, mitochondrial | 0.98 | 0.6248 |
| Sdhb | Succinate dehydrogenase [ubiquinone] iron-sulfur subunit, mitochondrial | 1.03 | 0.0343 |
| Ogdh | 2-oxoglutarate dehydrogenase, mitochondrial | 1.05 | 0.0032 |
| Sucla2 | Succinate--CoA ligase [ADP-forming] subunit beta, mitochondrial | 1.06 | 0.0046 |
| Suclg1 | Succinate--CoA ligase [ADP/GDP-forming] subunit alpha, mitochondrial | 1.10 | 0.0037 |
| Suclg2 | Succinate--CoA ligase [GDP-forming] subunit beta, mitochondrial | 1.06 | 0.0189 |
| Fh | Fumarate hydratase, mitochondrial | 1.01 | 0.4623 |
| Mdh1 | Malate dehydrogenase, cytoplasmic | 0.96 | 0.1202 |
| Mdh2 | Malate dehydrogenase, mitochondrial | 1.08 | 0.0073 |
| Asns | Asparagine synthetase [glutamine-hydrolyzing] | 0.85 | 0.1247 |
| Pc | Pyruvate carboxylase, mitochondrial | 1.00 | 0.8830 |
| Glud1 | Glutamate dehydrogenase 1, mitochondrial | 1.03 | 0.2844 |
| Glul | Glutamine synthetase | 0.86 | 0.0062 |
| Gad1 | Glutamate decarboxylase 1 | 1.00 | 0.9607 |
| Gad2 | Glutamate decarboxylase 2 | 1.15 | 0.0807 |
| Slc17a7 | Vesicular glutamate transporter 1 | 1.06 | 0.0547 |
| EAAT1 | Excitatory amino acid transporter 1 | 0.91 | 0.0100 |
| EAAT2 | Excitatory amino acid transporter 2 | 0.95 | 0.0440 |
| Glul | Glutamine synthetase | 0.86 | 0.0062 |

**Table S2.** Parameters of generalized tonic-clonic seizures during baseline (n=19) and during exposure to CD (n=8) or KD (n=10) in Dravet mice. Total seizure duration, seizure frequency, the number of days with seizures/week and seizure severity (mean±SEM) were evaluated.

| Group | Total seizure duration [s] | Seizure frequency (seizures/week) | Number of days with seizures/week | Racine score |
|---|---|---|---|---|
| Dra baseline | 340.7 ± 43.68 | 6.79 ± 0.86 | 2.21 ± 0.22 | 5.69 ± 0.07 |
| Dra CD | 289.4 ± 40.46 | 6.38 ± 0.94 | 2.75 ± 0.49 | 5.7 ± 0.12 |
| Dra KD | 259.5 ± 34.35 | 5.3 ± 0.72 | 2.1 ± 0.28 | 5.46 ± 0.19 |

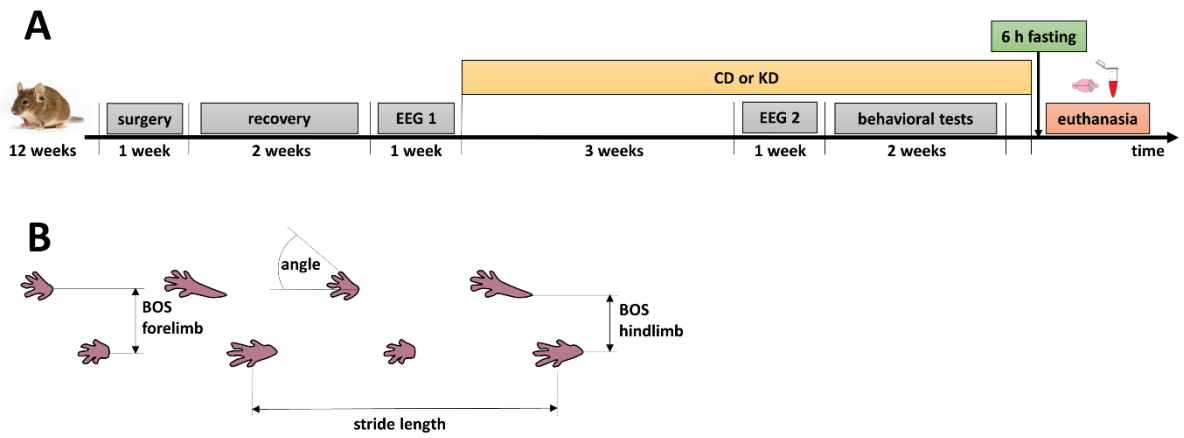


**Fig. S1 A** Experimental timeline. **B** This sketch illustrates chosen parameters for gait assessment in mice including stride length, angle between forelimb paw and body direction, forelimb and hindlimb base of support (BOS).

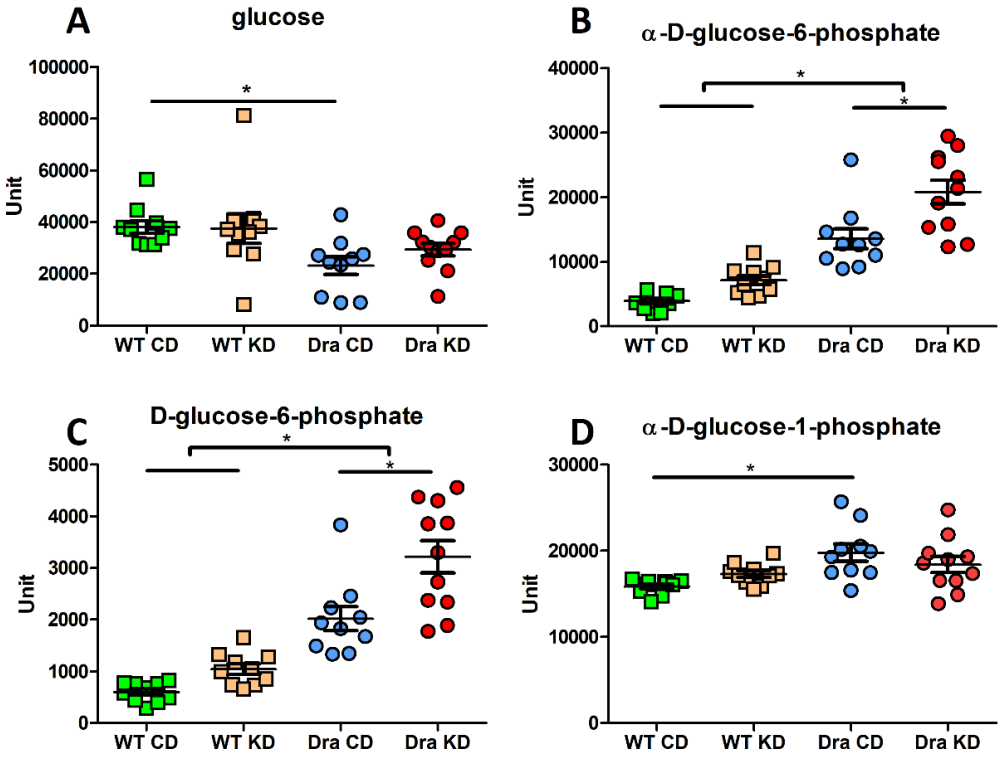


**Fig. S2 The abundance of glucose and its phosphorylated forms in hippocampal tissue. A** The glucose abundance in the hippocampus. Dravet mice fed CD had a lower abundance of glucose as compared to wildtype mice fed CD. **B-C** The level of α-D-glucose-6-phosphate (**B**) and D-glucose-6-phosphate (**C**) in hippocampal tissue. Both metabolites were up-regulated in Dravet mice when compared to wildtype mice. In addition, KD further increased metabolite abundance only in Dravet mice. **D** The hippocampal abundance of α-D-glucose-1-phosphate. This metabolite was up-regulated in Dravet mice fed CD, when compared to wildtype mice. Data shown are from 20 wildtype mice (10 CD, 10 KD) and 21 Dravet mice (10 CD, 11 KD). (Two-way ANOVA, FDR correction, Bonferroni post-hoc test, * = $p<0.05$, mean±SEM).

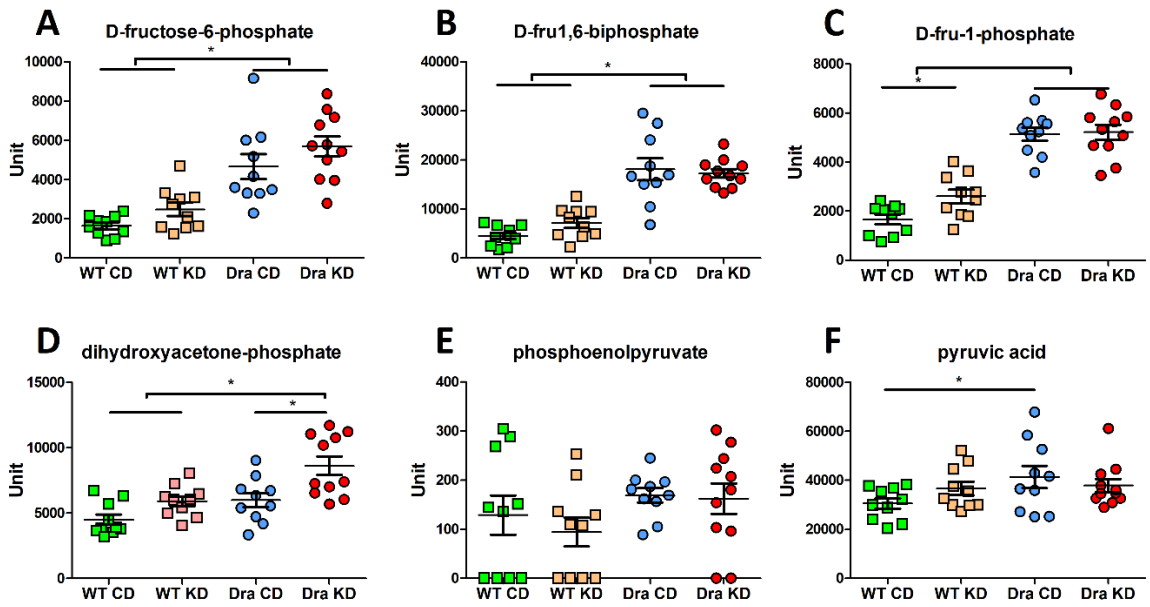


**Fig. S3 Intermediate metabolites of glycolysis in hippocampal tissue.** The abundance of D-fructose-6-phosphate (**A**) and D-fructose-1,6-biphosphate (**B**) in the hippocampus. Both metabolites were up-regulated in Dravet mice when compared to wildtype mice, regardless of the consumed diet. **C** The abundance of D-fructose-1-phosphate in the hippocampus. The metabolite level was increased in mice with the Dravet genotype when compared to wildtype mice. KD further increased metabolite levels only in wildtype mice. **D** The level of dihydroxyacetone-phosphate in the hippocampus. Dravet mice consuming KD had a significantly higher metabolite level than mice in the other three groups. **E** Phosphoenolpyruvate level in the hippocampus. No changes in the metabolite abundance were noted between the four groups. **F** Pyruvate abundance in the hippocampus. When consuming CD, Dravet mice showed an increased metabolite abundance as compared to wildtype mice. Data shown are from 20 wildtype mice (10 CD, 10 KD) and 21 Dravet mice (10 CD, 11 KD). (Two-way ANOVA, FDR correction, Bonferroni post-hoc test, * = $p<0.05$, mean±SEM).

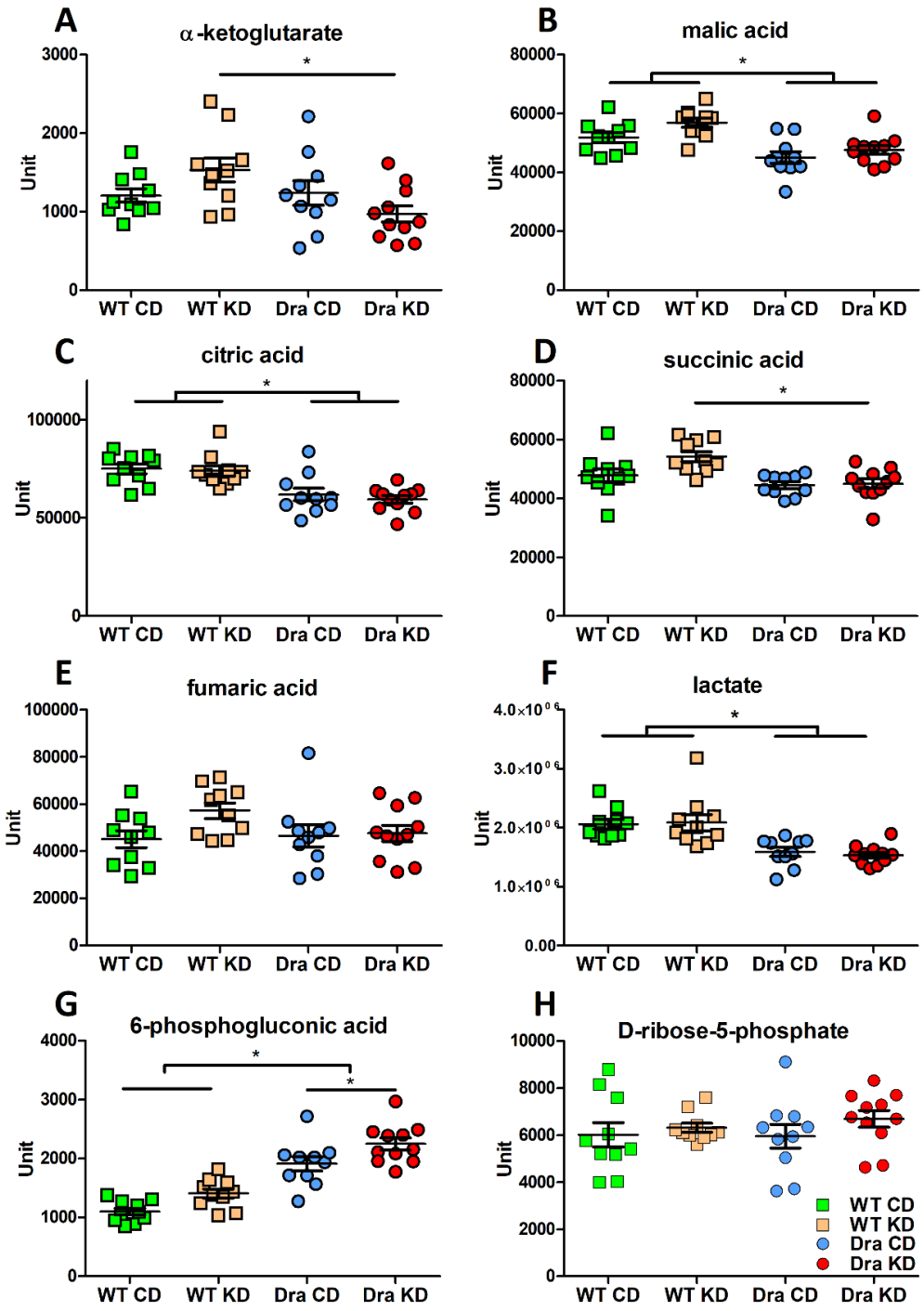


**Fig. S4 Intermediate metabolites of tricarboxylic acid cycle and the pentose phosphate pathway in hippocampal tissue.** Hippocampal abundance of α-ketoglutarate (**A**), malic acid (**B**), citric acid (**C**), succinic acid (**D**), fumaric acid (**E**), lactate (**F**), 6-phosphogluconic acid (**G**) and ribose-5-phosphate (**H**). **A, D** The levels of α-ketoglutarate and succinic acid were reduced in Dravet mice fed KD when compared to wildtype mice fed KD. **B-C** Dravet mice had a significantly lower level of malic and citric acid in hippocampal tissue than wildtype mice. **E** No change in the hippocampal level of fumaric acid was noted. **F** The hippocampal lactate abundance was significantly lower in Dravet mice, than in wildtype mice. **G** Dravet mice showed a significant increase in hippocampal 6-phosphogluconic acid abundance as compared

to wildtype mice. In addition, KD further increased metabolite levels only in Dravet mice. **H** The level of hippocampal D-ribose-5-phosphate was comparable between all groups. Data shown are from 20 wildtype mice (10 CD, 10 KD) and 21 Dravet mice (10 CD, 11 KD). (Two-way ANOVA, FDR correction, Bonferroni post-hoc test, * = $p<0.05$, mean±SEM).

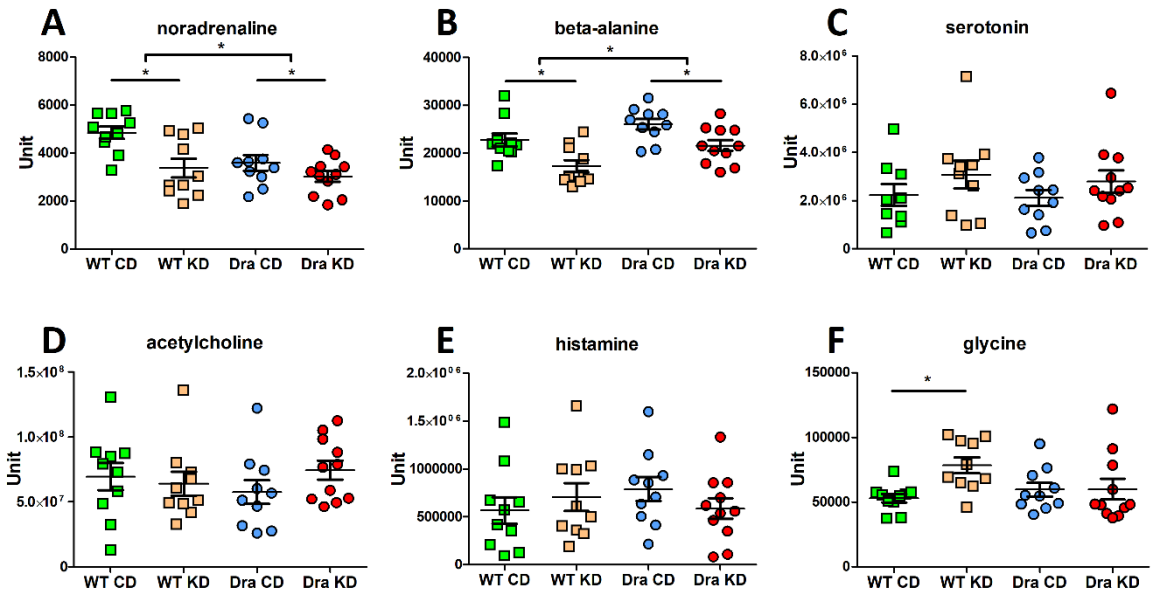


**Fig. S5 Neurotransmitters in the hippocampus.** Hippocampal level of noradrenaline (**A**), β-alanine (**B**), serotonin (**C**), acetylcholine (**D**), histamine (**E**) and glycine (**F**). **A-B** Dravet mice showed a reduced level of noradrenaline and an increased level of β-alanine in hippocampal tissue when compared to wildtypes. KD reduced neurotransmitter abundance in both wildtype and Dravet mice. **C-E** No differences in hippocampal abundance of serotonin, acetylcholine and histamine were noted between all four groups. **F** KD increased hippocampal levels of glycine only in mice with the wildtype genotype. Data shown are from 20 wildtype mice (10 CD, 10 KD) and 21 Dravet mice (10 CD, 11 KD). (Two-way ANOVA, FDR correction, Bonferroni post-hoc test, * = $p<0.05$, mean±SEM).

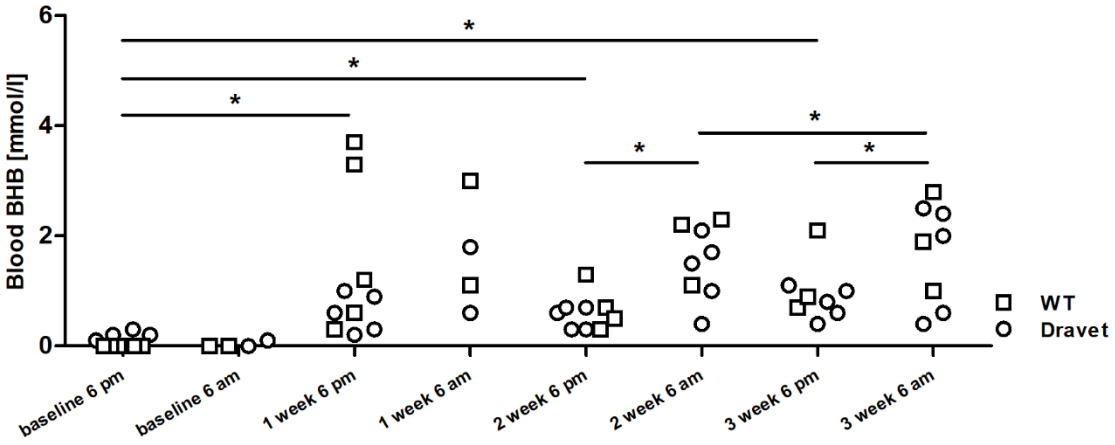


**Fig. S6 Ketosis confirmation.** Results of a pilot study showing the blood level of β-hydroxybutyrate (BHB) over 3 weeks of KD consumption. Ketosis was checked twice per day. Over time, the number of animals reaching ketosis state increased. Evening BHB levels at one, 2 and 3 weeks following the KD introduction were significantly increased when compared to the baseline (paired t-test, * $p<0.05$). Two and three weeks following KD onset, blood BHB levels were significantly higher in the morning measurement. The morning BHB level measured at 3 weeks post KD introduction, exceeded the BHB level measured at 2 weeks following KD onset.

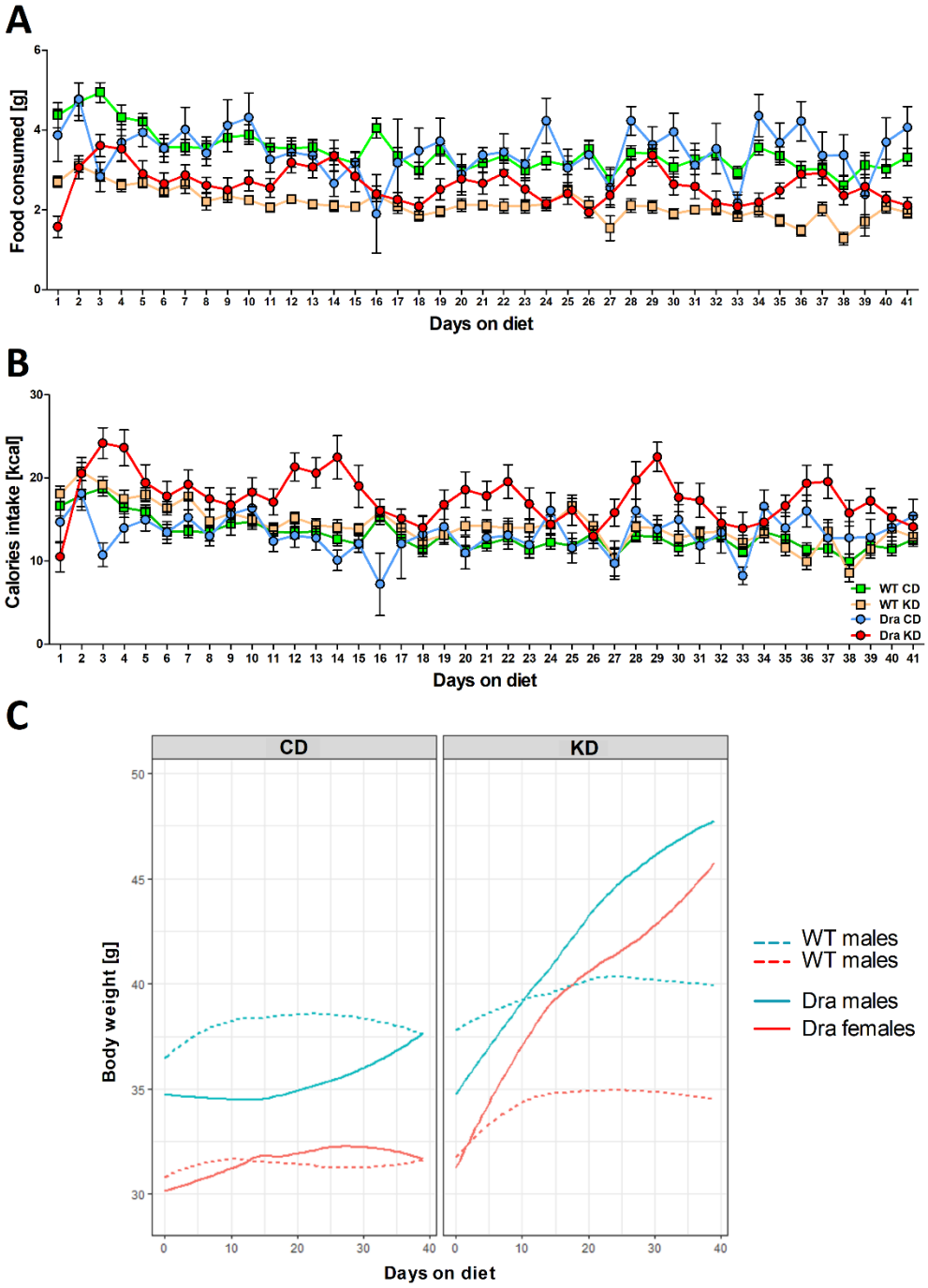


**Fig. S7 Food intake and body weight gain. A** The amount of CD or KD consumed over the course of the experiment. Wildtype and Dravet mice consumed more CD than KD. The amount of KD consumed by Dravet mice exceeded the amount consumed by wildtypes. **B** Calorie intake. Dravet mice consuming KD had an increased overall calorie intake as compared to the remaining three groups. (mean±SEM). **C** Body weight development following the onset of CD or KD exposure. All four groups gained body weight over the course of the experiment. However, weight gain in both male and female Dravet mice fed KD was significantly exceeding that in the remaining three groups. Data shown are from 20 wildtype mice (10 CD, 10 KD) and 21 Dravet mice (10 CD, 11 KD). (Two-way ANOVA, Bonferroni post hoc test).

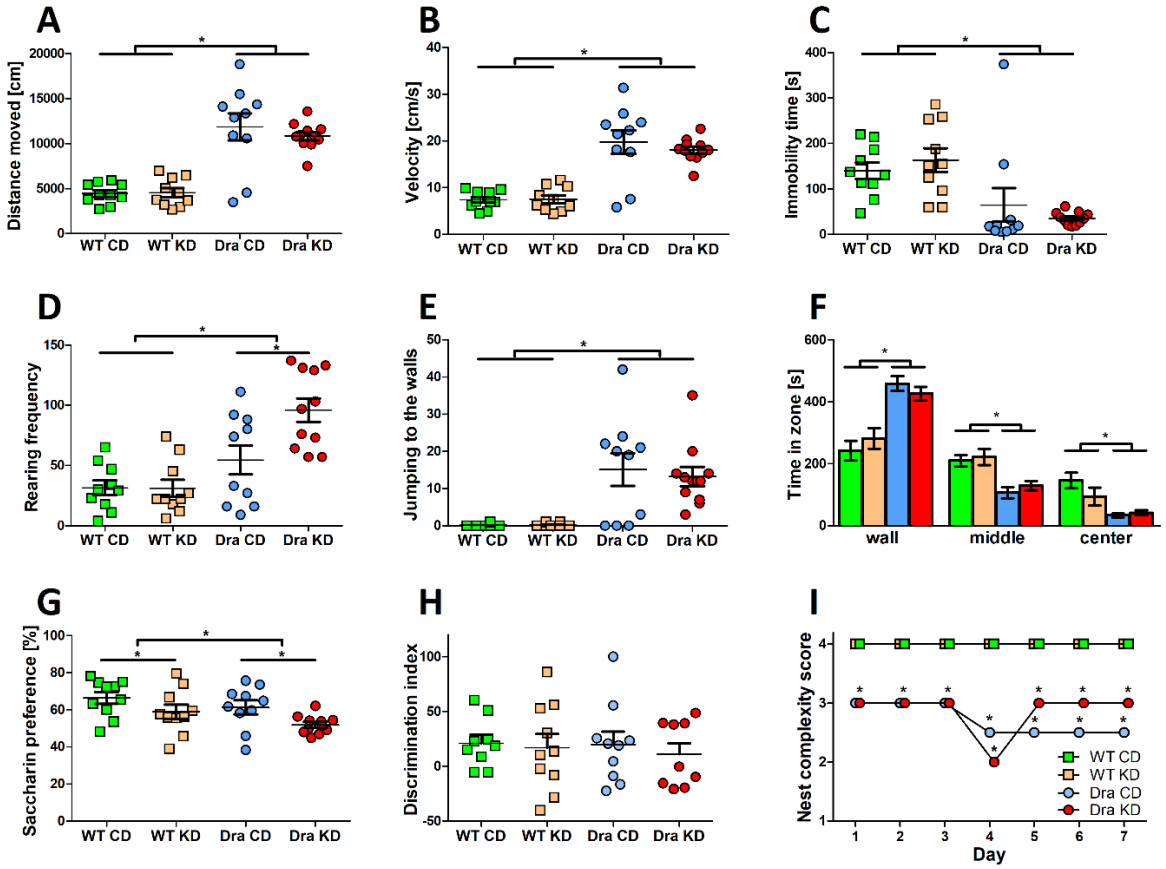


**Fig. S8 Open field test, novel object recognition, saccharin preference and nest complexity score. A** Distance moved in the open field paradigm over 10 minutes. The total distance moved was significantly greater in mice with the Dravet genotype as compared to wildtype mice. **B** Average velocity over 10 minutes. The average velocity of Dravet mice proved to be higher than that of wildtype mice. **C** Immobility time. Dravet mice spent significantly less time immobile when compared to wildtypes. **D** Rearing frequency. Rearing frequency in Dravet mice exceeded the frequency observed in wildtype mice. **E** Jumping on the walls of the open field paradigm. Dravet mice showed an increased jumping behavior when compared to wildtypes. **F** Time spent in wall, middle and center zones of the open field paradigm. Dravet mice showed thigmotaxic behavior by spending more time in the wall zone compared to the wildtypes and less time in both the middle and center zones of open field. **G** Total consumption of saccharin solution. Mice with the Dravet genotype consumed significantly less saccharin solution when compared to wildtypes. KD significantly reduced the preference for saccharin in wildtype and Dravet mice. (Data shown are from 20 wildtype mice (10 CD, 10 KD) and 21 Dravet mice (10 CD, 11 KD)). **H** Discrimination index in novel object recognition test. All four groups showed no difference in cognitive performance. Data shown are from 19 wildtype mice (9 CD, 10 KD) and 19 Dravet mice (10 CD, 9 KD) (Two-way ANOVA, Bonferroni post hoc test, * = $p<0.05$, mean±SEM). **I** Nest complexity score over seven consecutive days. Dravet mice showed poorer performance in building complex nests. (Friedman test, Dunn's Multiple Comparison Test, * = $p<0.05$ compared to wildtype groups, median). Data shown are from 20 wildtype mice (10 CD, 10 KD) and 21 Dravet mice (10 CD, 11 KD).

# DISCUSSION

## 1. *Face validity of the model*

The validity of a novel animal model should be determined to provide evidence about how suitable the model is for investigating the disease it attempts to recapitulate. Thus, the first aim of this study was to characterize the phenotype of this conditional mouse model carrying the Dravet syndrome mutation A1783V and compare it with symptoms observed in patients with Dravet syndrome. The first manuscript provided valuable data about model characteristics including thermally provoked seizures, spontaneous seizures, a high mortality rate and behavioral alterations including hyperactivity and attention deficits. In addition, the second manuscript confirmed the presence of motor deficits, which are common symptoms of Dravet syndrome. Therefore, the findings from both manuscripts provide a valuable basis for conclusions about face validity of the model. Further in the text, different phenotype characteristics are compared between mice and patients with Dravet syndrome in order to determine the translational significance of the model.

### *1.1. Sudden unexpected death in epilepsy*

Unfortunately, SUDEP rates are high in patients with Dravet syndrome (Shmuely et al., 2016). The reasons for the particularly high SUDEP risk in this epileptic encephalopathy have not yet been completely elucidated (Kalume, 2013; Shmuely et al., 2016). However, SUDEP is often attributed to frequent convulsive seizures (Harden et al., 2017) and the following postictal immobility, linked to peri-ictal respiratory dysfunction (Kuo et al., 2016). In another Dravet mouse model, sudden unexpected death has shown to be related to a high frequency of Racine V stage seizures (Kalume, 2013), which was also observed in this animal model. Taken together, the cause of death in these animals can be considered as probable SUDEP (Devinsky et al., 2018a). In the *Scn1a*-A1783V mice, mortality rates were high in the affected animals. This might be because the affected offspring had a 50:50 mixed C57BL/6J and 129S1

background. It has previously been described that C57BL/6 mice develop a severe phenotype upon the introduction of Dravet syndrome *Scn1a* mutations (Cheah et al., 2012; Kalume, 2013). In comparison to previously characterized Dravet mouse models with this mutation (Kuo et al., 2019; Ricobaraza et al., 2019), the model studied here exhibits a milder phenotype and a lower mortality rate, rendering it more preferable for further biomedical and pharmacological investigation.

The fact that an obvious peak became evident with most animals dying between P20 and 23, implies that the model is very well suited for studies analyzing the pathophysiological factors contributing to SUDEP and for studies assessing the impact of drug candidates on SUDEP rates. Decreasing SUDEP rates is one of the declared aims of future drug development for the management of Dravet syndrome (Genton et al., 2011). Thus, the commercial availability of an animal model for respective studies is of the utmost relevance.

## *1.2. Hyperthermia-induced seizures*

Hyperthermia-induced seizures are one of the hallmarks of epilepsy manifestation in patients with Dravet syndrome (Dravet, 2011). Thus, we aimed to check if mice with a Dravet genotype are prone to exhibit a seizure with exposure to hyperthermia. Interestingly, an increased susceptibility to hyperthermia-induced seizures with low thresholds was evident on all three test days: P23, P25 and P32. In addition, mean thresholds were rather comparable between P23 and P25 indicating that repeatedly using the animals may be possible. However, the level of intraindividual variation in thresholds between stimulation days must be taken into account for repeated drug testing.

With the subsequent testing 1 week later (P32), a reduction in the threshold became evident in comparison to P23 and P25 thresholds in both sexes. The lowered threshold at P32 might reflect

a progression of the disease with steadily increasing seizure susceptibility. However, a kindling phenomenon based on the previous induction of seizures might also have contributed.

### *1.3. Spontaneous seizures*

With progression of the disease, patients with Dravet syndrome develop further seizures, which then also occur without any thermal trigger (Dravet, 2011). In the first study, we obtained the first pilot information about spontaneous seizure activity in the novel Dravet mouse model. The information was based on video monitoring as continuous recordings are impossible in the very young animals. However, further electroencephalographic recordings in adult mice (manuscript I and II) confirmed the presence of seizure activity. Spontaneous motor seizures started at P16 with seizures recapitulating the convulsive generalized seizures observed in patients. Seizures often progressed with running and bouncing phases indicating spread of seizure activity to the brain stem. Considering the fact that discharges affecting the brain stem are considered a critical factor contributing to SUDEP (Aiba and Noebels, 2015), it will be of particular interest to perform electrophysiological studies in the model studying the cellular mechanisms of propagation to the brain stem in more detail. In addition to behavioral motor seizures, we repeatedly observed episodes with behavioral arrest and non-responsiveness to external stimuli. These episodes might reflect atypical absence seizures, which can occur in patients with Dravet syndrome with an onset at different ages between 4 months and 6 years (Ohki et al., 1997). However, further electrographic recordings will be essential to confirm seizure activity during these episodes.

### *1.4. Behavioral alterations*

Behavioral alterations contribute to the burden in Dravet patients (Besag, 2004; Dravet, 2011; Genton et al., 2011). As such, we gathered comprehensive behavioral information from the

same animals to form a better basis for drawing conclusions about altered behaviors. In addition, a battery of behavioral tests can help to identify factors of bias.

Lack of attention related to hyperactivity constitutes one of the common behavioral disturbances in Dravet patients (Battaglia et al., 2016; Besag, 2004; Dravet, 2011). In line with this clinical trait, we observed a pronounced increase in activity in the open field as well as in the elevated plus maze paradigm. In other Dravet mouse models including a knock-in model with a nonsense R1407X mutation and other knockout models, hyperactivity has become evident (Dutton et al., 2013; Han et al., 2012; Ito et al., 2013; Rubinstein et al., 2015a). While anxiety has not been reported in Dravet patients (Sinoo et al., 2019), our data showed a lower level of anxiety in Dravet mice observed in the elevated plus maze paradigm. However, when assessing anxiety-like behavior in these mice, the impact of evident hyperactivity on the test should also be considered as it may impact the time spent in different zones.

Development of motor abnormalities with features of cerebellar symptoms typically occur with disease progression in Dravet patients (Genton et al., 2011). While the rotarod test failed to demonstrate any motor disturbances in Dravet mice, the analysis of their gait proved to be a more sensitive approach and revealed alterations in body posture and motor coordination. Dravet mice had a different body posture in comparison to wildtype mice as a result of a significantly smaller distance between the hindlimbs. External torsion of the forelimbs may represent an attempt to regain stability. Considering great differences between the quadruped and biped gait, it is hard to say whether these changes mimic symptoms in humans. Nevertheless, these data certainly provide valuable information about how *Scn1a* deficiency in this mouse model results not only in seizure and behavioral alterations, but also in motor disturbances due to its expression in cerebellar Purkinje cells and in the nodes of Ranvier of motor neurons (Duflocq et al., 2008; Gataullina and Dulac, 2017).

Autistic features have been reported in subgroups of Dravet patients (Berkvens et al., 2015; Besag, 2004; Genton et al., 2011). With an increased level of active social interaction, Dravet mice did not show autistic-like behavior when compared to wildtype littermates. However, we must take into account that here we examined the social interaction between affected animals, and that respective data for an interaction between patients with Dravet syndrome have not been reported yet. In addition, it might be of interest to further study the development of social interaction at different ages and to perform another test where a novel stimulus animal is introduced.

Analyzing saccharine preference revealed prominent alterations as a consequence of the genetic deficiency. This finding might point to a slight increase in anhedonia-associated behavioral patterns. At the moment, there is a lack of clinical reports about anhedonia and depression in Dravet patients, perhaps attributable to the fact that depression is difficult to assess in patients with mental retardation and prominent behavioral disturbances.

Nest-building represents a behavioral pattern that is considered non-essential under laboratory conditions (Jirkof, 2014). Dravet mice, especially the females, proved to be less motivated to engage in nest-building activity as compared to their wildtype littermates. We obtained no evidence that nest complexity was compromised by spontaneous seizure activity in the home cage, thus, the data indicate that Dravet mice might not enjoy in this type of "luxury" behavior. The poor performance in nest-building might also reflect a failure to focus on a specific task thereby reflecting a hyperactivity-attention deficit syndrome, which is characteristic of Dravet patients (Berkvens et al., 2015). For instance, it has been described that children are restless and do not show an interest in playing with toys or in the other usual activities for their age group (Dravet, 2011).

Considering that the analyses were performed sequentially in the same animals, we cannot exclude an influence of the sequence of the testing. However, the additional information gained from individual animals allows better characterization of the animal model, with a possibility to find correlations between data from individual animals. For instance, the correlation between total distance moved as the main locomotion parameter and social interaction, elevated plus maze parameters and nest complexity score, indicates that hyperactivity may contribute to some of the behavioral results.

## *2. Comparison to other mouse models of Dravet syndrome*

The comprehensive characterization of this mouse model provided valuable information about the model´s similarity to the clinical symptoms of Dravet syndrome and its value for further scientific research. The model is also the first animal model of Dravet syndrome commercially available to a broad scientific audience. In addition, it is a conditional knock-in mouse model that avoids the breeding of affected animals. Besides these advantages, it is of particular relevance to compare this model to other available models (Table T1) to conclude about its value for the scientific community.

Interestingly, the time of spontaneous seizure onset in our model was on the identical day of postnatal brain development as another model with heterozygous conditional deletion of exon 7 (Ogiwara et al., 2013). In other *Scn1a* knockout models, later seizure onsets were reported including P18 (Cheah et al., 2012; Ogiwara et al., 2007), P20 (Miller et al., 2014; Tsai et al., 2015), P21(Dutton et al., 2013; Yu et al., 2006) and the third postnatal week (Ricobaraza et al., 2019).

As in most other models, we confirmed an increased susceptibility to hyperthermia. Furthermore, we confirmed a reduced seizure threshold following weaning but at a later time point. Moreover, we demonstrated a decrease in seizure threshold over time. Similar findings were reported only in one other mouse model, with no seizures occurring up to 42°C at P21, but apparent seizures in 50% of mice at P35 (Rubinstein et al., 2015a).

Besides the seizure phenotype, behavioral alterations are highly relevant for studies focusing on the pathophysiology and pharmacology of Dravet syndrome. While we failed to detect any social and cognitive deficits as in other models, we observed impaired motor coordination in Dravet mice so far reported only in a few mouse models (Ogiwara et al., 2007; Ricobaraza et al., 2019; Yu et al., 2006). Interestingly, cognitive decline was reported in a mouse model with the same mutation (Ricobaraza et al., 2019) thereby implying that a different battery of tests

may reveal the mutation´s impact on cognition. Furthermore, we also demonstrated poor nest building performance which, together with hyperactivity in these mice, may mimic attention deficits in humans. Interestingly, increased activity was reported in most of the other animal models. In contrast, the impact of hyperactivity on other behavioral tests was usually not assessed (Table T1). Here, we showed that hyperactivity in Dravet mice directly correlated with anxiety-like behavior, nest complexity score and social interaction. This suggests that hyperactivity impacts these other phenotypic features in Dravet mice.

Lastly, we also described an anhedonia-associated behavior in Dravet mice, a core symptom of depression in patients. It is possible that depression in patients with Dravet syndrome has been overlooked due to the often severe language and intellectual disabilities.

Besides excellent face validity for the investigation of Dravet syndrome, the *Scn1a*-A1873V mouse model showed several advantages over the other currently available models. Among these, the relatively low mortality rate and low threshold for hyperthermia-induced seizures are the model's main advantages when compared to other mouse models. These render it more favorable for the pharmacological assessment of different drug candidates.

**Table T1.** A comparison between the *Scn1a*-A1783V mouse model of Dravet syndrome, other available mouse models with a heterozygous *Scn1a* mutation and a clinical manifestation of Dravet syndrome (the first row). The arrow indicates an increased or a reduced phenotype characteristic. Minus (-) indicates no significant change in the evaluated parameter. P – postnatal day, PW – postnatal week, M – months, n.a. - not available, HIS – hyperthermia-induced seizure. [1](Ricobaraza et al., 2019); [2](Kuo et al., 2019); [3](Ogiwara et al., 2007); [4](Ito et al., 2013); [5](Dutton et al., 2013); [6](Han et al., 2012; Kalume, 2013; Oakley et al., 2009); [7](Yu et al., 2006); [8](Cheah et al., 2012); [9](Ogiwara et al., 2013); [10](Miller et al., 2014); [11](Mistry et al., 2014); [12](Tsai et al., 2015); [13](Dutton et al., 2017; Sawyer et al., 2016); [14](Martin et al., 2010); [15](Cooper et al., 2016). The table is adapted from manuscript I.

| Mouse model | BL/6:129S1 background [~%] | Mortality rate [%] | Spontaneous seizures onset | HIS threshold, test day (P) | Activity level | Anxiety-like behavior | Social behavior | Cognition | Anhedonia-related behavior | Motor coordination | Body weight |
|---|---|---|---|---|---|---|---|---|---|---|---|
| Clinical picture of Dravet syndrome | n.a. | 16[15] | 5-8 M | / | ↑ | - | ↓ | ↓ | n.a. | ↓ | n.a. |
| *Scn1a*-A1783V | 50:50 | 40 | P16 | 39.4 (P23) | ↑ | ↓ | ↑ | - | ↑ | ↓ | ↓ |
| [1]*Scn1a*$^{WT/A1783V}$ | 100:0 | 75 | PW3 | 38.2 (1-6 M) | ↑ | ↑ | - | ↓ | n.a. | ↓ | ↓ |
| [2]*Scn1a*$^{\Delta E26}$ | 90:10 | 100 | P14 | 41.1 (P12-14) | n.a | n.a. | n.a. | n.a. | n.a. | n.a. | - |
| [3] *Scn1a*$^{RX/+}$ | 75:25 | 40 | P18 | n.a. | n.a. | n.a. | n.a. | n.a. | n.a. | - | - |
| [4]*Scn1a*$^{RX/+}$ | 100:0 | 40 | P18 | n.a. | ↑ | ↓ | ↓ | ↓ | n.a. | - | - |
| [5]*Scn1a*$^{Flox/+}$Cre$^{+/-}$ | 100:0 | 100 | P21 | 40.7 (P22) | ↑ | ↑ | ↓ | ↓ | n.a. | n.a. | n.a. |
| [6]*Scn1a*$^{+/-}$ | 99.9: 0.1 | 40 | P21 | 39.5 (P20-46) | ↑ | ↑ | ↓ | ↓ | n.a. | ↓ | n.a. |
| [7]*Scn1a*$^{+/-}$ | 0:100 | 10 | P21 | n.a. | n.a. | n.a. | n.a. | n.a. | n.a. | n.a. | n.a. |
| [7]*Scn1a*$^{+/-}$ | 100:0 | 80 | P21 | n.a. | n.a. | n.a. | n.a. | n.a. | n.a. | n.a. | n.a. |
| [8]*Scn1a*$^{fl/+}$ | 100:0 | 70 | P18 | 39 (P35) | ↑ | n.a. | ↓ | ↓ | n.a. | n.a. | n.a. |
| [9]*Scn1a*$^{d/+}$ | 97:3 | 25 | PW3 | n.a. | n.a. | n.a. | n.a. | n.a. | n.a. | - | n.a. |
| [10]*Scn1a*$^{tm1Kea}$ | 75:25 | 54 | P24 | n.a. | n.a. | n.a. | n.a. | n.a. | n.a. | n.a. | n.a. |
| [11]*Scn1a*$^{tm1Kea}$ | 50:50 | 50 | P18 | n.a. | n.a. | n.a. | n.a. | n.a. | n.a. | n.a. | n.a. |
| [12]*Scn1a*$^{E1099X/+}$ | 75:25 | 46 | P20 | 40.2 (PW3-5) | n.a. | n.a. | n.a. | n.a. | n.a. | n.a. | n.a. |
| [13]*Scn1a*$^{RH/+}$ | 100:0 | 5 | n.a. | 41.3 (P14-15) | ↑ | - | ↓ | ↓ | n.a. | ↓ | - |
| [14]*Scn1a*$^{RH/+}$ | mix | 5 | n.a. | 43.1 (P14-15) | n.a. | n.a. | n.a. | n.a. | n.a. | n.a. | - |

## *3. Molecular and metabolic consequences of Scn1a genetic deficiency*

In the first manuscript, we provided relevant information about alterations in the hippocampal proteome of Dravet mice prior to and following epilepsy manifestation. The focus of research in the second manuscript was the investigation of the metabolome in the plasma and hippocampal tissue of Dravet mice. This approach might identify potential candidate mechanisms contributing to the course of Dravet Syndrome.

Dravet syndrome is closely related to *SCN1A* deficiency and the loss of function of sodium channels on GABAergic interneurons, leading to overall hyperexcitability and ictogenesis (Catterall, 2018). In 2006, this was demonstrated for the first time in an animal model of Dravet syndrome (Yu et al., 2006). Further electrophysiological studies confirmed this finding but also pointed towards other processes contributing to disease development such as excitability of hippocampal excitatory neurons (Almog et al., 2019; Mistry et al., 2014; Ogiwara et al., 2013; Tsai et al., 2015). In line with that, data from proteomic and metabolomic studies demonstrated significant alterations in inhibitory and excitatory signaling in the hippocampus of Dravet mice following the onset of spontaneous seizures.

Significant changes in the expression of several $GABA_A$ and $GABA_B$ receptor proteins, as well as a lower level of GABA in the hippocampus of Dravet mice, indicated disrupted GABAergic signaling which may contribute to ictogenesis in Dravet mice.

Interestingly, both studies also pointed towards a strong regulation of glutamatergic signaling in the hippocampus of Dravet mice. These changes might reflect compensatory mechanisms occurring as a consequence of hyperexcitability in Dravet mice. Whilst some of these aspects have already been discussed in the second manuscript, due to space limitations and the focus of the manuscript, some were shortened or excluded. Therefore, they are discussed in detail here.

In the second manuscript, we showed that glutamate, the main excitatory neurotransmitter in the brain, was down-regulated in the hippocampus of Dravet mice. Even though glutamate levels were reduced in the hippocampus, its distribution within synapses may be changed, as indicated by our proteomics data. Dravet mice showed a trend for the up-regulation of the vesicular glutamate transporter 1 (VGLUT1), leading to increased presynaptic vesicle filling and presynaptic glutamate release (Du et al., 2020). Once released into the synaptic cleft, the majority of glutamate is taken up by astrocytes via the excitatory amino acid transporters 1 and 2 (EAAT1, EAAT2) and converted into glutamine via glutamine synthetase. In manuscript I we reported a down-regulation of respective proteins, which, combined with a strong up-regulation of GFAP (glial fibrillary acidic protein), may imply reactive astrogliosis in Dravet mice. Altogether, this can result in glutamate accumulation in the synaptic cleft and astrocytes, thus contributing to neuronal hyperexcitability. Moreover, once taken up by astrocytes, glutamate conversion to glutamine in Dravet mice is reduced, possibly leading to glutamate accumulation in astrocytes and further increasing plasma membrane thresholds for its uptake by excitatory amino acid transporters (Mahmoud et al., 2019). This could explain why even with reduced hippocampal glutamate levels, its distribution within synapses could still lead to excitotoxicity and promote seizures in these animals.

Interestingly, both GABA and glutamate were down-regulated in Dravet mice hippocampus. Yet, GABA levels were reduced to a lesser extent, resulting in an increased GABA:glutamate ratio in Dravet mice. This could be a compensatory mechanism to the overall lack of glutamate, which is known to convert to both GABA and α-ketoglutarate in cells. As already mentioned in the second manuscript, lower glutamate levels and alterations in the glutamate/GABA-glutamine cycle, may also be a consequence of a decreased TCA cycle-mediated supply of the glutamate precursor α-ketoglutarate. However, the enzyme directing conversion of glutamate to α-ketoglutarate and vice versa (glutamate dehydrogenase), showed no changes in expression.

On the contrary, glutamic acid decarboxylase 2 is one of the two key enzymes for GABA formation from glutamate (Erlander et al., 1991) that showed a trend towards an up-regulation in four-week-old Dravet mice. This may suggest altered glutamate fueling of GABA, which can further contribute to the disrupted balance between GABA and glutamate observed in these animals. However, further studies exploring the alterations in the glutamate/GABA-glutamine cycle in different disease phases of Dravet syndrome are needed to confirm this concept.

Ionotropic glutamatergic receptors, NMDA or AMPA, are frequently linked to epilepsy in patients and animals, as are mutations in NMDA receptor genes (Xu and Luo, 2018). Agonists of these receptors can provoke seizures in animals or humans while their antagonists can inhibit seizures in animal models, listing them as potential anti-seizure medications (Hanada, 2020). However, to date, perampanel is the only glutamatergic receptor antagonist that has proved efficacious in the treatment of focal and generalized tonic-clonic seizures (French et al., 2012; French et al., 2013; French et al., 2015; Krauss et al., 2012; Nishida et al., 2018).

Aside from low glutamate levels in the hippocampus, we also noted a strong down-regulation of both ionotropic and metabotropic glutamatergic receptors, predominantly expressed on the postsynaptic neuronal and glial membranes (Hanada, 2020). These changes may be a result of glutamate excitotoxicity and consequential receptor internalization or apoptosis (Scott et al., 2004).

In addition to changes in GABAergic and glutamatergic signaling, alterations in other neurotransmitters systems and signaling molecules became evident in the hippocampus of Dravet mice. For instance, the abundance of several proteins involved in dopaminergic signaling was altered in Dravet mice. In addition, an interesting finding was an overall down-regulation of calcium and potassium channel subunits with possibly contrasting consequences. However, the actual consequences of these changes, such as dopaminergic signaling and the function of channels in the hippocampus, remain to be further examined.

Next, the nitric oxide signaling pathway, dominated by the up-regulation of neuronal nitric oxide synthetase (nNOS), was significantly regulated in Dravet mice. As a result of NMDA overstimulation, calcium entry through cation channels triggers nNOS, which induces the synthesis of nitric oxide (Lipton et al., 1993; Mahmoud et al., 2019; Yamauchi et al., 1998). Nitric oxide is known to further mediate oxidative stress, reactive glial cell proliferation and promote angiogenesis, all of which have been discussed as potential contributors to epileptogenesis and overall hyperexcitability in the epileptic brain (Arhan et al., 2011; Mahmoud et al., 2019; Morbidelli et al., 2004). In line with this, we have reported reactive astrogliosis and increased angiogenesis in the hippocampus of Dravet mice. However, follow up studies addressing the functional consequences of these alterations would be essential to confirm our findings.

In addition, recent findings also proposed a link between excessive central nitric oxide production and hypothalamic-pituitary-adrenocortical (HPA) axis dysregulation (Bruenig et al., 2017; Chen et al., 2015a). Interestingly, investigation of the Dravet mice metabolome revealed plasma depletion of corticosterone, the main glucocorticoid in rodents. Corticosterone is released by the adrenal glands as a result of HPA axis activation in response to stress or other triggers (Herman et al., 2016). While the activation of the HPA axis serves as an important adaptive function preparing the body for increased demands, long-term activation by chronic stressors can be associated with detrimental effects and, in particular, with epileptic activity (Castro et al., 2012; Herman et al., 2016). The lower corticosterone levels in Dravet mice are rather unexpected, considering its direct role in promoting seizures (Joëls, 2009). However, a down-regulation of HPA axis activity and reduced plasma corticosterone may represent a compensatory mechanism to the long-term overstimulation. Therefore, it would be of interest to check corticosterone levels in younger animals following the highest incidence of seizures and SUDEP and thus inspect when negative feedback of the HPA axis occurs.

One of the main findings in this study were pronounced alterations in bioenergetics in the hippocampus of Dravet mice, specifically in glucose metabolism and TCA cycle activity. These metabolic changes may be associated with increased interictal activity and a failure to fulfill higher energy demands. Furthermore, these alterations may not only represent a consequence of seizure activity, but can also contribute to an increased susceptibility to seizures and ictogenesis. This has also been observed in metabolic epilepsies, which in many cases also have a genetic cause (Scheffer et al., 2016).

As mentioned above, the interneuron energy hypothesis may further explain the particularly high seizure incidence, one of the clinical manifestations of Dravet syndrome. The hypothesis is based on evidence that inhibitory interneurons require a higher amount of energy (Kann, 2016). This may in turn result in excitatory neuron disinhibition and hyperexcitability, as previously discussed (Henke et al., 2020). This could explain how energy depletion in neurons caused by an increased interictal spiking may further contribute to lowering of seizure threshold and ictogenesis. In line with this hypothesis, intermediates of glucose metabolism and the TCA cycle significantly correlated with the severity of spontaneous motor seizures in Dravet mice.

Lastly, we have also observed some possible compensatory changes to energy deficits, including increased glycolysis and glycogenogenesis. Particularly interesting were alterations pointing towards a dysregulation in the metabolic coupling between neurons and astrocytes in Dravet mice. These changes could affect glycolysis in astrocytes, lactate shuttle to neurons and TCA cycle regulation in neurons (Turner and Adamson, 2011), altogether affecting the brain's energetic state.

## *4. The impact of the ketogenic diet on the phenotype and metabolome of Dravet mice*

A ketogenic diet has been recommended as a second-line therapy in Dravet syndrome (Cross et al., 2019). The diet is known to shift energy metabolism towards a more fat-based energy supply, thus providing indirect evidence for metabolic and bioenergetic alterations in patients with Dravet syndrome. In the second manuscript, we aimed to identify metabolic changes in the hippocampus and plasma samples of Dravet mice. In addition, we aimed to investigate the impact of a ketogenic diet on these alterations and its therapeutic potential in the mouse model of Dravet syndrome here evaluated.

The ketogenic diet failed to improve the seizure and behavioral phenotype in Dravet mice. However, the diet succeeded to partially improve their impaired gait. This might be related to an increase in intracellular forms of glucose in the hippocampus. In line with this assumption, this improvement in gait positively correlated with hippocampal levels of glucose and glucose-6-phosphate. Therefore, replacing glucose utilization by ketone bodies, may be sufficient to improve the gait in Dravet animals. Importantly, the level of ketosis did not show a significant correlation with this improvement. Altogether, these findings trigger an interest to further investigate the therapeutic potential of the ketogenic diet in the treatment of gait abnormalities in patients with Dravet syndrome, so far shown in only one clinical study (Tian et al., 2019).

Due to word count limitations and the focus of the manuscript, some interesting aspects regarding the application of the ketogenic diet and its metabolic consequences in Dravet mice were not discussed in the manuscript. Therefore, they are discussed here. A lower intake of ketogenic diet than the control diet was expected, considering that its caloric value is almost twice as high as the control diet. However, an interesting finding was that mutant mice consumed significantly higher amounts of the ketogenic diet than wildtype mice, which resulted in a much steeper body weight curve as compared to the remaining three groups. This phenomenon could be a consequence of an increased appetite in Dravet mice on the high-fat

diet. In patients with epilepsy, an increase of appetite and body weight is frequently observed especially when taking antiseizure drugs (Ben-Menachem, 2007). Seizures are high-energy events for the brain (Yang et al., 2013a), which could promote appetite in Dravet animals, the results of which would be much more pronounced on a high-energy diet, such as the ketogenic diet. However, this behavior has not been observed in Dravet patients. Conversely, in some patients with Dravet syndrome, loss of appetite has been described, particularly when taking stiripentol, topiramate and zonisamide as antiseizure drugs (Knupp and Wirrell, 2018). Since we did not detect any differences between Dravet and wildtype mice on the control diet, the change in appetite may also be triggered by the lower glucose intake and an attempt to compensate for the already depleted glucose levels.

Even though mutant mice consumed a higher amount of ketogenic diet, they still exhibited a lower level of ketosis in the hippocampus and plasma, when compared to wildtype controls. This may explain a failure to refill reduced TCA cycle intermediates from ketone bodies, compensate energy deficiency and reduce seizures in these mice. Consistent with this, we have observed a negative correlation between intracellular phosphorylated glucose forms, lactate, glutamate precursors (α-ketoglutarate, L-glutamine, L-asparagine and L-aspartic acid) and the GABA:glutamate ratio, the main representation of inhibitory/excitatory balance in the brain postulated as one mechanism of epileptogenesis and seizure generation (Fritschy, 2008). Except for an increased abundance of phosphorylated glucose in Dravet mice, all other metabolites directly or indirectly fueling the TCA cycle, were down-regulated in Dravet mice and the ketogenic diet failed to restore wildtype levels, thus confirming our hypothesis. On the other hand, reduced free glucose import, glucose concentration in cells and up-regulated glucose-6-phosphate in the hippocampus of Dravet mice might point towards a mechanism compensating for energy deficiency and an attempt of cells to shift glucose metabolism towards glycolysis. Furthermore, an increased level of glucose-1-phosphate may indicate a higher degradation or lower synthesis of glycogen reserves (Obel et al., 2012). An introduction of the ketogenic diet

seemed to further increase glucose-6-phosphate forms in the hippocampus. This could be explained by the dominant use of ketone bodies for energetic needs and saving glucose for other relevant processes such as the pentose phosphate pathway, a non-oxidative metabolic pathway for the synthesis of nucleotides (Soty et al., 2017). An observed increase of 6-phosphogluconic acid, an intermediate in the pentose phosphate pathway, further supported this claim.

## *5. Study limitations*

As mentioned above, “Omics” studies are a useful approach for the broad screening of data and obtaining the first information about disease-associated molecular alterations. Similarly, here we managed to demonstrate overall information about neuronal signaling in the brain of Dravet mice. However, we must not overlook some of the inevitable study limitations.

Firstly, proteomic data can only provide information about protein abundance but not about the functional relevance of this molecular change. Therefore, future studies will be essential to provide further information, thus confirming or opposing our hypotheses.

Secondly, proteomic and metabolic screening of hippocampal tissue cannot provide information about protein or metabolite distribution within hippocampal cell structures, neuronal or glial cells or the intra- or extracellular space. Respective data may provide crucial information about the functional relevance of proteome and metabolome alterations and help the interpretation of our results. Immunohistochemical studies could provide information about the localization and distribution of selected proteins in the hippocampus and are thus of particular interest for the future.

Moreover, we should also consider the difference in age of mice sampled in these two studies. Four-week-old mice in manuscript I are considered early adolescent mice, while mice in manuscript II are fully adult (Brust et al., 2015). Considering that the adolescent brain still undergoes intense developmental changes, this may result in differences in the expression of certain proteins which were compared to metabolites of adult mice in the second study. However, we must state that the different sampling time in the two studies was due to the different study aims. The proteomics study focused on molecular alterations at the early developmental age in order to capture all changes before and shorty following epilepsy manifestation. The later time point was chosen in order to pass the period with the highest seizure frequency thus aiming to limit the direct impact of seizures on the proteome. On the

other hand, the metabolomics study aimed to assess which metabolic changes are linked to Dravet syndrome and the use of the ketogenic diet. In order to capture the impact of these alterations on both seizures and the behavioral phenotype of Dravet mice, we needed to conduct experiments in adult animals. In addition, the minimum duration of ketogenic diet application to induce ketosis is 3 weeks, which also influenced the time point of sampling.

Lastly, four-week-old Dravet mice still exhibited lowered body weight as compared to wildtype littermates, an observation that disappeared by adulthood. Therefore, certain proteome changes may also result from poor brain and body weight development, which by themselves are known to deteriorate disease pathology in both animal models and humans (Crepin et al., 2009). Still, body weight loss is part of the phenotype of Dravet mice and should therefore be considered when investigating Dravet syndrome pathology in these mice.

# CLOSING REMARKS

Taken together, our findings revealed excellent face validity of the conditional, heterozygous *Scn1a*-A1783V Dravet mouse model bred on a mixed (50:50) C57BL/6J and 129S1 background with *Hprt* promotor-mediated neuronal knock-in. The model accurately replicates the clinical syndrome in patients with Dravet syndrome with an increased susceptibility to hyperthermia-induced seizures, development of spontaneous seizures, a relatively high incidence of SUDEP, hyperactivity and motor deficits. The model is therefore highly valuable for the evaluation of pharmacological strategies in Dravet syndrome and emerging novel "personalized" treatment options. In addition, the rate of mortality within a narrow time frame makes this model highly suitable for studies investigating mechanisms of SUDEP and approaches for its prevention.

The untargeted proteomic profiling in Dravet mice revealed significant proteome differences and molecular alterations in hippocampal tissue both before and following disease manifestation. Several proteins involved in synaptic plasticity were affected before epilepsy manifestation. Thus, it would be of relevance for future studies to investigate if these molecular alterations represent early consequences of *Scn1a* genetic deficiency or can contribute to disease onset. Following epilepsy manifestation, molecular alterations beyond GABAergic interneuron dysfunction became evident. More complex pathophysiological mechanisms underlying the disease's pathology should be considered in the future development of treatment strategies. Among those, glutamatergic synaptic transmission stood out as the most affected molecular mechanism in the hippocampus, later confirmed by the metabolome analysis in Dravet mice. The findings also indicated further alterations of components of the glutamate/GABA-glutamine cycle. These may serve as an endogenous compensatory mechanism, which can be supported by GABAergic drugs, already recommended as first line drugs for the treatment of Dravet syndrome.

The extensive metabolomic screening revealed prominent alterations in energy metabolism in the hippocampus of Dravet mice. Interestingly, some of these metabolites directly correlated with the severity of motor seizures observed in Dravet mice, including the hippocampal level of glucose-6-phosphate, TCA cycle intermediates and several amino acids. Their potential as target candidates for the treatment of Dravet syndrome should be explored in future studies.

The ketogenic diet improved the motor deficits observed in Dravet mice, thus pointing to a potential role of metabolic alterations in ataxia and gait disturbances in Dravet syndrome. The development of therapeutic modulating concentrations of glucose and glucose-6-phosphate may be considered in the future for the treatment of Dravet syndrome and associated gait disturbances. Lastly, the ketosis state in Dravet and wildtype mice differed. This might explain why the diet failed to improve seizure susceptibility. In line with this, the diet is frequently prescribed in combination with other antiseizure drugs for therapeutic management of Dravet syndrome.

Altogether, our findings revealed several molecular alterations beyond *SCN1A* deficiency that might contribute to the pathophysiology of Dravet syndrome. Their role as possible candidates for novel pharmacological treatments should be explored in future studies. However, further research addressing the functional consequences of these molecular alterations in different disease states of Dravet syndrome will be essential to validate our findings.

# *References*


Accurso, A., et al., 2008. Dietary carbohydrate restriction in type 2 diabetes mellitus and metabolic syndrome: time for a critical appraisal. Nutrition & Metabolism. 5**,** 9.

Acha, J., et al., 2015. Cognitive characterization of children with Dravet syndrome: A neurodevelopmental perspective. Child Neuropsychology. 21**,** 693-715.

Aiba, I., Noebels, J. L., 2015. Spreading depolarization in the brainstem mediates sudden cardiorespiratory arrest in mouse SUDEP models. Sci Transl Med. 7**,** 282ra46.

Aljaafari, D., et al., 2017. Adult motor phenotype differentiates Dravet syndrome from Lennox-Gastaut syndrome and links SCN1A to early onset parkinsonian features. Epilepsia. 58**,** e44-e48.

Almog, Y., et al., 2019. Early hippocampal hyperexcitability followed by disinhibition in a mouse model of Dravet syndrome. bioRxiv. 790170.

Alonso Gómez, C., et al., 2018. P.2.029 - Characterisation of a Dravet syndrome knock-in mouse model useful for investigating cannabinoid-based treatments. European Neuropsychopharmacology. 28**,** S41.

Aras, L. M., et al., 2015. The European patient with Dravet syndrome: results from a parent-reported survey on antiepileptic drug use in the European population with Dravet syndrome. Epilepsy Behav. 44**,** 104-9.

Arhan, E., et al., 2011. Effects of epilepsy and antiepileptic drugs on nitric oxide, lipid peroxidation and xanthine oxidase system in children with idiopathic epilepsy. Seizure. 20**,** 138-42.

Auvin, S., et al., 2018. Altered vaccine-induced immunity in children with Dravet syndrome. Epilepsia. 59**,** e45-e50.

Avanzini, G., et al., 2013. Do seizures and epileptic activity worsen epilepsy and deteriorate cognitive function? Epilepsia. 54 Suppl 8**,** 14-21.

Bao, Y., et al., 2018. RASgrf1, a Potential Methylatic Mediator of Anti-epileptogenesis? Neurochem Res. 43**,** 2000-2007.

Barañano, K. W., Hartman, A. L., 2008. The ketogenic diet: uses in epilepsy and other neurologic illnesses. Curr Treat Options Neurol. 10**,** 410-9.

Battaglia, D., et al., 2016. Outlining a core neuropsychological phenotype for Dravet syndrome. Epilepsy Res. 120**,** 91-7.

Bauer, A., et al., 2016. Identification of cyclins A1, E1 and vimentin as downstream targets of heme oxygenase-1 in vascular endothelial growth factor-mediated angiogenesis. Scientific reports. 6**,** 29417.

Ben-Hamo, M., et al., 2016. Differential effects of photoperiod length on depression- and anxiety-like behavior in female and male diurnal spiny mice. Physiol Behav. 165**,** 1-6.

Ben-Menachem, E., 2007. Weight issues for people with epilepsy--a review. Epilepsia. 48 Suppl 9**,** 42-5.

Bender, A. C., et al., 2013. Focal Scn1a knockdown induces cognitive impairment without seizures. Neurobiol Dis. 54**,** 297-307.

Berg, A. T., 2011. Epilepsy, cognition, and behavior: The clinical picture. Epilepsia. 52 Suppl 1**,** 7-12.

Berkvens, J. J., et al., 2015. Autism and behavior in adult patients with Dravet syndrome (DS). Epilepsy Behav. 47**,** 11-6.

Besag, F. M., 2004. Behavioral aspects of pediatric epilepsy syndromes. Epilepsy Behav. 5 Suppl 1**,** S3-13.

Bhutia, Y. D., et al., 2017. Plasma Membrane $Na^+$-Coupled Citrate Transporter (SLC13A5) and Neonatal Epileptic Encephalopathy. Molecules. 22.

Bitsika, V., et al., 2016. High-throughput LC–MS/MS proteomic analysis of a mouse model of mesiotemporal lobe epilepsy predicts microglial activation underlying disease development. Journal of proteome research. 15**,** 1546-1562.

Boison, D., 2017. New insights into the mechanisms of the ketogenic diet. Curr Opin Neurol. 30**,** 187-192.

Boison, D., Steinhäuser, C., 2018. Epilepsy and astrocyte energy metabolism. Glia. 66**,** 1235-1243.

Bosque, J. R., et al., 2019. Molecular tools for the characterization of seizure susceptibility in genetic rodent models of epilepsy. Epilepsy Behav. 106594.

Bough, K. J., et al., 2006. Mitochondrial biogenesis in the anticonvulsant mechanism of the ketogenic diet. Ann Neurol. 60**,** 223-35.

Bozzi, Y., Borrelli, E., 2013. The role of dopamine signaling in epileptogenesis. Front Cell Neurosci. 7**,** 157.

Brambilla, R., et al., 1997. A role for the Ras signalling pathway in synaptic transmission and long-term memory. Nature. 390**,** 281-286.

Brigo, F., et al., 2018. Emerging drugs for the treatment of Dravet syndrome. Expert Opinion on Emerging Drugs. 23**,** 261-269.

Bruenig, D., et al., 2017. Nitric oxide pathway genes (NOS1AP and NOS1) are involved in PTSD severity, depression, anxiety, stress and resilience. Gene. 625**,** 42-48.

Brunklaus, A., Zuberi, S. M., 2014. Dravet syndrome--from epileptic encephalopathy to channelopathy. Epilepsia. 55**,** 979-84.

Brust, V., et al., 2015. Lifetime development of behavioural phenotype in the house mouse (Mus musculus). Front Zool. 12 Suppl 1**,** S17.

Buck, M. L., Goodkin, H. P., 2019. Stiripentol: A Novel Antiseizure Medication for the Management of Dravet Syndrome. Ann Pharmacother. 53**,** 1136-1144.

Bureau, M., Dalla Bernardina, B., 2011. Electroencephalographic characteristics of Dravet syndrome. Epilepsia. 52 Suppl 2**,** 13-23.

Cao, D., et al., 2012. Efficacy of stiripentol in hyperthermia-induced seizures in a mouse model of Dravet syndrome. Epilepsia. 53**,** 1140-1145.

Caraballo, R. H., 2011. Nonpharmacologic treatments of Dravet syndrome: focus on the ketogenic diet. Epilepsia. 52 Suppl 2**,** 79-82.

Carola, V., et al., 2002. Evaluation of the elevated plus-maze and open-field tests for the assessment of anxiety-related behaviour in inbred mice. Behav Brain Res. 134**,** 49-57.

Cassé-Perrot, C., et al., Neuropsychological aspects of severe myoclonic epilepsy in infancy. Neuropsychology of childhood epilepsy. Springer, 2001, pp. 131-140.

Castro, J. E., et al., 2012. Personality traits in rats predict vulnerability and resilience to developing stress-induced depression-like behaviors, HPA axis hyper-reactivity and brain changes in pERK1/2 activity. Psychoneuroendocrinology. 37**,** 1209-23.

Catarino, C. B., et al., 2011. Dravet syndrome as epileptic encephalopathy: evidence from long-term course and neuropathology. Brain. 134**,** 2982-3010.

Catterall, W. A., 2018. Dravet Syndrome: A Sodium Channel Interneuronopathy. Curr Opin Physiol. 2**,** 42-50.

Catterall, W. A., et al., 2010. NaV1.1 channels and epilepsy. J Physiol. 588**,** 1849-59.

Cavus, I., et al., 2005. Extracellular metabolites in the cortex and hippocampus of epileptic patients. Ann Neurol. 57**,** 226-35.

Cetica, V., et al., 2017. Clinical and genetic factors predicting Dravet syndrome in infants with SCN1A mutations. Neurology. 88**,** 1037-1044.

Cheah, C. S., et al., 2013. Correlations in timing of sodium channel expression, epilepsy, and sudden death in Dravet syndrome. Channels (Austin). 7**,** 468-72.

Cheah, C. S., et al., 2012. Specific deletion of NaV1.1 sodium channels in inhibitory interneurons causes seizures and premature death in a mouse model of Dravet syndrome. Proc Natl Acad Sci U S A. 109**,** 14646-51.

Chen, F., et al., 2015a. Hypothalamic-pituitary-adrenal axis hyperactivity accounts for anxiety- and depression-like behaviors in rats perinatally exposed to bisphenol A. J Biomed Res. 29**,** 250-8.

Chen, G., et al., 2015b. Amino acid metabolic dysfunction revealed in the prefrontal cortex of a rat model of depression. Behav Brain Res. 278**,** 286-92.

Chen, H., et al., 2018. RASGRF1 hypermethylation, a putative biomarker of colorectal cancer. Annals of Clinical & Laboratory Science. 48**,** 3-10.

Chieffo, D., et al., 2016. Disorders of early language development in Dravet syndrome. Epilepsy & Behavior. 54**,** 30-33.

Chieffo, D., et al., 2011. Early development in Dravet syndrome; visual function impairment precedes cognitive decline. Epilepsy Res. 93**,** 73-9.

Chiron, C., 2005. Stiripentol. Expert Opin Investig Drugs. 14**,** 905-11.

Chiron, C., 2007. Stiripentol. Neurotherapeutics. 4**,** 123-5.

Chiron, C., et al., 2000. Stiripentol in severe myoclonic epilepsy in infancy: a randomised placebo-controlled syndrome-dedicated trial. STICLO study group. Lancet. 356**,** 1638-42.

Claes, L., et al., 2001. De novo mutations in the sodium-channel gene SCN1A cause severe myoclonic epilepsy of infancy. Am J Hum Genet. 68**,** 1327-32.

Connolly, H. M., et al., 1997. Valvular heart disease associated with fenfluramine-phentermine. N Engl J Med. 337**,** 581-8.

Connolly, M. B., 2016. Dravet Syndrome: Diagnosis and Long-Term Course. Can J Neurol Sci. 43 Suppl 3**,** S3-8.

Constantinou, C., et al., 2011. GC-MS metabolomic analysis reveals significant alterations in cerebellar metabolic physiology in a mouse model of adult onset hypothyroidism. J Proteome Res. 10**,** 869-79.

Cooper, M. S., et al., 2016. Mortality in Dravet syndrome. Epilepsy Res. 128**,** 43-47.

Cox, J., Mann, M., 2007. Is proteomics the new genomics? Cell. 130**,** 395-8.

Crepin, S., et al., 2009. Malnutrition and epilepsy: a two-way relationship. Clin Nutr. 28**,** 219-25.

Cross, J. H., et al., 2019. Dravet syndrome: Treatment options and management of prolonged seizures. Epilepsia. 60 Suppl 3**,** S39-S48.

D'Andrea Meira, I., et al., 2019. Ketogenic Diet and Epilepsy: What We Know So Far. Front Neurosci. 13**,** 5.

Danış, O., et al., 2011a. Changes in intracellular protein expression in cortex, thalamus and hippocampus in a genetic rat model of absence epilepsy. Brain Res Bull. 84**,** 381-8.

Danış, Ö., et al., 2011b. Changes in intracellular protein expression in cortex, thalamus and hippocampus in a genetic rat model of absence epilepsy. Brain research bulletin. 84**,** 381-388.

Dave, J. M., Bayless, K. J., 2014. Vimentin as an integral regulator of cell adhesion and endothelial sprouting. Microcirculation. 21**,** 333-44.

Davidovic, L., et al., 2011. A metabolomic and systems biology perspective on the brain of the fragile X syndrome mouse model. Genome Res. 21**,** 2190-202.

Deberardinis, R. J., et al., 2008. Brick by brick: metabolism and tumor cell growth. Curr Opin Genet Dev. 18**,** 54-61.

Dedeurwaerdere, S., et al., 2015. In the grey zone between epilepsy and schizophrenia: alterations in group II metabotropic glutamate receptors. Acta Neurol Belg. 115**,** 221-32.

Devinsky, O., et al., 2018a. Resolving ambiguities in SUDEP classification. Epilepsia. 59**,** 1220-1233.

Devinsky, O., et al., 2018b. Randomized, dose-ranging safety trial of cannabidiol in Dravet syndrome. Neurology. 90**,** e1204-e1211.

Devinsky, O., et al., 2013. Glia and epilepsy: excitability and inflammation. Trends Neurosci. 36**,** 174-84.

Dibué-Adjei, M., et al., 2017. Efficacy of adjunctive vagus nerve stimulation in patients with Dravet syndrome: A meta-analysis of 68 patients. Seizure. 50**,** 147-152.

Dingledine, R., McBain, C., 1999. Glutamate and aspartate are the major excitatory transmitters in the brain. Basic Neurochemistry: Molecular, Cellular and Medical Aspects. Ed. GJ Siegel, BW Agranoff, RW Albers, SK Fisher, MD Uhler. Philadelphia.

Dlouhy, B. J., et al., 2016. Palliative epilepsy surgery in Dravet syndrome-case series and review of the literature. Childs Nerv Syst. 32**,** 1703-8.

Domon, B., Aebersold, R., 2006. Mass spectrometry and protein analysis. Science. 312**,** 212-7.

Donatti, A., et al., 2020. Circulating Metabolites as Potential Biomarkers for Neurological Disorders-Metabolites in Neurological Disorders. Metabolites. 10.

Douglas, J. G., et al., 1981. Pulmonary hypertension and fenfluramine. Br Med J (Clin Res Ed). 283**,** 881-3.
Dravet, C., 2011. The core Dravet syndrome phenotype. Epilepsia. 52 Suppl 2**,** 3-9.
Dravet, C., Oguni, H., 2013. Dravet syndrome (severe myoclonic epilepsy in infancy). Handb Clin Neurol. 111**,** 627-33.
Dressler, A., et al., 2015. Efficacy and tolerability of the ketogenic diet in Dravet syndrome - Comparison with various standard antiepileptic drug regimen. Epilepsy Res. 109**,** 81-9.
Du, X., et al., 2020. Research progress on the role of type I vesicular glutamate transporter (VGLUT1) in nervous system diseases. Cell Biosci. 10**,** 26.
Duflocq, A., et al., 2008. Nav1.1 is predominantly expressed in nodes of Ranvier and axon initial segments. Mol Cell Neurosci. 39**,** 180-92.
Dugger, S. A., et al., 2018. Drug development in the era of precision medicine. Nature Reviews Drug Discovery. 17**,** 183.
Dutton, S. B., et al., 2013. Preferential inactivation of Scn1a in parvalbumin interneurons increases seizure susceptibility. Neurobiol Dis. 49**,** 211-20.
Dutton, S. B., et al., 2011. Protective effect of the ketogenic diet in Scn1a mutant mice. Epilepsia. 52**,** 2050-2056.
Dutton, S. B. B., et al., 2017. Early-life febrile seizures worsen adult phenotypes in Scn1a mutants. Exp Neurol. 293**,** 159-171.
Erlander, M. G., et al., 1991. Two genes encode distinct glutamate decarboxylases. Neuron. 7**,** 91-100.
Escayg, A., Goldin, A. L., 2010. Sodium channel SCN1A and epilepsy: mutations and mechanisms. Epilepsia. 51**,** 1650-8.
Fabene, P. F., et al., 2010. The emerging role for chemokines in epilepsy. J Neuroimmunol. 224**,** 22-7.
Fasano, A., et al., 2014. Antecollis and levodopa-responsive parkinsonism are late features of Dravet syndrome. Neurology. 82**,** 2250-2251.
Fisher, J. L., 2011. The effects of stiripentol on GABA(A) receptors. Epilepsia. 52 Suppl 2**,** 76-8.
Fisher, R. S., et al., 2014. ILAE official report: a practical clinical definition of epilepsy. Epilepsia. 55**,** 475-82.
Fisher, R. S., et al., 2005. Epileptic seizures and epilepsy: definitions proposed by the International League Against Epilepsy (ILAE) and the International Bureau for Epilepsy (IBE). Epilepsia. 46**,** 470-2.
Freeman, J. M., et al., 2007. The ketogenic diet: one decade later. Pediatrics. 119**,** 535-43.
French, J. A., et al., 2012. Adjunctive perampanel for refractory partial-onset seizures: randomized phase III study 304. Neurology. 79**,** 589-96.
French, J. A., et al., 2013. Evaluation of adjunctive perampanel in patients with refractory partial-onset seizures: results of randomized global phase III study 305. Epilepsia. 54**,** 117-25.
French, J. A., et al., 2015. Perampanel for tonic-clonic seizures in idiopathic generalized epilepsy A randomized trial. Neurology. 85**,** 950-7.
Fritschy, J. M., 2008. Epilepsy, E/I Balance and GABA(A) Receptor Plasticity. Front Mol Neurosci. 1**,** 5.
Gao, Q., et al., 1999. The E6 oncoproteins of high-risk papillomaviruses bind to a novel putative GAP protein, E6TP1, and target it for degradation. Molecular and cellular biology. 19**,** 733-744.
Gardin, J. M., et al., 2000. Valvular abnormalities and cardiovascular status following exposure to dexfenfluramine or phentermine/fenfluramine. JAMA. 283**,** 1703-9.
Gataullina, S., Dulac, O., 2017. From genotype to phenotype in Dravet disease. Seizure. 44**,** 58-64.
Geffrey, A. L., et al., 2015. Drug-drug interaction between clobazam and cannabidiol in children with refractory epilepsy. Epilepsia. 56**,** 1246-51.
Genton, P., et al., 2011. Dravet syndrome: the long-term outcome. Epilepsia. 52 Suppl 2**,** 44-9.
Geschwind, D. H., Konopka, G., 2009. Neuroscience in the era of functional genomics and systems biology. Nature. 461**,** 908-15.
Giordano, F., et al., 2017. Vagus nerve stimulation: Surgical technique of implantation and revision and related morbidity. Epilepsia. 58 Suppl 1**,** 85-90.

Giorgi, F. S., et al., 2004. The role of norepinephrine in epilepsy: from the bench to the bedside. Neurosci Biobehav Rev. 28, 507-24.

Gitiaux, C., et al., 2016. Motor neuropathy contributes to crouching in patients with Dravet syndrome. Neurology. 87, 277-281.

González-Domínguez, R., et al., 2015. Metabolomic investigation of systemic manifestations associated with Alzheimer's disease in the APP/PS1 transgenic mouse model. Mol Biosyst. 11, 2429-40.

Grant, S. M., DeMorrow, S., 2020. Bile Acid Signaling in Neurodegenerative and Neurological Disorders. Int J Mol Sci. 21.

Grosenbaugh, D. K., Mott, D. D., 2013. Stiripentol is anticonvulsant by potentiating GABAergic transmission in a model of benzodiazepine-refractory status epilepticus. Neuropharmacology. 67, 136-43.

Haginoya, K., et al., 2018. [(18)F]fluorodeoxyglucose-positron emission tomography study of genetically confirmed patients with Dravet syndrome. Epilepsy Res. 147, 9-14.

Han, S., et al., 2012. Autistic-like behaviour in Scn1a+/- mice and rescue by enhanced GABA-mediated neurotransmission. Nature. 489, 385-90.

Hanada, T., 2020. Ionotropic Glutamate Receptors in Epilepsy: A Review Focusing on AMPA and NMDA Receptors. Biomolecules. 10.

Harden, C., et al., 2017. Practice Guideline Summary: Sudden Unexpected Death in Epilepsy Incidence Rates and Risk Factors: Report of the Guideline Development, Dissemination, and Implementation Subcommittee of the American Academy of Neurology and the American Epilepsy Society. Epilepsy Curr. 17, 180-187.

Hawkins, N. A., et al., 2019. Gene expression profiling in a mouse model of Dravet syndrome. Exp Neurol. 311, 247-256.

Henke, C., et al., 2020. Disruption of the sodium-dependent citrate transporter SLC13A5 in mice causes alterations in brain citrate levels and neuronal network excitability in the hippocampus. Neurobiol Dis. 143, 105018.

Herman, J. P., et al., 2016. Regulation of the Hypothalamic-Pituitary-Adrenocortical Stress Response. Compr Physiol. 6, 603-21.

Heron, S. E., et al., 2010. De novo SCN1A mutations in Dravet syndrome and related epileptic encephalopathies are largely of paternal origin. J Med Genet. 47, 137-41.

Hollywood, K., et al., 2006. Metabolomics: current technologies and future trends. Proteomics. 6, 4716-23.

Holter, S. M., et al., 2015. Tests for Anxiety-Related Behavior in Mice. Curr Protoc Mouse Biol. 5, 291-309.

Hu, X. J., Ticku, M. K., 1994. Chronic benzodiazepine agonist treatment produces functional uncoupling of the gamma-aminobutyric acid-benzodiazepine receptor ionophore complex in cortical neurons. Mol Pharmacol. 45, 618-25.

Ito, S., et al., 2013. Mouse with Nav1.1 haploinsufficiency, a model for Dravet syndrome, exhibits lowered sociability and learning impairment. Neurobiol Dis. 49, 29-40.

Ivanisevic, J., et al., 2014. Brain region mapping using global metabolomics. Chem Biol. 21, 1575-84.

Ivanov, A. I., et al., 2015. Metabolic responses differentiate between interictal, ictal and persistent epileptiform activity in intact, immature hippocampus in vitro. Neurobiol Dis. 75, 1-14.

Jeyabalan, N., Clement, J. P., 2016. SYNGAP1: Mind the Gap. Front Cell Neurosci. 10, 32.

Jirkof, P., 2014. Burrowing and nest building behavior as indicators of well-being in mice. J Neurosci Methods. 234, 139-46.

Jirkof, P., et al., 2013. Assessment of postsurgical distress and pain in laboratory mice by nest complexity scoring. Lab Anim. 47, 153-61.

Joëls, M., 2009. Stress, the hippocampus, and epilepsy. Epilepsia. 50, 586-97.

Jogamoto, T., et al., 2017. Add-on stiripentol elevates serum valproate levels in patients with or without concomitant topiramate therapy. Epilepsy Res. 130, 7-12.

Joshi, S., Kapur, J., GABA(A) Receptor Plasticity During Status Epilepticus. In: J. L. Noebels, et al., (Eds.), Jasper's Basic Mechanisms of the Epilepsies. National Center for Biotechnology Information (US)

Copyright © 2012, Michael A Rogawski, Antonio V Delgado-Escueta, Jeffrey L Noebels, Massimo Avoli and Richard W Olsen., Bethesda (MD), 2012.

Kalume, F., 2013. Sudden unexpected death in Dravet syndrome: respiratory and other physiological dysfunctions. Respir Physiol Neurobiol. 189**,** 324-8.

Kalume, F., et al., 2015a. Sleep impairment and reduced interneuron excitability in a mouse model of Dravet Syndrome. Neurobiol Dis. 77**,** 141-54.

Kalume, F., et al., 2015b. Sleep impairment and reduced interneuron excitability in a mouse model of Dravet Syndrome. Neurobiology of disease. 77**,** 141-154.

Kalume, F., et al., 2007. Reduced sodium current in Purkinje neurons from Nav1.1 mutant mice: implications for ataxia in severe myoclonic epilepsy in infancy. J Neurosci. 27**,** 11065-74.

Kamburov, A., et al., 2009. ConsensusPathDB—a database for integrating human functional interaction networks. Nucleic acids research. 37**,** D623-D628.

Kanai, K., et al., 2004. Effect of localization of missense mutations in SCN1A on epilepsy phenotype severity. Neurology. 63**,** 329-34.

Kanani, H., et al., 2008. Standardizing GC-MS metabolomics. J Chromatogr B Analyt Technol Biomed Life Sci. 871**,** 191-201.

Kann, O., 2016. The interneuron energy hypothesis: Implications for brain disease. Neurobiol Dis. 90**,** 75-85.

Kaplan, J. S., et al., 2017. Cannabidiol attenuates seizures and social deficits in a mouse model of Dravet syndrome. Proceedings of the National Academy of Sciences. 114**,** 11229-11234.

Kassel, K. M., et al., 2010. Regulation of human cytidine triphosphate synthetase 2 by phosphorylation. Journal of Biological Chemistry. 285**,** 33727-33736.

Keck, M., et al., 2017. A systems level analysis of epileptogenesis-associated proteome alterations. Neurobiology of disease. 105**,** 164-178.

Keck, M., et al., 2018. Proteomic profiling of epileptogenesis in a rat model: Focus on cell stress, extracellular matrix and angiogenesis. Neurobiol Dis. 112**,** 119-135.

Khurana, M., et al., 2020. Application of contemporary neuroproteomic techniques in unravelling neurological disorders. Curr Protein Pept Sci.

Kim, Y., 2017. Mechanisms and prevention of SUDEP in Dravet Syndrome.

Kiriyama, Y., Nochi, H., 2019. The Biosynthesis, Signaling, and Neurological Functions of Bile Acids. Biomolecules. 9.

Klein, P., et al., 2018. Commonalities in epileptogenic processes from different acute brain insults: Do they translate? Epilepsia. 59**,** 37-66.

Klein, S., et al., 2015. Sucrose consumption test reveals pharmacoresistant depression-associated behavior in two mouse models of temporal lobe epilepsy. Exp Neurol. 263**,** 263-71.

Knupp, K. G., Wirrell, E. C., 2018. Correction to: Treatment Strategies for Dravet Syndrome. CNS Drugs. 32**,** 783.

Koch, H., Weber, Y. G., 2019. The glucose transporter type 1 (Glut1) syndromes. Epilepsy Behav. 91**,** 90-93.

Kossoff, E. H., et al., 2018. Optimal clinical management of children receiving dietary therapies for epilepsy: Updated recommendations of the International Ketogenic Diet Study Group. Epilepsia Open. 3**,** 175-192.

Kovács, R., et al., 2018. Bioenergetic Mechanisms of Seizure Control. Front Cell Neurosci. 12**,** 335.

Krapivinsky, G., et al., 2003. The NMDA receptor is coupled to the ERK pathway by a direct interaction between NR2B and RasGRF1. Neuron. 40**,** 775-784.

Krauss, G. L., et al., 2012. Randomized phase III study 306: adjunctive perampanel for refractory partial-onset seizures. Neurology. 78**,** 1408-15.

Kumar, A., et al., 2018. Evolution of Brain Glucose Metabolic Abnormalities in Children With Epilepsy and SCN1A Gene Variants. J Child Neurol. 33**,** 832-836.

Kuo, F.-S., et al., 2019. Disordered breathing in a mouse model of Dravet syndrome. Elife. 8**,** e43387.
Kuo, J., et al., 2016. Postictal immobility and generalized EEG suppression are associated with the severity of respiratory dysfunction. Epilepsia. 57**,** 412-7.
Lagae, L., et al., 2018. Quality of life and comorbidities associated with Dravet syndrome severity: a multinational cohort survey. Dev Med Child Neurol. 60**,** 63-72.
Lagae, L., et al., 2019. Fenfluramine hydrochloride for the treatment of seizures in Dravet syndrome: a randomised, double-blind, placebo-controlled trial. Lancet. 394**,** 2243-2254.
Lai, W. W., et al., 2020. Cardiovascular safety of fenfluramine in the treatment of Dravet syndrome: Analysis of an ongoing long-term open-label safety extension study. Epilepsia. 61**,** 2386-2395.
Langan, Y., 2000. Sudden unexpected death in epilepsy (SUDEP): risk factors and case control studies. Seizure. 9**,** 179-83.
Laux, L., Blackford, R., 2013. The ketogenic diet in Dravet syndrome. J Child Neurol. 28**,** 1041-4.
Lepper, M. F., et al., 2018. Proteomic landscape of patient-derived CD4+ T cells in recent-onset type 1 diabetes. Journal of proteome research. 17**,** 618-634.
Li, A., et al., 2010. Proteomic profiling of the epileptic dentate gyrus. Brain pathology. 20**,** 1077-1089.
Liao, L., et al., 2008a. Quantitative proteomic analysis of primary neurons reveals diverse changes in synaptic protein content in fmr1 knockout mice. Proceedings of the National Academy of Sciences. 105**,** 15281-15286.
Liao, L., et al., 2008b. Quantitative proteomic analysis of primary neurons reveals diverse changes in synaptic protein content in fmr1 knockout mice. Proc Natl Acad Sci U S A. 105**,** 15281-6.
Licheni, S. H., et al., 2018. Sleep problems in Dravet syndrome: a modifiable comorbidity. Developmental Medicine & Child Neurology. 60**,** 192-198.
Lichtman, J. W., et al., 2014. The big data challenges of connectomics. Nature Neuroscience. 17**,** 1448-1454.
Likhodii, S. S., et al., 2003. Anticonvulsant properties of acetone, a brain ketone elevated by the ketogenic diet. Ann Neurol. 54**,** 219-26.
Lipton, S. A., et al., 1993. A redox-based mechanism for the neuroprotective and neurodestructive effects of nitric oxide and related nitroso-compounds. Nature. 364**,** 626-32.
Lisman, J., et al., 2002. The molecular basis of CaMKII function in synaptic and behavioural memory. Nature Reviews Neuroscience. 3**,** 175-190.
Liu, W., Hajjar, K. A., 2016. The annexin A2 system and angiogenesis. Biol Chem. 397**,** 1005-16.
Liu, X. Y., et al., 2008. Comparative proteomics and correlated signaling network of rat hippocampus in the pilocarpine model of temporal lobe epilepsy. Proteomics. 8**,** 582-603.
Lossin, C., 2009. A catalog of SCN1A variants. Brain Dev. 31**,** 114-30.
Lueptow, L. M., 2017. Novel Object Recognition Test for the Investigation of Learning and Memory in Mice. J Vis Exp.
Maa, E., Figi, P., 2014. The case for medical marijuana in epilepsy. Epilepsia. 55**,** 783-6.
Magiorkinis, E., et al., 2010. Hallmarks in the history of epilepsy: epilepsy in antiquity. Epilepsy Behav. 17**,** 103-8.
Mahmoud, S., et al., 2019. Astrocytes Maintain Glutamate Homeostasis in the CNS by Controlling the Balance between Glutamate Uptake and Release. Cells. 8.
Mantegazza, M., Broccoli, V., 2019. SCN 1A/NaV1. 1 channelopathies: Mechanisms in expression systems, animal models, and human iPSC models. Epilepsia. 60**,** S25-S38.
Martin, M. S., et al., 2010. Altered function of the SCN1A voltage-gated sodium channel leads to gamma-aminobutyric acid-ergic (GABAergic) interneuron abnormalities. J Biol Chem. 285**,** 9823-34.
Martin, P., et al., 2020. Fenfluramine acts as a positive modulator of sigma-1 receptors. Epilepsy Behav. 105**,** 106989.
Masino, S. A., et al., 2012. Purines and neuronal excitability: links to the ketogenic diet. Epilepsy Res. 100**,** 229-38.
Masino, S. A., Rho, J. M., Mechanisms of Ketogenic Diet Action. In: J. L. Noebels, et al., (Eds.), Jasper's Basic Mechanisms of the Epilepsies. National Center for Biotechnology Information (US)

Copyright © 2012, Michael A Rogawski, Antonio V Delgado-Escueta, Jeffrey L Noebels, Massimo Avoli and Richard W Olsen., Bethesda (MD), 2012.

Masino, S. A., Rho, J. M., 2019. Metabolism and epilepsy: Ketogenic diets as a homeostatic link. Brain Res. 1703**,** 26-30.

Mason, S., 2017. Lactate Shuttles in Neuroenergetics-Homeostasis, Allostasis and Beyond. Front Neurosci. 11**,** 43.

McDonald, T., et al., 2018. Impairments in Oxidative Glucose Metabolism in Epilepsy and Metabolic Treatments Thereof. Front Cell Neurosci. 12**,** 274.

McGonigle, P., Ruggeri, B., 2014. Animal models of human disease: challenges in enabling translation. Biochem Pharmacol. 87**,** 162-71.

McIntosh, A. M., et al., 2010. Effects of vaccination on onset and outcome of Dravet syndrome: a retrospective study. Lancet Neurol. 9**,** 592-8.

McMillin, M., DeMorrow, S., 2016. Effects of bile acids on neurological function and disease. Faseb j. 30**,** 3658-3668.

Meisler, M. H., Kearney, J. A., 2005. Sodium channel mutations in epilepsy and other neurological disorders. J Clin Invest. 115**,** 2010-7.

Mergenthaler, P., et al., 2013. Sugar for the brain: the role of glucose in physiological and pathological brain function. Trends Neurosci. 36**,** 587-97.

Michael-Titus, A. T., Priestley, J. V., 2014. Omega-3 fatty acids and traumatic neurological injury: from neuroprotection to neuroplasticity? Trends Neurosci. 37**,** 30-8.

Miller, A. R., et al., 2014. Mapping genetic modifiers of survival in a mouse model of Dravet syndrome. Genes Brain Behav. 13**,** 163-72.

Mistry, A. M., et al., 2014. Strain- and age-dependent hippocampal neuron sodium currents correlate with epilepsy severity in Dravet syndrome mice. Neurobiol Dis. 65**,** 1-11.

Molin, S., et al., 2015. The hand eczema proteome: imbalance of epidermal barrier proteins. British Journal of Dermatology. 172**,** 994-1001.

Morbidelli, L., et al., 2004. Role of nitric oxide in tumor angiogenesis. Cancer Treat Res. 117**,** 155-67.

Morin-Brureau, M., et al., 2012. Why and how to target angiogenesis in focal epilepsies. Epilepsia. 53 Suppl 6**,** 64-8.

Myers, K. A., et al., 2018. Randomized controlled trial of melatonin for sleep disturbance in dravet syndrome: the DREAMS study. Journal of Clinical Sleep Medicine. 14**,** 1697-1704.

Nabbout, R., et al., 2011. Ketogenic diet also benefits Dravet syndrome patients receiving stiripentol: a prospective pilot study. Epilepsia. 52**,** e54-7.

Nabbout, R., et al., 2020. Fenfluramine for Treatment-Resistant Seizures in Patients With Dravet Syndrome Receiving Stiripentol-Inclusive Regimens: A Randomized Clinical Trial. JAMA Neurol. 77**,** 300-308.

Nashef, L., et al., 2012. Unifying the definitions of sudden unexpected death in epilepsy. Epilepsia. 53**,** 227-233.

Nichol, K., et al., The proposed multimodal mechanism of action of cannabidiol (CBD) in epilepsy: Modulation of intracellular calcium and adenosine-mediated signaling (P5. 5-007). AAN Enterprises, 2019.

Niday, Z., Tzingounis, A. V., 2018. Potassium Channel Gain of Function in Epilepsy: An Unresolved Paradox. Neuroscientist. 24**,** 368-380.

Nishida, T., et al., 2018. Adjunctive perampanel in partial-onset seizures: Asia-Pacific, randomized phase III study. Acta Neurol Scand. 137**,** 392-399.

O'Donnell, J., et al., 2012. Norepinephrine: a neuromodulator that boosts the function of multiple cell types to optimize CNS performance. Neurochem Res. 37**,** 2496-512.

O'Sullivan, G. J., et al., 2008. Dopamine D1 vs D5 receptor-dependent induction of seizures in relation to DARPP-32, ERK1/2 and GluR1-AMPA signalling. Neuropharmacology. 54**,** 1051-61.

Oakley, J. C., et al., 2011. Insights into pathophysiology and therapy from a mouse model of Dravet syndrome. Epilepsia. 52 Suppl 2**,** 59-61.

Oakley, J. C., et al., 2009. Temperature- and age-dependent seizures in a mouse model of severe myoclonic epilepsy in infancy. Proc Natl Acad Sci U S A. 106**,** 3994-9.

Obel, L. F., et al., 2012. Brain glycogen-new perspectives on its metabolic function and regulation at the subcellular level. Front Neuroenergetics. 4**,** 3.

Ogiwara, I., et al., 2013. Nav1.1 haploinsufficiency in excitatory neurons ameliorates seizure-associated sudden death in a mouse model of Dravet syndrome. Hum Mol Genet. 22**,** 4784-804.

Ogiwara, I., et al., 2007. Nav1.1 localizes to axons of parvalbumin-positive inhibitory interneurons: a circuit basis for epileptic seizures in mice carrying an Scn1a gene mutation. J Neurosci. 27**,** 5903-14.

Ohki, T., et al., 1997. Severe myoclonic epilepsy in infancy: evolution of seizures. Seizure. 6**,** 219-24.

Olivieri, G., et al., 2016. Cognitive-behavioral profiles in teenagers with Dravet syndrome. Brain and Development. 38**,** 554-562.

Oyarzabal, A., Marin-Valencia, I., 2019. Synaptic energy metabolism and neuronal excitability, in sickness and health. J Inherit Metab Dis. 42**,** 220-236.

Paoli, A., et al., 2014. Ketogenic diet in neuromuscular and neurodegenerative diseases. Biomed Res Int. 2014**,** 474296.

Patel, M., 2018. A Metabolic Paradigm for Epilepsy. Epilepsy Curr. 18**,** 318-322.

Patri, M., Synaptic Transmission and Amino Acid Neurotransmitters. Neurochemical Basis of Brain Function and Dysfunction. IntechOpen, 2019.

Patti, G. J., et al., 2012. Innovation: Metabolomics: the apogee of the omics trilogy. Nat Rev Mol Cell Biol. 13**,** 263-9.

Peterman, M., 1924. The ketogenic diet in the treatment of epilepsy: a preliminary report. American journal of diseases of children. 28**,** 28-33.

Pong, A. W., et al., 2012. Glucose transporter type I deficiency syndrome: epilepsy phenotypes and outcomes. Epilepsia. 53**,** 1503-10.

Porter, B. E., Jacobson, C., 2013. Report of a parent survey of cannabidiol-enriched cannabis use in pediatric treatment-resistant epilepsy. Epilepsy Behav. 29**,** 574-7.

Poryo, M., et al., 2017. Dravet syndrome: a new causative SCN1A mutation? Clin Case Rep. 5**,** 613-615.

Prins, M. L., 2008. Cerebral metabolic adaptation and ketone metabolism after brain injury. J Cereb Blood Flow Metab. 28**,** 1-16.

Puchalska, P., Crawford, P. A., 2017. Multi-dimensional Roles of Ketone Bodies in Fuel Metabolism, Signaling, and Therapeutics. Cell Metab. 25**,** 262-284.

Racine, R. J., 1972. Modification of seizure activity by electrical stimulation. II. Motor seizure. Electroencephalogr Clin Neurophysiol. 32**,** 281-94.

Ragona, F., 2011. Cognitive development in children with Dravet syndrome. Epilepsia. 52 Suppl 2**,** 39-43.

Ragona, F., et al., 2011. Cognitive development in Dravet syndrome: a retrospective, multicenter study of 26 patients. Epilepsia. 52**,** 386-392.

Reid, C. A., et al., 2014. Epilepsy, energy deficiency and new therapeutic approaches including diet. Pharmacol Ther. 144**,** 192-201.

Rho, J. M., 2017. How does the ketogenic diet induce anti-seizure effects? Neurosci Lett. 637**,** 4-10.

Rho, J. M., et al., 2002. Acetoacetate, acetone, and dibenzylamine (a contaminant in l-(+)-beta-hydroxybutyrate) exhibit direct anticonvulsant actions in vivo. Epilepsia. 43**,** 358-61.

Ricobaraza, A., et al., 2019. Epilepsy and neuropsychiatric comorbidities in mice carrying a recurrent Dravet syndrome SCN1A missense mutation. Scientific reports. 9**,** 1-15.

Rigau, V., et al., 2007. Angiogenesis is associated with blood-brain barrier permeability in temporal lobe epilepsy. Brain. 130**,** 1942-56.

Rilstone, J. J., et al., 2012. Dravet syndrome: seizure control and gait in adults with different SCN1A mutations. Epilepsia. 53**,** 1421-1428.

Rodda, J. M., et al., 2012. Progressive gait deterioration in adolescents with Dravet syndrome. Arch Neurol. 69**,** 873-8.

Rosander, C., Hallbook, T., 2015. Dravet syndrome in Sweden: a population-based study. Dev Med Child Neurol. 57**,** 628-633.

Rowley, S., Patel, M., 2013. Mitochondrial involvement and oxidative stress in temporal lobe epilepsy. Free Radic Biol Med. 62**,** 121-131.

Rubinstein, M., et al., 2015a. Dissecting the phenotypes of Dravet syndrome by gene deletion. Brain. 138**,** 2219-33.

Rubinstein, M., et al., 2015b. Genetic background modulates impaired excitability of inhibitory neurons in a mouse model of Dravet syndrome. Neurobiol Dis. 73**,** 106-17.

Sada, N., et al., 2015. Epilepsy treatment. Targeting LDH enzymes with a stiripentol analog to treat epilepsy. Science. 347**,** 1362-7.

Sakauchi, M., et al., 2011. Mortality in Dravet syndrome: search for risk factors in Japanese patients. Epilepsia. 52**,** 50-54.

Salek, R. M., et al., 2010. A metabolomic study of the CRND8 transgenic mouse model of Alzheimer's disease. Neurochem Int. 56**,** 937-47.

Salgueiro-Pereira, A. R., et al., 2019. A two-hit story: Seizures and genetic mutation interaction sets phenotype severity in SCN1A epilepsies. Neurobiol Dis. 125**,** 31-44.

Sanchez, R. E., et al., 2019. Circadian regulation of sleep in a pre-clinical model of Dravet syndrome: dynamics of sleep stage and siesta re-entrainment. Sleep. 42**,** zsz173.

Sawyer, N. T., et al., 2016. Scn1a dysfunction alters behavior but not the effect of stress on seizure response. Genes Brain Behav. 15**,** 335-47.

Scharfman, H. E., Brooks-Kayal, A. R., 2014. Is plasticity of GABAergic mechanisms relevant to epileptogenesis? Adv Exp Med Biol. 813**,** 133-50.

Scheffer, I. E., et al., 2017. ILAE classification of the epilepsies: Position paper of the ILAE Commission for Classification and Terminology. Epilepsia. 58**,** 512-521.

Scheffer, I. E., et al., 2016. Classification of the epilepsies: New concepts for discussion and debate-Special report of the ILAE Classification Task Force of the Commission for Classification and Terminology. Epilepsia Open. 1**,** 37-44.

Schoonjans, A.-S., et al., 2019. More daytime sleepiness and worse quality of sleep in patients with Dravet Syndrome compared to other epilepsy patients. European Journal of Paediatric Neurology. 23**,** 61-69.

Schoonjans, A. S., et al., 2015. Low-dose fenfluramine in the treatment of neurologic disorders: experience in Dravet syndrome. Ther Adv Neurol Disord. 8**,** 328-38.

Schoonjans, A. S., et al., 2017. Cardiovascular safety of low-dose fenfluramine in Dravet syndrome: a review of its benefit-risk profile in a new patient population. Curr Med Res Opin. 33**,** 1773-1781.

Schwindinger, W. F., et al., 2012. Synergistic roles for G-protein γ3 and γ7 subtypes in seizure susceptibility as revealed in double knock-out mice. Journal of Biological Chemistry. 287**,** 7121-7133.

Scott, D. B., et al., 2004. Endocytosis and degradative sorting of NMDA receptors by conserved membrane-proximal signals. J Neurosci. 24**,** 7096-109.

Seyfried, T. N., Mukherjee, P., 2005. Targeting energy metabolism in brain cancer: review and hypothesis. Nutr Metab (Lond). 2**,** 30.

Shiotsuki, H., et al., 2010. A rotarod test for evaluation of motor skill learning. J Neurosci Methods. 189**,** 180-5.

Shmuely, S., et al., 2016. Mortality in Dravet syndrome: A review. Epilepsy Behav. 64**,** 69-74.

Sills, G. J., Rogawski, M. A., 2020. Mechanisms of action of currently used antiseizure drugs. Neuropharmacology. 168**,** 107966.

Sinoo, C., et al., 2019. Behavior problems and health-related quality of life in Dravet syndrome. Epilepsy Behav. 90**,** 217-227.

Skluzacek, J. V., et al., 2011. Dravet syndrome and parent associations: the IDEA League experience with comorbid conditions, mortality, management, adaptation, and grief. Epilepsia. 52**,** 95-101.

Smith, D., et al., 2003. Lactate: a preferred fuel for human brain metabolism in vivo. J Cereb Blood Flow Metab. 23**,** 658-64.

Soty, M., et al., 2017. Gut-Brain Glucose Signaling in Energy Homeostasis. Cell Metab. 25**,** 1231-1242.

Südhof, T. C., 2008. Neuroligins and neurexins link synaptic function to cognitive disease. Nature. 455**,** 903-911.

Sun, H., et al., 2010. Analysis of SCN1A mutation and parental origin in patients with Dravet syndrome. J Hum Genet. 55**,** 421-7.

Suvorov, A., Takser, L., 2008. Facing the challenge of data transfer from animal models to humans: the case of persistent organohalogens. Environ Health. 7**,** 58.

Swulius, M. T., Waxham, M. N., 2008. Ca(2+)/calmodulin-dependent protein kinases. Cell Mol Life Sci. 65**,** 2637-57.

Tai, C., et al., 2014. Impaired excitability of somatostatin- and parvalbumin-expressing cortical interneurons in a mouse model of Dravet syndrome. Proc Natl Acad Sci U S A. 111**,** E3139-48.

Tang, S. H. E., et al., 2002. A Cre/loxP-deleter transgenic line in mouse strain 129S1/SvImJ. genesis. 32**,** 199-202.

Team, R. C., 2017. R Core Team (2017). R: A language and environment for statistical computing. R Found. Stat. Comput. Vienna, Austria.

Teran, F. A., et al., 2019. Time of Day and a Ketogenic Diet Influence Susceptibility to SUDEP in Scn1aR1407X/+ Mice. Frontiers in Neurology. 10**,** 278.

Terrone, G., et al., 2017. Inflammation and Epilepsy: Preclinical Findings and Potential Clinical Translation. Curr Pharm Des. 23**,** 5569-5576.

Tian, X., et al., 2019. The Efficacy of Ketogenic Diet in 60 Chinese Patients With Dravet Syndrome. Front Neurol. 10**,** 625.

Tiedje, K. E., et al., 2010. Beta-alanine as a small molecule neurotransmitter. Neurochem Int. 57**,** 177-88.

Tonini, R., et al., 2001. Involvement of CDC25Mm/Ras-GRF1-dependent signaling in the control of neuronal excitability. Molecular and Cellular Neuroscience. 18**,** 691-701.

Tran, C. H., et al., 2020. Interneuron Desynchronization Precedes Seizures in a Mouse Model of Dravet Syndrome. J Neurosci. 40**,** 2764-2775.

Tro-Baumann, B., et al., 2011. A retrospective study of the relation between vaccination and occurrence of seizures in Dravet syndrome. Epilepsia. 52**,** 175-8.

Tsai, M. S., et al., 2015. Functional and structural deficits of the dentate gyrus network coincide with emerging spontaneous seizures in an Scn1a mutant Dravet Syndrome model during development. Neurobiol Dis. 77**,** 35-48.

Turner, D. A., Adamson, D. C., 2011. Neuronal-astrocyte metabolic interactions: understanding the transition into abnormal astrocytoma metabolism. J Neuropathol Exp Neurol. 70**,** 167-76.

Vasilopoulou, C. G., et al., 2016. Metabolomic Analysis in Brain Research: Opportunities and Challenges. Front Physiol. 7**,** 183.

Verheyen, K., et al., 2019. Motor development in children with Dravet syndrome. Developmental Medicine & Child Neurology. 61**,** 950-956.

Verleye, M., et al., 2016. Neuroprotective activity of stiripentol with a possible involvement of voltage-dependent calcium and sodium channels. J Neurosci Res. 94**,** 179-89.

Vezzani, A., 2014. Epilepsy and inflammation in the brain: overview and pathophysiology. Epilepsy Curr. 14**,** 3-7.

Vidal, M., et al., 2011. Interactome networks and human disease. Cell. 144**,** 986-98.

Villa, C., Combi, R., 2016. Potassium Channels and Human Epileptic Phenotypes: An Updated Overview. Front Cell Neurosci. 10**,** 81.

Villas, N., et al., 2017. Dravet syndrome: characteristics, comorbidities, and caregiver concerns. Epilepsy & Behavior. 74**,** 81-86.

Vlaskamp, D. R., et al., 2019. SYNGAP1 encephalopathy: a distinctive generalized developmental and epileptic encephalopathy. Neurology. 92**,** e96-e107.

von Spiczak, S., et al., 2011. A retrospective population-based study on seizures related to childhood vaccination. Epilepsia. 52**,** 1506-12.

Waldbaum, S., Patel, M., 2010. Mitochondrial dysfunction and oxidative stress: a contributing link to acquired epilepsy? J Bioenerg Biomembr. 42**,** 449-55.

Walker, A., et al., 2016. Proteomic profiling of epileptogenesis in a rat model: Focus on inflammation. Brain Behav Immun. 53**,** 138-158.

Wallace, A., et al., 2016. Pharmacotherapy for Dravet Syndrome. Paediatr Drugs. 18**,** 197-208.

Wang, Y. Q., et al., 2020. Efficacy of the ketogenic diet in patients with Dravet syndrome: A meta-analysis. Seizure. 81**,** 36-42.

Warnes, M. G. R., et al., 2016. Package 'gplots'. Various R Programming Tools for Plotting Data.

Weber, Y. G., et al., 2014. Genetic biomarkers in epilepsy. Neurotherapeutics. 11**,** 324-33.

Wexler, I. D., et al., 1997. Outcome of pyruvate dehydrogenase deficiency treated with ketogenic diets. Studies in patients with identical mutations. Neurology. 49**,** 1655-61.

Wheless, J. W., 2008. History of the ketogenic diet. Epilepsia. 49 Suppl 8**,** 3-5.

WILDER, R. M., The effects of ketonemia on the course of epilepsy. Mayo Clin Proc, Vol. 2, 1921, pp. 307-308.

Wirrell, E. C., et al., 2017. Optimizing the Diagnosis and Management of Dravet Syndrome: Recommendations From a North American Consensus Panel. Pediatr Neurol. 68**,** 18-34 e3.

Woodyatt, R., 1921. Objects and method of diet adjustment in diabetes. Archives of internal Medicine. 28**,** 125-141.

Wu, N., et al., 2016. Alpha-Ketoglutarate: Physiological Functions and Applications. Biomol Ther (Seoul). 24**,** 1-8.

Wyers, L., et al., 2019. Gait deviations in patients with dravet syndrome: A systematic review. European Journal of Paediatric Neurology. 23**,** 357-367.

Xu, B., et al., 2018. Proteomic Profiling of Brain and Testis Reveals the Diverse Changes in Ribosomal Proteins in fmr1 Knockout Mice. Neuroscience. 371**,** 469-483.

Xu, X. X., Luo, J. H., 2018. Mutations of N-Methyl-D-Aspartate Receptor Subunits in Epilepsy. Neurosci Bull. 34**,** 549-565.

Yamauchi, M., et al., 1998. Direct evidence for the role of nitric oxide on the glutamate-induced neuronal death in cultured cortical neurons. Brain Res. 780**,** 253-9.

Yan, N., et al., 2018. Prospective study of the efficacy of a ketogenic diet in 20 patients with Dravet syndrome. Seizure. 60**,** 144-148.

Yang, H., et al., 2013a. Glycolysis in energy metabolism during seizures. Neural Regeneration Research. 8**,** 1316-1326.

Yang, H., et al., 2013b. Glycolysis in energy metabolism during seizures. Neural Regen Res. 8**,** 1316-26.

Youngson, N. A., et al., 2017. The mechanisms mediating the antiepileptic effects of the ketogenic diet, and potential opportunities for improvement with metabolism-altering drugs. Seizure. 52**,** 15-19.

Yu, F. H., et al., 2006. Reduced sodium current in GABAergic interneurons in a mouse model of severe myoclonic epilepsy in infancy. Nature Neuroscience. 9**,** 1142.

Yudkoff, M., et al., 2005. Response of brain amino acid metabolism to ketosis. Neurochem Int. 47**,** 119-28.

Zhang, Y., et al., 2015. Pharmacological characterization of an antisense knockdown zebrafish model of Dravet syndrome: inhibition of epileptic seizures by the serotonin agonist fenfluramine. PloS one. 10**,** e0125898.

Zuberi, S. M., et al., 2011. Genotype-phenotype associations in SCN1A-related epilepsies. Neurology. 76**,** 594-600.

# *Acknowledgments*

First of all, I would like to thank my supervisor Prof. Dr. Heidrun Potschka for giving me this incredible opportunity to conduct my Ph.D. thesis in her lab and work on such an amazing project. As in every Ph.D. project, there were many challenges on the way and I am very grateful for all the support and guidance on the way. Having her as a mentor was equally inspiring and motivational for progress in my work. Therefore, I truly appreciate the given chance which allowed me to learn and develop not only as a scientist but also as a person.

I would like to thank the members of my Thesis Advisory Committee, for their time, constructive suggestions, and directing my Ph.D. Also, I am very grateful to the GSN for this great opportunity and for enriching my life with numerous social events. Special thanks to Stefanie and Lena for their support and guidance towards the end of my Ph.D.

Next, I would like to thank my lab colleagues for their great support and help with my project. I am of course very grateful for all the fun over the past few years and their help with improving my German. A particular tribute to all doctoral students who made the time in the office enjoyable and memorable, and to Marta and Sarah for lovely tea breaks and their friendship. I owe a special thanks to Dr. Roelof Maarten van Dijk for sharing his in-depth knowledge and all constructive discussions about my project that helped me develop as a scientist.

I especially appreciate the time taken to read my thesis and therefore, I am very thankful to my supervisor, Dr. van Dijk, Helen, and Shruti.

I would like to thank my friends from Serbia for all long-distance love and support, and always a lovely vacation time with a special note to Bojana, Dušica, and Zorica. My stay in Munich would not be as pleasant without dear friends and weekend coffees with Mirjana, Milica, Tamara, Monica, and Imme. Also, many thanks to my friends around the globe and in particular to Shruti and Fernanda, for all the online support and comfort during hard times.

I cannot thank enough to my brother, my mother, my boyfriend Vladimir, and my family for their unconditional love, which remained the main motivation for completing my thesis. I deeply appreciate their support over my time in Munich and therefore this thesis is dedicated to them. I am truly lucky to have you in my life!

# *Curriculum Vitae*

## ***Education***

| | |
|---|---|
| Oct. 2016 – currently | *Ph.D. in Systemic Neurosciences*<br>Graduate School of Systemic Neurosciences (GSN)<br>Ludwig-Maximilians-Universität (LMU), Munich, Germany |
| Oct. 2011 - Sept. 2016 | *Master in Pharmacy*<br>Integrated Undergraduate and Master Academic Studies<br>University of Novi Sad, Novi Sad, Serbia |

## ***Research experience***

| | |
|---|---|
| Nov. 2016 – currently | *Research Investigator*<br>Institute of Pharmacology, Toxicology and Pharmacy,<br>Ludwig-Maximilians-Universität (LMU), Munich, Germany |
| July 2015 – Aug. 2015 | *Research Intern*<br>Brain Mind Institute,<br>École polytechnique fédérale de Lausanne (EPFL),<br>Lausanne, Switzerland |
| Jan. 2015 – Feb. 2015 | *Research Intern*<br>VISRA Undergraduate Internship Program,<br>Vanderbilt University, Nashville, USA |
| Nov. 2013 – June 2016 | *Research student (part-time)*<br>Faculty of Medicine<br>University of Novi Sad, Novi Sad, Serbia |

# *List of publications*

**Miljanovic N.**, Hauck SM., van Dijk RM., Di Liberto V., Rezaei A., Potschka H. Proteomic signature of the Dravet syndrome in the genetic mouse model Scn1a-A1783V. [Journal article] *Neurobiol Dis.* (submitted).

**Miljanovic N.**, van Dijk RM., Buchecker V., Potschka H. Metabolomic signature of the Dravet syndrome: a genetic mouse model study. [Journal article] *Epilepsia* (submitted).

Boldt L., Koska I., van Dijk R.M, Talbot S.R., **Miljanovic N.**, Palme R., Bleich A., Potschka H. Toward evidence-based severity assessment in mouse models with repeated seizures: I. Electrical kindling. *Epilepsy Behav*. 2021 Jan 5;115:107689. doi: 10.1016/j.yebeh.2020.107689. Epub ahead of print. PMID: 33418481.

Henke C., Töllner K., van Dijk R.M., **Miljanovic N.**, Cordes T., Twele F., Bröer S., Ziesak V., Rohde M., Hauck S.M., Vogel C., Welzel L., Schumann T., Willmes D.M., Kurzbach A., El-Agroudy N.N., Bornstein S.R., Schneider S.A., Jordan J., Potschka H., Metallo C.M., Köhling R., Birkenfeld A.L., Löscher W. Disruption of the sodium-dependent citrate transporter SLC13A5 in mice causes alterations in brain citrate levels and neuronal network excitability in the hippocampus. *Neurobiol Dis.* 2020 Sep;143:105018. doi: 10.1016/j.nbd.2020.105018. Epub 2020 Jul 16. PMID: 32682952.

Talbot S.R., Biernot S., Bleich A., van Dijk R.M., Ernst L., Häger C., Helgers S.O.A., Koegel B., Koska I., Kuhla A., **Miljanovic N.**, Müller-Graff F.T., Schwabe K., Tolba R., Vollmar B., Weegh N., Wölk T., Wolf F., Wree A., Zieglowski L., Potschka H., Zechner D. Defining body-weight reduction as a humane endpoint: a critical appraisal. *Lab Anim*. 2020 Feb;54(1):99-110. doi: 10.1177/0023677219883319. Epub 2019 Oct 30. PMID: 31665969.

Ernst L., Kopaczka M., Schulz M., Talbot S.R., Struve B., Häger C., Bleich A., Durst M., Jirkof P., Arras M., van Dijk R.M., **Miljanovic N.**, Potschka H., Merhof D., Tolba R.H.. Semi-automated generation of pictures for the Mouse Grimace Scale: A multi-laboratory analysis (Part 2). *Lab Anim.* 2020 Feb;54(1):92-98. doi: 10.1177/0023677219881664. Epub 2019 Oct 29. PMID: 31660777.

# *Declaration of author contributions*

**1. manuscript: Miljanovic N., Hauck SM., van Dijk RM., Di Liberto V., Rezaei A., Potschka H. Proteomic signature of the Dravet syndrome in the genetic mouse model *Scn1a*-A1783V. Submitted to *Neurobiology of Disease*.**

The author of the thesis is the first author of this manuscript. **N.M**. designed and performed all in vivo experiments, completed statistical analysis and provided the original manuscript draft. **S.M.H.** performed proteomic screening and provided raw data. **R.M.v.D.** contributed to study design and statistical analysis. **D.L.V.** contributed to establishing experiment methodology and assisted in experiments. **R.A.** performed immunohistochemical staining. **H.P.** provided conception and funding for the study, wrote sections of the manuscript. All authors contributed to manuscript revision, read and agreed on the submitted version.

**2. manuscript: Miljanovic N., van Dijk RM., Buchecker V., Potschka H. Metabolomic signature of the Dravet syndrome: a genetic mouse model study. Submitted to *Epilepsia*.**

The author of the present thesis is the first author of this manuscript. **N.M**. designed and performed all experiments, completed statistical analysis and provided the original manuscript draft. **R.M.v.D.** contributed to study design and statistical analysis. **V.B.** contributed to experiments execution. **H.P.** provided conception and funding for the study, wrote sections of the manuscript. All authors contributed to the manuscript revision and approved the submitted version.

Munich, 9.12.2020 Nina Miljanović Prof. Dr. Heidrun Potschka

# *Eidesstattliche Versicherung/Affidavit*

Hiermit versichere ich an Eides statt, dass ich die vorliegende Dissertation „*Proteomic and metabolomic signature of Dravet Syndrome: analysis in a genetic mouse model Scn1a-A1783V*“ selbstständig angefertigt habe, mich außer der angegebenen keiner weiteren Hilfsmittel bedient und alle Erkenntnisse, die aus dem Schrifttum ganz oder annähernd übernommen sind, als solche kenntlich gemacht und nach ihrer Herkunft unter Bezeichnung der Fundstelle einzeln nachgewiesen habe.

I hereby confirm that the dissertation “*Proteomic and metabolomic signature of Dravet Syndrome: analysis in a genetic mouse model Scn1a-A1783V*” is the result of my own work and that I have only used sources or materials listed and specified in the dissertation.

München, den 11.03.2021
Munich, date 11.03.2021 Nina Miljanović